INVESTIGATIONS ON USABILITY OF POROUS MEDIA IN KEROSENE PRESSURE STOVES FOR IMPROVEMENT OF THERMAL PERFORMANCE

A Thesis

Submitted by

MONIKANKANA SHARMA

for the award of the degree

of

DOCTOR OF PHILOSOPHY

CENTRE FOR ENERGY

INDIAN INSTITUTE OF TECHNOLOGY GUWAHATI

DECEMBER 2010

CERTIFICATE

It is certified that the work contained in the thesis entitled **Investigations on Usability of Porous Media in Kerosene Pressure Stoves for Improvement of Thermal Performance** by **Monikankana Sharma**, a student in the Centre for Energy, Indian Institute of Technology Guwahati, India, for the award of the degree of the **Doctor of Philosophy** has been carried out under our supervision and that this work has not been submitted elsewhere for any degree.

Dr. Subhash C. Mishra
Professor
Department of Mechanical Engineering
Indian Institute of Technology Guwahati
Guwahati – 781039, Assam, India.

Dr. P. Mahanta
Professor
Department of Mechanical Engineering &
Head, Centre for Energy
Indian Institute of Technology Guwahati
Guwahati – 781039, Assam, India.

Dedicated to my parents, parents-in-law and my loving husband

Acknowledgements

I am heartily thankful to my supervisor, **Prof. Subhash C. Mishra**, whose guidance and support from the initial to the final level have enabled me to develop an understanding of the subject. His constant encouragements have been a great motivation for me to take up the work as a challenge and complete the same with great enthusiasm. He taught me the "mantra of having patience" which helped me to remain bold and work towards betterment, even in the adverse situations. I can never forget his dedication in teaching me the art of writing. He has been a great source of inspiration for me. I also have received an overwhelming inspiration and support from my second supervisor **Prof. P. Mahanta,** for which I am always grateful. His wide knowledge and his logical way of thinking have been of great value for me. His understanding, encouraging and personal guidance have provided a good basis for the present thesis.

Besides, my supervisors, I want to offer my special thanks to my doctoral committee chairman, **Dr. U.K. Saha** for his insightful comments and invaluable suggestions during my progress seminars. My thanks are also due to other members of my doctoral committee **Dr. V.S. Moholkar, Prof. A.K. Dass** and **Dr. C. Somayaji** for their critical assessment of my work and their valuable comments towards its improvement.

I would like to thank Petroleum Conservation and Research Association (PCRA), New Delhi for their partial support in the form of a project to **Prof. Mishra** and **Dr. P, Muthukumar** that helped me in carrying out some of my experimental investigations. I am highly grateful

to **Dr. P, Muthukumar** for his kind permission to do my experiments in the Thermal Science Laboratory of the Department of Mechanical Engineering, IIT Guwahati.

I wish to express my warm and sincere thanks to **Dr. D.K. Sharma,** Assistant Workshop Superintendent, IIT Guwahati, for his kind support in allotting highly skilled technicians for helping me in the fabrication work of my experimental setups. **Mr. U Gohain, Mr. M Sharma** and **Mr. D. Chetri** deserve special thanks for their kind assistance. I am also thankful to the technical and non-technical staff members of the Centre for Energy and the Department of Mechanical Engineering who have helped me in different phases of my research work.

.

I warmly thank **Prof. M. Nishioka** of University of Tsukuba, Japan for giving me the opportunity to do some computational work. I am highly impressed with his patience, motivation and sincere dedication towards research. I thank all his research students who provided me a congenial environment to work with them.

I owe my most sincere gratitude to **Prof. H.S Mukunda** of IISc Bangalore who developed my interest in the area of combustion during my stay in his group, before coming to IIT Guwahati. His teaching has immensely benefited me in developing a good understanding of the subject.

My special thanks are due to my fellow lab-mate **Mr. Vijaya K. Pantangi** who had been a good companion since my M.Tech days, for his kind help and cooperation during the entire period of my PhD work. I also wish to express my warm thanks to Mr. **Paltu Acharjree,** who helped me in the initial stages of my experiments, during his stay here for his Master's

project. **Mr. N. Sarma, Mr. S. Das, Mr. R. Malakar** and **Mr. M. Hazarika** are highly acknowledged for their assistances offered during various stages of my experiments.

I would also like to thank many of my friends from the Centre for Energy and the Department of Mechanical Engineering for their timely helps in the last five years of my PhD tenure. **Buljit, Gaurishankar, Swapnita, Bibhuti, Ranjit, Pankaj, Lepakshi, Dipti**, **Anupa**, **Ramchandra, Perumal** and **Anbarasu** are to name a few.

Few of my hostel-mates who made my stay enjoyable need special mention here. They are **Jashmini, Cosmika, Purabi, Sumitra, Minaxi, Shampa, Tapashi** and **Rumi**. I thank them all for offering me nice friendship and providing me emotional support as and when needed.

I offer my deepest gratitude to my parents for their unflagging love and support throughout my life. Without their due care, I could not have come to the present stage. My father who obtained his PhD in Economics has always been a great source of inspiration for me. He took his utmost care to build a research oriented mind in me. I thank him for providing me good education. I also would like to thank my parents-in-law and husband for their kind support during my PhD. For me, my husband is a real teacher. Without his help it would have been certainly much harder to write this thesis. Despite being a researcher in Chemistry, he gave me many valuable suggestions which helped me in my experimental work. I thank my brother **Panku**, sister-in-law **Mili**, brother-in-law **Bhaity** for their unwavering love and encouragement. Last but not the least, what moves without the blessings of the Almighty. I thank Him for giving me the strength to face every difficulty and keep me on the right track.

December 2010 **Monikankana Sharma**

Abstract

In developing countries, kerosene is considered as one of the principal cooking fuels and it is normally burnt in two kinds of stoves: wick type and pressure type. The pressure type stoves perform reasonably well; however the growing awareness about conservation of energy and reduction of pollution has necessitated their further improvements. Towards the above goal, in this study, a conventional kerosene pressure stove was modified to incorporate a bi-layered porous media consisting of alumina (Al_2O_3) and silicon carbide (SiC) enclosed in 6 different types of casing in the combustion zone. The thermal performance of the stove was evaluated with each type of casing. The main aspects of the thermal performance include temperature, emission and efficiency measurements. The emission and efficiency studies were conducted for different fuel and air flow rates. It was observed that the burner could be operated in a much leaner condition without affecting the stability of the flame. CO and NO_x were measured at different air fuel ratios. The lowest CO emission (30 ppm) was observed for the fuel flow rate: 220 g/hr and air flow rate 120 lpm. CO emission was found sensitive to heat input and air flow rate. While, NO_x behaviour was found insensitive to both heat input and air flow rate. The lowest NO_x recorded was 1.2 ppm. The temperature measurements were taken at different radial and axial locations. The average surface temperature was found ~800 ^oC and it was found to increase with increase in air and fuel flow rates. The efficiency test of the burner was conducted as per the standard water boiling test (WBT) in accordance with the BIS standard: IS 10109: 2002. The highest efficiency (~57%) was recorded for the fuel flow rate: 160 g/hr and air flow rate rate: 150 lpm and this was obtained for a conical casing. Further, the efficiency also varied with vessel sizes and the different spacings between the vessel and the burner. The optimum distances giving the best thermal performance have been identified. An analysis has been carried out to calculate the efficiencies of the burner,

working in different operating conditions, from the second law point of view. It was found that with increase in air flow rate the energy efficiency or the first law efficiency increases, while the exergy efficiency decreases. Similarly, the exergy efficiency increases with increase in fuel flow rate which is reverse in case of the first the efficiency. Thus, considering both first law and second law efficiencies, the air flow rate 120-130 lpm was found optimum. The conical casing shows the highest second law efficiency too. Finally, the thermal performances of the stove with new burner were compared with a conventional BIS specified stove. For the same heat input, the conventional stove showed higher CO (80-90 ppm) and NO_x (3-4 ppm) but first (thermal efficiency) and second law efficiencies (exergy efficiency) were comparable.

Contents

List of Figures

List of Tables

Nomenclature

ϕ	:	Equivalence ratio
Q_1	:	Heat taken by water (kJ)
Q_2	:	Heat taken by water vapour (kJ)
Q_3	:	Heat taken by vessel (kJ)
m_w	:	Mass of water in the vessel (kg)
m_v	:	Mass of aluminum vessel (kg)
c_{pv}	:	Specific heat of aluminum vessel (kJ/kgK)
c_{pw}	:	Specific heat of water (kJ/kgK)
T_{iw}	:	Initial temperature of water (K)
T_{fw}	:	Final temperature of water (K)
T_{iv}	:	Initial temperature of vessel (K)
T_{fv}	:	Final temperature of vessel (K)
L	:	Latent heat of vaporization of water (kJ/kg)
$\dot{m}_f$	:	Mass of fuel consumed per unit time (kg/s)
CV	:	Calorific value of fuel (kJ/kg)
t	:	Heating time (s)
Q_i	:	Heat input (kW)

W_c : Compressor work (kW)

$\dot{m}_a$: Mass flow rate of air (kg/s)

R : Characteristics gas constants of air (kJ/Kg-K)

P_2 : Air pressure after compression (bar)

P_1 : Initial pressure of air before compression (bar)

T_1 : Initial temperature of air before compression (K)

η_I : Thermal efficiency/first law efficiency

$\dot{m}_g$: Mass flow rate of gas (kg/s)

c_{pg} : Specific heat of gas (kJ/kgK)

T_g : Gas temperature (K)

T_o : Ambient temperature (K)

A_g : Available energy with hot gases at the exit of the burner (kW)

ΔS_w : Change in entropy of water (kJ/K)

A_1 : Available energy of water (kW)

ΔS_{wvp} : Change in entropy of water vapor (kJ/K)

A_2 : Available energy of water vapour (kW)

ΔS_v : Change in entropy of vessel (kJ/K)

A_3 : Available energy of vessel (kW)

η_{II} : Exergy efficiency/second law efficiency

C : Heat capacity of the calorimeter (J/K)

H_{OB} : Heat of combustion of Benzoic acid (J/g)

m_{OB} : Mass of Benzoic acid (g)

Q_F : Ignition energy (J)

ΔT : Change in water temperature in calorimeter

m_f : Mass of fuel (g)

Pe : Peclet number

S_L : Laminar flame speed (m/s)

d_m : Mean pore diameter (cm)

ρ : Density of air-fuel mixture (kg/m^3)

k : Thermal conductivity air-fuel mixture (W/mK)

Abbreviations

PMC	**:**	Porous media combustion
PM	**:**	Porous media/material
PB	**:**	Porous burner
CCT	**:**	Conventional combustion technology
CB	**:**	Conventional burner
ppi	**:**	Pores per inch
ppcm	**:**	Pores per centimetre
LPG	**:**	Liquefied petroleum gas
60SCC	**:**	60 mm straight cylindrical casing
70SCC	**:**	70 mm straight cylindrical casing
80SCC	**:**	80 mm straight cylindrical casing
70SCCWHS	**:**	70 mm straight cylindrical casing with heat shield
70TCWHS	**:**	70 mm taper casing with heat shield
70CCWHS	**:**	70 mm conical casing with heat shield
WHO	**:**	World Health Organization

CHAPTER 1

INTRODUCTION

1.1 BACKGROUND

The energy consumption pattern in the world varies widely. The developed countries use more energy in industrial and transport sectors; while in the developing countries, the major share goes in fulfilling their basic needs such as cooking and home lighting (Gupta and Köhlin, 2006). In India, the cooking energy consumption is nearly 45% of the total energy (Jungbluth et al., 1997). This large share of the cooking energy comes mainly from 3 different fuels, viz., biomass, kerosene and liquefied petroleum gas (LPG). Table 1.1 indicates the share of different cooking fuels used in rural and urban Indian households.

Table 1.1: Cooking fuel usage, percentage of households (Gangopadhyay et al., 2005)

Serial No.	Primary cooking fuel	1999-2000	
		Rural	Urban
1.	Coal	1.52	4.12
2.	Firewood and chips	**75.44**	**22.24**
3.	Gas (coal, oil or LPG)	**5.40**	**44.09**
4.	Gobar gas	0.31	0.5
5.	Dungcake	**10.61**	2.06
6.	Charcoal	0.04	0.14
7.	Kerosene	**2.70**	**21.67**
8.	Electricity	0.08	0.40
9.	Others	2.67	0.74
10.	No cooking arrangement	1.09	4.24

As is evident, LPG and kerosene are consumed mainly in the urban areas, while in rural sectors the use of biomass (firewood and chips, dungcake and gobar gas) is more prevalent. The dominance of LPG share in the urban areas is influenced mainly by two

factors, viz., (i) higher income of the people and, (ii) easy availability of the fuel (Reddy, 2003). Unlike this, in rural areas, majority of the people do not have access to LPG due to its higher cost and poor distribution network (Dixit et al., 2006). Similarly, in urban areas, even though the distribution networks are good, the higher cost of LPG has limited its accessibility to the lower income group. Hence, the choice of the lower income group remains between kerosene and biomass.

Kerosene has emerged as a preferred fuel over biomass because combustion of kerosene is relatively clean, and its handling is easier (Alam et al., 1998). By using kerosene, several other problems of biomass such as human drudgery, storage difficulty, ignition difficulty, smoky operation etc. can be reduced (Dunkerley et al., 1990). In recent times, its usage has been widely emphasized because it has the potential to reduce the thrust on deforestation, and also to reduce the indoor air pollution associated with biomass burning. The Indian Government has promoted its widespread usage by providing subsidy on it and made it available to both rural and urban households (Thukral and Bhandari, 1994).

Currently in India, the annual growth rate of kerosene usage is as high as 11%, and in near future, it is expected to increase further. Due to remote locations, the possibility of penetration of LPG in the rural areas will continue to remain poor (Ravindranath et al., 2005). In the last two decades, kerosene has remained as the transition fuel as there has been a marginal shifting of fuel consumption pattern from biomass to kerosene (Viswanathan and Kumar, 2005). This shifting is promoted by improvement of economy and desire for clean fuel. However, the increased demand for kerosene is of great concern since the fossil fuel reserves are depleting, and the indoor air pollutions from kerosene stoves are high (Pandit et al., 2001).

Kerosene is normally burnt in two types of stoves, viz., wick type and pressure type. The pressure type stove is preferred due to their higher thermal efficiencies (Natarajan et al., 2008). The average thermal efficiencies of the most popular kerosene pressure stoves are 45% (Thukral and Bhandari, 1994 and Smith et al., 2000), while, the rated thermal efficiencies of the Bureau of Indian Standard (BIS) specified stoves stand between 55-58% (IS:10109, 2002). However, depending upon the input power and other operating conditions, the thermal efficiencies may vary widely (Natarajan et al., 2008, Smith et al., 2000). It is to be mentioned that in comparison to the thermal efficiencies of the traditional biomass stoves (5-10%), the kerosene stoves perform much better (Dendukuri and Mittal, 1993). Nevertheless, inspired by the need for conservation of fuel, it is preferable to raise the efficiency even further.

In the emission front also, the kerosene stoves perform better than the biomass stoves. Because of higher thermal and combustion efficiencies, the carbon dioxide (CO_2) and carbon monoxide (CO) emissions from the kerosene stoves are much lower than the biomass stoves. However, as an individual entity, the CO emissions from the kerosene stoves are considered high, and in fact, higher than the prescribed limit of the World health organization (WHO) for indoor air pollution (Kandpal et al., 1995, Zhang et al., 1999).

CO is produced when fuel burns incompletely due to lack of oxygen (O_2). It is a toxic air pollutant, and its prolonged exposure can cause severe health problems. The presence of CO molecule in haemoglobin forms carboxyhaemoglobin which decreases the overall capacity of the blood to carry O_2 to the cells. Besides, CO is considered as an indirect greenhouse gas due to its close coupling to atmospheric methane (CH_4), a strong

greenhouse gas whose sole effect is to make the earth warm (Khalil and Rasmussen, 1985). Thus, the regulation of CO from the cooking stoves is essential and this further adds to the motivation to improve the design of the combustion devices.

The existing cooking stoves need improvement in their thermal performance. This is indeed essential to avoid the imminent energy crisis the world is about to face, and the health hazards from the various types of pollutants emitted from cooking stoves. It is to be noted that in India, the share of cooking energy is increasing annually at a rate of 8.1% (Pohekar et al., 2005), and this results in a greater demand for inefficient cooking devices which are fabricated in small-scale industries and marketed all over the country (Thukral and Bhandari, 1994). Thus, looking at the increased share of cooking energy demand, it is necessary to focus on improving the performances of existing cooking stoves so that they can be environment friendly and fuel efficient.

In recent times, a new combustion technology called porous media combustion (PMC) is gaining attention in improving the thermal performances of the existing combustion devices (Mujeebu et al., 2009a). The porous combustor has been identified as an excellent choice to solve the problem of pollutant emissions (Huang et al., 2002). Besides, it offers several other advantages such as fuel flexibility, ability to operate at low equivalence ratio, effective flame speed greater than the laminar flame speeds etc. (Barra et al., 2003). Recently, this concept has been used in many thermal systems like IC engine, water heater, air heater, etc. (Mößbauer, 1999, Delalic et al., 2004, Avdic et al., 2010). In the present work also, this very concept has been utilized in a conventional kerosene pressure stove for its thermal improvement. In the following pages, PMC is briefly described.

1.2 POROUS MEDIA COMBUSTION (PMC)

PMC is a technology which utilizes a novel concept of employing a highly conductive and radiative porous solid medium in the combustion zone of a premixed flame for better heat transport. This technology is significantly different from the conventional combustion technology (CCT) characterized by a free-flame where the combustion takes place in a gaseous environment, and convection remains the dominant mode of heat transfer. In contrast to this, in PMC, the reaction zone remains fully submerged in the inert porous matrix with almost no visible flame at the exit of the burner (Mital et al., 1997). The porous material/media (PM) being highly conducive and emissive, in the PMC, the contributions of conduction and radiation heat transfers are significant. Additionally, due to large internal surface area of the PM, the convective heat transfer is also improved. Thus, in the PMC, the heat transfer process is more efficient and this result in an internally self-organized process of heat recuperation yielding much lower temperature of the combustion zone than that found in the CCT (Weinberg, 1971).

Owing to better conductive, radiative and convective heat transfer, the burner made of PM has several advantages, such as higher radiant output, higher power density, higher power modulation, lower NO_x, etc. (Howell et al., 1996). Besides that, owing to higher effective diffusion and heat transfer between the phases, in porous burner (PB), the combustible mixture stabilizes over a wide range of reactant velocities, air-fuel ratios and heat input (Mujeebu et al., 2009a). Figure 1.1 schematically describes the heat transfer mechanism in a PM constructed with 4 spherical solids where combustion takes places within the pores of the solids. The air-fuel mixture is passed from the bottom of the media which find its way through the convoluted path of the solid porous bed and the exhaust gases are expelled from the top. The reaction zone is stabilized within the porous bed, and

there is a transfer of heat from the reaction zone to the incoming mixture which involves all the three modes, viz., convection, radiation and conduction.

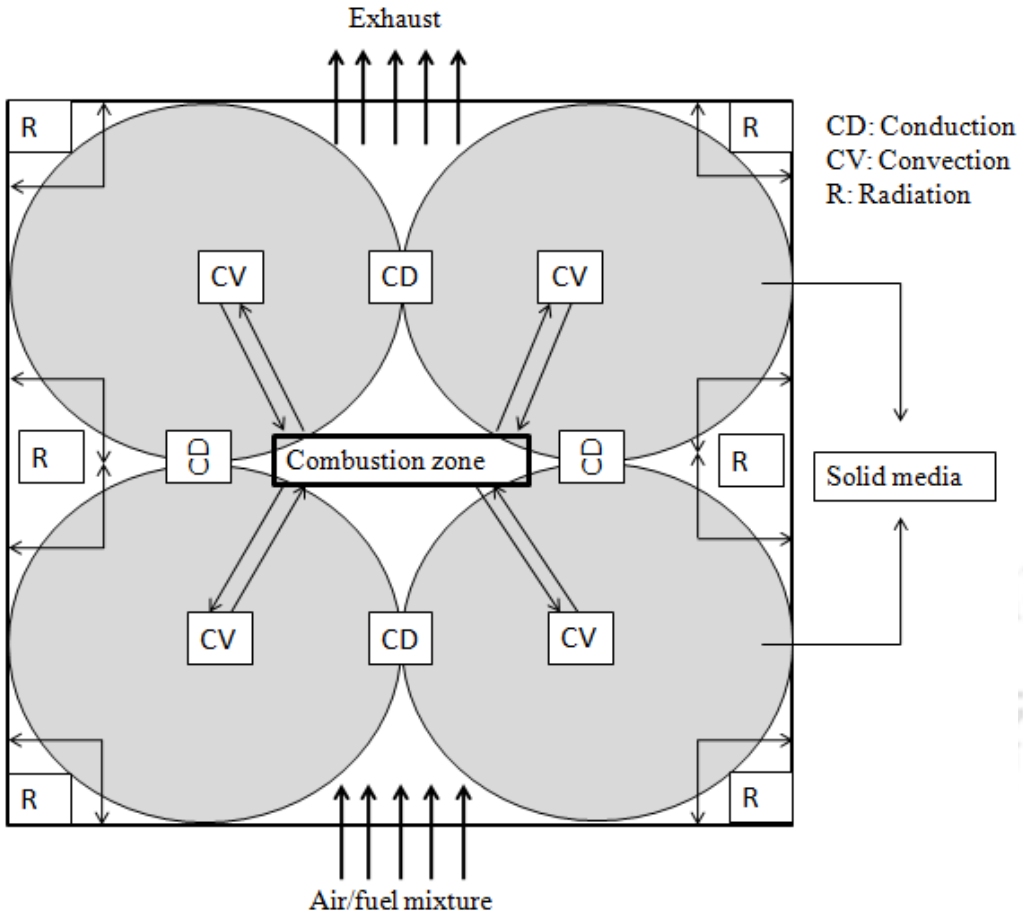

Fig. 1.1: Heat recirculation in a porous burner.

(i) Convection is involved because there is a transfer of heat from the hot combustion products to the porous solids. (ii) Radiation occurs as the porous solid takes up sensible heat of hot gases and becomes incandescent (iii) Likewise, conduction takes place as the solids are interconnected. This self-organized internal heat recirculation makes the PMC technology unique and facilitates preheating of reactants which thereby allows the combustion to start at a relatively low temperature. Preheating offers several advantages such as increase in flammability limit, reduction of CO, increase in burn rate, increase in

flame speed, etc. Unlike this in a conventional burner (CB), because of poor heat conductivity of gases, the chemical reaction occurs in a small region of the combustion chamber leading to the maximum energy release in that region itself, while the rest of the combustion chamber remains unused. Thus, the temperature gradient across the combustion zone of a CB is very steep leading to an increased formation of NO_x.

In recent times, the use of PB has been increasing as it gives the benefits of infrared heating which provides much faster heating as compared to the convective heat transfer alone that relies on the temperature difference between the heated air and the surface of the product (Howell et al., 1996). The rate of heat transfer in an infrared heater is determined by the temperature of the source and the absorption characteristics of the product being heated. The source temperature dominates the performance since the radiation output is proportional to the fourth power of the temperature. The source temperature is dependent on (i) the emissivity of the radiating material, (ii) the rate of energy release of the reactants and, (iii) the heat transfer rates between the hot combustion products and the PM (Howell et al., 1996). High radiation output is found beneficial as it increases the heating rate which is important for thermal process. In recent years, the concept of radiant heating through use of PB has been applied to many thermal systems and the applications vary from industry to households. The following paragraph highlights a few of the applications explored so far.

1.3 APPLICATIONS OF PMC

The applications of PBs are widespread. Wood and Harris (2008) in their review paper on application of PMC technology reported that PBs are already commercially available, and the gas fired PBs are used in a number of manufacturing processes such as paper drying,

paper finishing, powder and paint curing, baking, textile drying, glass and chemical processing, polymer processing, metal heat treating, etc. They are also used in household air and water system, IC engines (pre-heaters of vehicles), gas turbine combustion chamber, steam generator, etc. The domestic cooking applications of the PB are, however, limited, and also not much literature is available on this. Till date, Jugjai and Rungsimuntuchart (2002) and Pantangi (2010) analyzed the combustion behaviour of LPG stoves, while Kakati et al. (2007) studied the performance of the conventional kerosene stove. Pantangi (2010) employed the complete concept of PMC whereby LPG was combusted within the PB. However, Jugjai and Rungsimuntuchart (2002), and Kakati et al. (2007) used the PM as radiant inserts only. They used PM to preheat the incoming air and also to increase the heat transfer from the conventional stove which operates in the convective mode to the cooking vessel. It is to be noted that in all the cases, significant improvements were found over the CBs.

1.4 SCOPE OF THE PRESENT STUDY

The need for development of a low emission and high efficiency cooking stove is strongly felt as there has been a global concern for reduction of pollutants especially from fossil fuel fired devices, and also to conserve energy. In this regard, mostly in other applications (Mößbauer, 1999, Delalic et al., 2004, Qui and Hayden, 2006 and Avdic et al., 2010) and some studies made with cooking stoves (Jugjai and Rungsimuntuchart, 2002, Kakati et al., 2007, Pantangi 2010), the use of the PMC has been promising. In the last decade, several applications of this technology have been reported (Mujeebu, 2009a). However, for domestic cooking applications, no significant development has taken place. In fact, to the best of author's knowledge, such study is limited to just 3 published reports, (Jugjai and Rungsimuntuchart, 2002, Kakati et al., 2007, Pantangi 2010). Out of these, only

Pantangi (2010) employed the complete concept of the PMC in developing PBs for LPG stoves. Jugjai and Rungsimuntuchart (2002) and Kakati et al. (2007) used the PM as radiant inserts only, as in their setups, the combustion did not take place inside the porous matrix but in the gaseous mode as in case of CBs. The results obtained are, however, motivating as there were significant improvements on the performances. Till date, there is no report on kerosene stove working on PB and hence an interesting scope lies to develop the same and evaluate its usability in terms of thermal performance. Besides, there is also a scope to evaluate the performance of the burner from exergy point of view based on the second law of thermodynamics which gives the realistic measure of energy utilization and its losses.

The traditional way of evaluating the performance of a cooking stove is based on their energy efficiency defined as the ratio of output energy to the input energy supplied. However, the true measure of the performance of a thermal system can be obtained only from the exergy efficiency. The exergy efficiency is a useful tool for evaluating the relative performances of different designs. It accounts for the temperatures associated with energy transfer to and from the cooking stove, and it provides a measure of how closely the efficiency of the cooking stove approaches the ideal efficiency.

To estimate the true efficiency, the exergy analysis has been used in other thermal systems including solar cookers (Dincer et al., 2004, Ozturk, 2004, Saidur et al., 2007, Pope et al., 2010). However, in a fuel fired cooking stove, such as LPG and kerosene stoves, this analysis has not been made. When a new stove is developed or an existing one is improved, this exergy analysis is important to identify the sources of irreversibility while transferring energy from a cooking stove to the vessel. Thus, in addition to develop

a PB incorporated kerosene pressure stove and doing its energy analysis according to the first law of thermodynamics, its thermal performance in terms of exergy analysis, is also one of the objectives of the present study. Below the objectives of the present work are outlined.

1.5 OBJECTIVES OF THE PRESENT STUDY

The overall objective of this study is to investigate the usefulness of PB in the conventional kerosene pressure stoves. In a broad sense, considering the scope of the present study the following specific objectives have been set.

1. Development of a PB incorporated kerosene pressure stove.
2. Performance evaluation of the new stove in terms of temperature profiles, thermal efficiency and emissions.
3. Performance evaluation of the new stove in terms of exergy analysis.
4. Comparison of the performance of the new stove with the conventional stove.

1.6 ORGANISATION OF THE THESIS

The thesis has been organized in six chapters. In the second chapter, first a brief history of the kerosene pressure stove is presented. This is followed by a review of the literature dealing with the important aspects of the PMC such as flame stabilization, heat recirculation etc. Next, the investigations on different materials for PB construction are discussed. Finally the reported experimental as well as theoretical investigations related to PMC of liquid fuels are presented. The third chapter contains detailed descriptions of the various experimental tools and the measurement techniques that are relevant for the present work. The formulations used for the calculations of different parameters are also

discussed. In the fourth chapter, the thermal performance of the kerosene stove equipped with PB under different operating conditions is discussed, and the strategy adopted for improvements are highlighted. This is followed by a comparison of the performance of the developed PB with the existing CB. The fifth chapter contains the exergy analysis based on the second law thermodynamics for evaluation of the relative performance of the PB enclosed in different casing geometries. The sixth chapter is the concluding chapter. Therein, the major findings from the current study are summarized first, and then the conclusions and the possible future scope are discussed.

भारतीय प्रौद्योगिकी संस्थान गुवाहाटी
Indian Institute of Technology Guwahati

CHAPTER 2

LITERATURE REVIEW

2.1 INTRODUCTION

The research on PMC started towards the end of 19th century. However, it has started gaining momentum only in the last two decades. In recent times, this technology has shown a promising approach in solving the problems arising on the onset of global concern over climate change, energy security and rising fossil fuel prices. PMC offers several advantages like extension of reaction zone, extension of flammability limit, homogenization of temperature field, reduction of emissions etc (Howell et al., 1996, Mujeebu et al., 2009a). Since the last two decades, this technology has been the subject of interest of many researchers, and as an outcome, it has seen a multifaceted advancement. This chapter basically discusses some of the important research findings of the PMC that are useful in design and development of a new thermal system. The chapter begins with a discussion on the history and working of the conventional kerosene pressure stoves, and this is followed by a brief history of the PMC highlighting the various stages of advancement. Next, the investigations related to various aspects of PMC such as heat recirculation, flame stabilization, excess enthalpy combustion are discussed. Following this, the investigations on materials, their thermo-physical properties and their usability are highlighted, and then some important results on performance characteristics of gaseous fuel-fired PB are presented. This is followed by an introductory discussion on emission of pollutants and their control strategies. Following this, various investigations of liquid fuel combustion within PM are elaborated. The important findings have been highlighted with the clear diagrams of their experimental setups. Finally, with a summary of the available literature, the scope of the present study has been presented.

2.2 HISTORY OF KEROSENE PRESSURE STOVE

The first kerosene pressure stove was developed in 1892 by a Swedish person named Frans Wilhelm Lidqvist (Primus stove, Wikipedia, 2010). The stove was known as the primus stove. This stove has gained popularity since its early days, as it was found reliable and durable in everyday use and also under adverse conditions. In yesteryears, a number of similarly-designed stoves of different models and sizes were built and commercialized. The modern kerosene pressure stoves are basically the modified version of the primus stove.

The first model of the primus stove (Figure 2.1) consisted of a fuel tank with a hand operated plunger, a spirit cup and a burner. A steel ring was provided on the top of the burner for supporting cooking vessel.

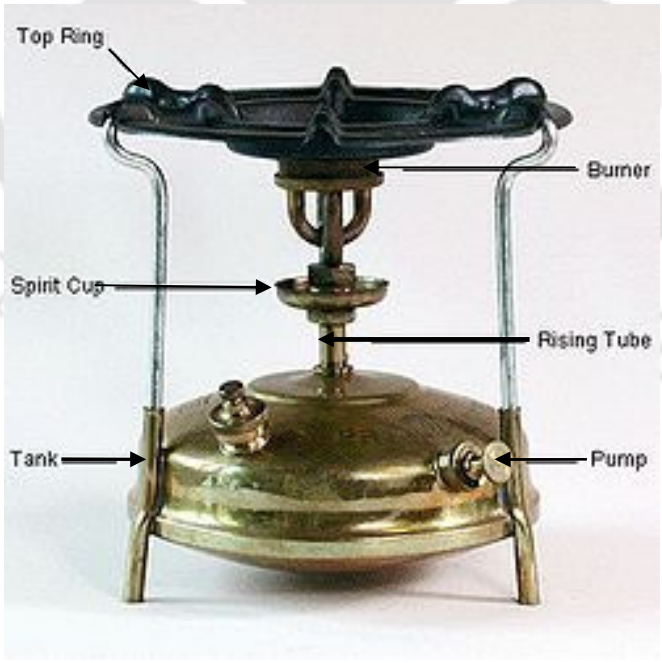

Fig. 2.1: Picture of a primus stove and its various components (Primus stove, Wikipedia, 2010).

In primus stove (Figure 2.1), the burner is an assembly of two ascending and two descending tubes with a flat circular chamber at the top called burner head. The lower portions of the ascending tubes are connected to another tube called rising tube which on the other end is connected to the pressure tank. A spray nozzle is provided in between the two descending tubes. Figure 2.2 shows the schematic of the burner assembly.

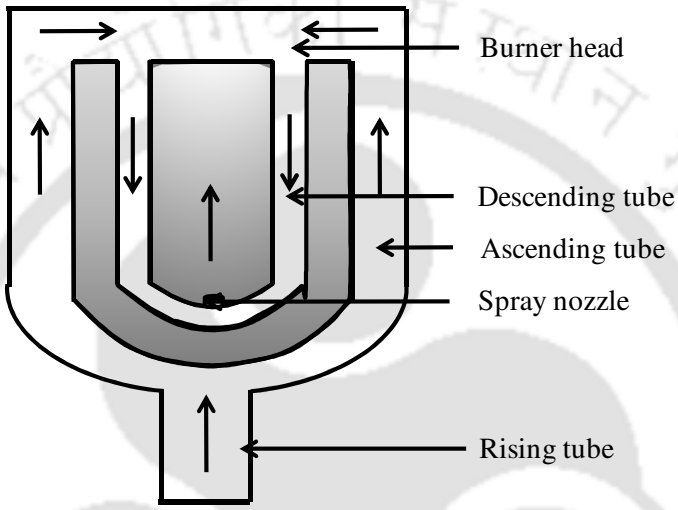

Fig. 2.2: Schematic of the primus stove burner (Primus stove, Wikipedia, 2010).

The operation of the stove is as follows. Initially, a small amount of alcohol poured in the spirit cup, provided in between the rising tube and the ascending and descending tubes, is ignited with the help of a burning wick. Once heated, the fuel tank is pressurized by means of the hand operated plunger and the pressure forces kerosene from the tank up through the rising tube and the ascending tubes to the pre-heated burner head. The burner head receives heat from the spirit cup through convection and the kerosene receives heat from it on its way through the ascending tubes and gets converted to vapour. The kerosene vapour is then forced under pressure through the descending tubes and is sprayed through the nozzle, where it mixes with air and burns. The burner head then

receives heat from the kerosene/air flame and the alcohol flame at the spirit cup is put off. Thus, the vaporization and combustion cycle continues during the cooking process.

The basic designs of the modern primus-style stoves are same as the older version. They are operated in a similar way. However, there are constructional differences between the earlier and the latter versions. Figure 2.3 shows the schematic of a kerosene pressure stove available these days in the market. In this, the fuel tank is not just below the burner but little away. For easy cleaning, the tank is made detachable. The dimensions of the burners are also different; the new burner is well optimised for higher thermal efficiency.

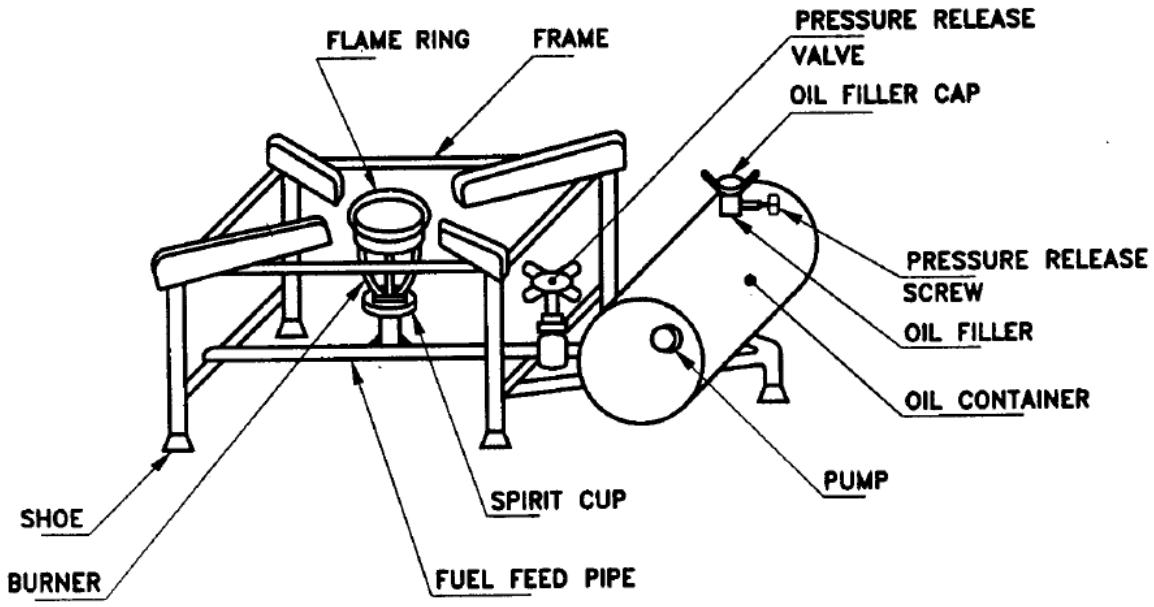

Fig. 2.3: Schematic of a BIS specified kerosene pressure stove (IS: 10109, 2002).

Prior to the invention of the primus stove, the kerosene stoves were constructed in the same manner as the oil lamps, which use a wick to draw fuel from the tank to the burner. Those stoves known as wick stoves are still very popular due to its easy construction and low initial cost. But these stoves produce a great deal of soot due to incomplete

combustion. The primus stove's design, which uses pressure and heat to vaporize kerosene before ignition, results in efficient combustion, resulting relatively lower emissions of CO. The reports on emission measurement of the primus stove are, however, limited, although there have been ample reports on efficiency measurements (Thukral and Bhandari, 1994, Jungbluth et al. 1997, Pohekar et al. 2005). In the Indian context, emission characteristics of the primus stove have been reported by Zhang et al., (1999), Smith et al., (2000) and Kakati et al., (2007).

Zhang et al. (1999) measured the CO from different kinds of stoves available in the Indian market, and they found that the CO emissions from the kerosene stoves are higher than the LPG stoves. They also found that the CO exposure is higher than the exposure equivalents of health-based national standards and WHO guidelines. Kakati et al. (2007) examined the CO emission characteristics of a conventional BIS pressure stove and also of a stove incorporated with a PM. They found that the PM incorporated stove exhibited better thermal performance over the conventional counterpart due to improved heat transfer. In recent times, the use of PM has been prevalent in many other thermal systems as outlined in Chapter 1. The subsequent paragraphs report the various findings of PMC.

2.3 EARLY HISTORY OF PMC

PMC is a two-century old technology. Its first research activity started in the beginning of the 19th century. Many scientists, mostly from the USA, Germany, Great Britain and Russia, tried to explain its physics and they provided methods to regulate the combustion process (Avdic, 2004). Their major challenge lied in stabilizing the flame as there was difficulty in having smooth thermal performances, avoiding flash-back or blow off. In course of time, however, many solutions were conceived and successfully implemented;

even then, somehow the technology did not attain the state of commercialization and was eventually forgotten. A continued exploration for its applications has started only in the last two decades (Kaplan, 1995, Mößbauer, 1999).

In the first quarter of the 19th century, Sir Humphry Davy (Jarosinski and Veyssiere, 2009) postulated an important concept which states that below a certain radius of pores in a PM the combustion cannot occur. He termed the minimum pore radius supporting combustion as the "quenching radius". This finding was important and laid the foundation for flameless combustion which in the recent times has gained popularity due to its intrinsic characteristics of low emission of pollutants.

Following the findings of Davy, a number of researchers have come up with new kinds of burners made of PM. A few among them which have been given in the recent review article by Mujeebu et al., (2009a) are: Krause, Welch, Mitchell, Ruby, Schnabel, Bone, Lucke and Hays. They built burners for different applications such as steam generators, radiant room heaters, crucible furnaces etc.

The path breaking invention in the field of PMC is the concept given by Smith (Avdic, 2004). He invented a device and showed that the stabilization of a reaction zone in a PB is possible through use of a structure composed of corrugated sheets which contact each other only at their ridges. He reported that for making corrugated sheets, sintered ceramic materials such as alumina (Al_2O_3), silicon carbide (SiC), beryllia (BeO), titania (TiO_2), zirconia (ZrO_2) and petalite and metal powders such as tungsten, molybdenum and tantalum are useful. Following these early findings, many different versions of the PBs have been developed.

2.4 RECENT ADVANCEMENTS IN PMC

In the recent years, the interest in PMC has revived owing to strict legislation on environmental protection and conservation of fuel. The research in PMC has now found different dimensions. Many new burners have been developed for different applications. Different materials have been explored. The flame stabilization, heat recirculation processes have been adequately studied. Experimental as well as numerical studies have been undertaken to understand the combustion behaviour of different kinds of fuels within PM. In the following pages, some of the important aspects of the PMC are briefly discussed.

2.4.1 Heat recirculation

In a combustion device, heat recirculation is a desirable feature. It raises the temperature of the reactants which yields high reaction rate and high thermodynamic efficiencies (Barra and Ellzey, 2004). It is Weinberg (1971) who discussed the benefits of recirculation, and he suggested that this can be better achieved using the heat exchanges rather than recirculating hot combustion products into the reactants. Following his idea, Takeno and Sato (1979) proposed the innovative way of recirculating heat from downstream of the flame to the upstream of the burner through insertion of a porous, highly conductive solid material in the flame. With combustion in a porous matrix, the recirculation is accomplished through solid conduction and solid-to-solid radiation and thus, the greater temperature differential between the hot solid and gas results in an increased solid-to-gas convection, resulting preheating of the reactants.

Barra and Ellzey (2004) numerically analyzed the heat recirculation using a one-dimensional time dependent formulation with complete chemistry. They found that the

degree of heat recirculation increased with the thermal conductivity or convective heat transfer coefficient. They obtained the temperature profiles and heat release rate of a PB and compared the same with the results Mallard and Le Chatelier (Glassman, 1996) who had studied a laminar premixed flame. They reported that in a PB the flame structure was different from that of the conventional flame. The preheat zone in the PB was found much wider in comparison to the freely propagating laminar premixed flame. The stable operating range was also higher for the material with high thermal conductivity and large heat transfer coefficient. They also confirmed that there is an optimum value for the radiative extinction coefficient. Inappropriate value results in spreading of the radiation confined to either too small area or too large area. They quantified the heat recirculation in terms of heat recirculation efficiency which is the ratio of the amount of solid-to-gas convection in the preheat zone to the firing rate. Figure 2.4 shows the variation of heat recirculation efficiency as a function of the flame speed ratio (defined as the ratio of effective flame speed to the laminar flame speed) for a range of equivalence ratios (ϕ), defined as the ratio of stoichiometric air fuel mixture to the actual air fuel mixture.

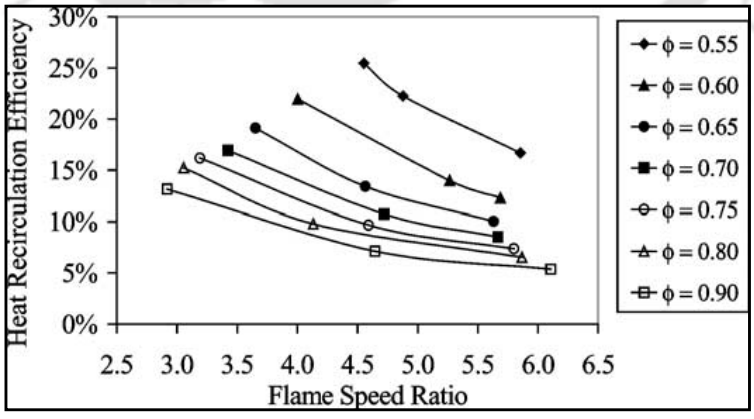

Fig. 2.4: Heat recirculation efficiency as a function of flame speed ratio for a range of equivalence ratios (Barra and Ellzey, 2004). (Figure reproduced with copyright permission, licence number: 2572880696508).

The effective flame speed is the interstitial velocity of the gas in the PM that results in a stable flame. It is evident from Figure 2.4 that the flame speed ratio increases with decrease in equivalence ratio (ϕ). For a given equivalence ratio (ϕ), heat recirculation efficiency decreases with increase in the flame speed ratio. At an equivalence ratio (ϕ) of 0.55, 16-26% of the heat is recirculated to the preheat zone, whereas at an equivalence ratio (ϕ) of 0.90, only 5 to 13% of the heat is recirculated.

Barra and Ellzey (2004) also examined the relative contributions of conduction and radiation to the recirculation process. Figures 2.5 (a)-(c) show the variation of various efficiencies, viz., heat recirculation, preheat conduction and preheat radiation with flame speeds for three different equivalence ratios (ϕ), i.e, 0.55, 0.65 and 0.90. It is observed that at the lowest equivalence ratio investigated (ϕ = 0.55), conduction is more than radiation at lower flow velocities or flame speed ratios. However, at higher velocities, radiation is dominant. This is due to the fact that at lower velocity, flames stabilize further upstream, and in this case, conduction is more important in upstream since the conductivity of the upstream is more than that of the downstream. At a fixed equivalence ratio (ϕ), the preheat and the radiant efficiency, are relatively constant over the stable operating range. As the equivalence ratio (ϕ) increases, conduction becomes less important and eventually radiation becomes the dominant mechanism due to higher temperatures in the reaction zone. These findings of Barra and Ellzey (2004) were in line with the results of Min and Shin (1991) who used a one-dimensional model that considered all three modes of heat transfer with single step combustion chemistry. They predicted that 28% of the total heat released would be recirculated to the incoming reactants, and that the contributions of conduction and radiation were approximately equivalent in magnitude (at ϕ =0.55).

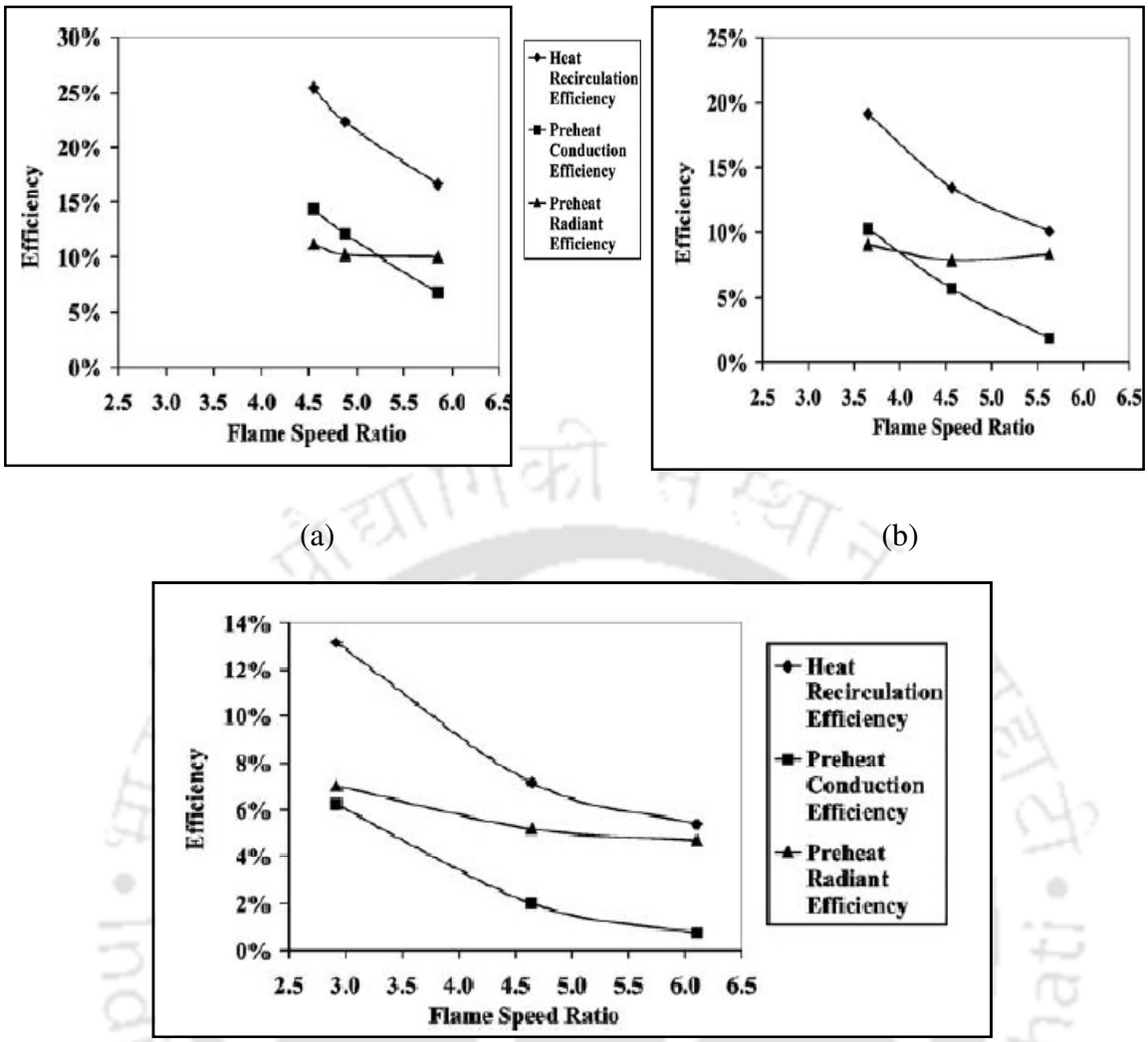

Fig. 2.5: Heat recirculation processes (a) ϕ=0.55, (b) ϕ =0.65 and (c) ϕ =0.90 (Barra and Ellzey, 2004). (Figure reproduced with copyright permission, licence number: 2572880696508).

From the above findings it is found that the heat recirculation is dependent on both conductive and radiative heat transfer and the magnitudes of heat transfer by conduction and radiation will be dependent on materials of the PM. Thus, the proper selection of a PM supporting effective heat recirculation results is important. Also, heat recirculation, gives rise to additional energy called excess enthalpy and the pertinent process is known as the excess enthalpy combustion. The following section briefly describes this concept.

2.4.2 Excess enthalpy combustion

The excess enthalpy combustion is one of the interesting characteristics of the PMC which indicates that the peak flame temperature is higher than the corresponding adiabatic flame temperature. The adiabatic flame temperature for a laminar premixed flame is defined as the theoretical temperature obtained if all the heat released by the reaction is used to raise the temperature of the combustion products (Glassman, 1996).Thus, the adiabatic flame temperature is the maximum possible temperature that can be obtained. However, Weinberg (1971) theoretically proved that it is possible to obtain the flame temperatures in excess of the adiabatic flame temperature through recirculation of heat from the hot combustion products to the cold reactants, without diluting the reactants.

The term excess enthalpy refers to the process of 'borrowing' enthalpy from the combustion products to preheat the incoming reactants (Hardesty and Weinberg, 1974). Takeno and Sato (1979) used a one-dimensional model to study the effects of mass flow rate and heat transfer coefficient on flame characteristics in excess enthalpy flames. They reported that by insertion of higher thermal conductivity solid in the flame zone, the heat transfer efficiency increases and the flame moves upstream. Thus, the maximum temperature decreases, and the reaction zone widens. With increase in mass flow rate, the reaction zone becomes narrower, the flame moves downstream, and the maximum temperature increases. However, the flame stabilization is possible for a wide of range of flow rates. They described this in the following manner: if for momentary increase in flow rate, the flame moves downstream, unreacted mixture is exposed to higher temperature solid which transfer heat to the gas causing increasing the flame speed and this brings back the flame to upstream and vice versa.

In PMC, this desirable heat is recirculated by thermal radiation and conduction to preheat the unburnt mixture upstream of the reaction zone. Preheating offers several advantages, such as higher laminar flame speed, higher burn rate, lower CO emission, extended flammability limit' etc., thus, in the recent times, this concept has attracted attention (Natarajan et al., 2009). It has been identified as one of the most practical and effective means of saving energy. Many researchers have studied the effect of preheating on burning characteristics of laminar premixed flame. External preheating, is, however, somewhat different from the internal heat recirculation because external preheating increases the energy input to the burner (Barra and Ellzey, 2004). Nonetheless, for the sake of comparison, numerical studies (Barra and Ellzey (2004)) have been made for a premixed flame with different unburnt mixture temperatures. Barra and Ellzey (2004) also did this study to know the laminar flame speed in a PB. They studied a premixed flame with PREMIX code (Kee et al., 1985) and compared their results of laminar flame speed with the flame speed as obtained in the PMC. At an equivalence ratio (ϕ) of 0.65, the flame speed ratio was found to be 4, and the laminar flame speed was 15.5 cm/s, meaning that the effective flame speed in the PB to be $62\,{}^{\mathrm{cm}}\!/_{\mathrm{s}}\,(=15.5\times4)$. In a premixed flame, this value corresponds to the temperature of 550 K of the unburnt mixture.

For a better understanding of the effect of preheating on burning characteristics, a similar work was undertaken by Sharma et al. (2010a, 2010b). This includes the calculations of laminar flame speeds of methane and propane at different unburnt temperatures and equivalence ratios (ϕ). Methane was chosen because it is the building block of all the fuel (Warnatz et al., 2001) and propane represents the higher hydrocarbons (Mishra et al., 2006). The reaction mechanisms used for simulations of methane/air and propane/air flames were GRI-Mech 3.0 and Dagaut respectively. The GRI-Mech 3.0 mechanism

consists of 53 species and the Dagaut contains 91 species. The reactions considered in GRI Mech-3.0 and Dagaut were 325 and 704, respectively. The simulation was done for an unburnt temperature in the range of 300-700 K for the methane/air flame and 300-800 K for the propane/air flame. The equivalence ratio (ϕ) was varied from 0.6 to 1.4, for the unburnt temperature 300 K. For the higher unburnt temperature, the simulation was extended to lower equivalence ratio (ϕ), since preheating extends the stability limit, supporting stable combustion even at leaner conditions. Results are presented in Annexure A. The following subsection describes the flame stabilization process in a PB.

2.4.3 Flame stabilization

Flame stabilization in a PB is a critical issue, since in order to stabilize the combustion process within a PM, a balance must be achieved between heat recirculation, heat release and heat losses, such that the effective flame speed is equal to the incoming flow velocity. When the flow velocity is more than the flame speed, the flame propagates downstream, resulting in blow off, and if it is contrary, flashback results. It is difficult to predict a priori whether for a given air/fuel mixture, the flame will stabilize or not, and if stabilized, at what position the flame will actually be located. Flame location depends on various parameters, such as the flow velocity, the heat transfer coefficient, the thermal properties of the PM, etc. (Kamal and Mohamad, 2006).

Buckmaster and Takeno (1981) provided an intuitive explanation on the flame stabilization process, thereby defining the conditions for blow-off and flashback. They reported that in response to any change in inlet conditions, for instance, if the flow velocity is increased, the flame moves downstream. However, if this movement causes an increase in flame speed, the flame will eventually search for a new location where the

flame speed again matches the flow velocity, and it will stabilize in that location only. The requisite increase in flame speed will occur due to the incoming gases being preheated more effectively. In general, as the flame moves downstream, the amount of preheating will increase (as less heat will be lost from the upstream end of the burner). Thus, the flame location and upstream internal heat recirculation are mutually related and this makes the process more complex. A few of the findings on flame stabilization are summarized below.

Sathe et al. (1990) used a conduction, convection, radiation and combustion model and studied the flame stabilization process in a PB. They studied the dependence of various parameters such as the flame location, the radiative properties of the PM, the solid thermal conductivity, the stoichiometry on the flame speed and the stability. It was observed that the flame propagation near the edge of the porous layer was controlled mostly by solid-phase conduction. In the interior, both solid conduction and radiation heal transfer were important.

Malico and Pereira (1999) reported that with decrease in fuel concentration, flame moves downstream. Decrease in equivalence ratio (ϕ) results in a corresponding decrease in the flame speed, and thus, in order to match the flow velocity, the flame moves to a new downstream location.

Trimis and Durst (1996) proposed an interesting concept of stabilizing the flame over a wider range of operating conditions by employing a bi-layered design whereby different PM are used in the upstream and downstream regions. They reported that with the use of

a small-pored material in the upstream, and a large-pored material in the downstream section, the flame stabilizes in the downstream section at or near the interface.

The critical pore size of the PM is the most important criterion which determines whether a combustion process takes place inside a PM or not. If the size of the pores is smaller than the critical dimension, flame propagation is prohibited and the flame is quenched. This is because, in this case, the magnitude the heat release rate is less than the rate of heat dissipation through pores. On the other hand, if the pore size exceeds the critical dimension, the free ignition takes place and the flame propagates within the porous structure.

Babkin et al. (1991) dealt with the physics of flame propagation velocities of methane/air and propane/air mixtures within PM. They identified five steady-state regimes for gas combustion in an inert PM and also explained the phenomenon of flame quenching within the PM. This was important for defining the stable velocity of flame propagation and thus stable combustion. Besides, they also identified the criterion of the Peclet number (ratio of heat flow by transport to heat flow by conduction) which is an important concept closely associated with prevention of flash-back. They reported that there is a supercritical Peclet number (Pe) for flame development corresponding to the porosity at which ignition can take place. The proposed limiting condition for the flame propagation is given by

$$Pe \geq 65$$

where

$$Pe = \frac{S_L d_m c_p \rho}{k}$$

where S_L is the laminar flame speed, d_m is the mean pore diameter, c_p is the specific heat, ρ is the density and k is the thermal conductivity of air-fuel mixture. If $Pe \leq 65$, then the flame quenches (extinguishes), since heat is transferred to the porous matrix at a higher rate than it is produced. However, this critical value of the Peclet number (Pe) might be different for the different fuels. Dilon (1999) found the same as 37 in case of hydrogen/air combustion against the 65 for methane/air flame.

Using the concept of Babkin et al. (1991), Trimis and Durst (1996) developed a bi-layerd PB which could be operated with stable combustion over a wide thermal power range (20:1) without flash-back. They adopted a new technique to control the flame stabilization by changing the porosity (defined as the ratio of free volume of pores to PM volume) of the material along the combustion chamber in such a way that the pore size increased from inlet to the outlet in the direction of flow of the gas/air mixture. A steep gradient in the pores sizes results in stabilization of the flame in that region. Thus, the basis of the bi-layered PB lies on stabilization of the combustion process within PM through sudden change of pore size.

2.4.4 Bi-layered PB

A bi-layered PB is characterised by two distinct zones, viz., preheating and combustion zones. The thumb rule for designing a bi-layered PB is that the preheating zone should consist of less porous and less conducting materials, while the combustion zone should be highly conductive and porous in nature. The reason for choosing materials with two different thermo-physical properties is to support stable combustion, thereby avoiding combustion in the preheating zone. By proper selection of PM for the two zones, the combustion reaction can be initiated at the interface of the two zones and made to occur

over the entire volume of the combustion zone. Besides, flashback can be avoided as the local quenching of flame occurs owing to sudden change in pore size at the interface of the two media. Thus, the preheating zone of a bi-layered PB can be defined as a flashback arrestor or flame support layer. Figure 2.6 presents the schematic of a bi-layered PB in which air/fuel mixture enters from the bottom and exhaust gases come out from the burner top. The flame stabilizes at the interface due to change in porosities of the two zone viz., preheat and combustion zones. The preheat zone is the small pore region and the combustion zone is the large pore region. Heat is shown to recirculate from the downstream to the upstream through conduction, convection and radiation.

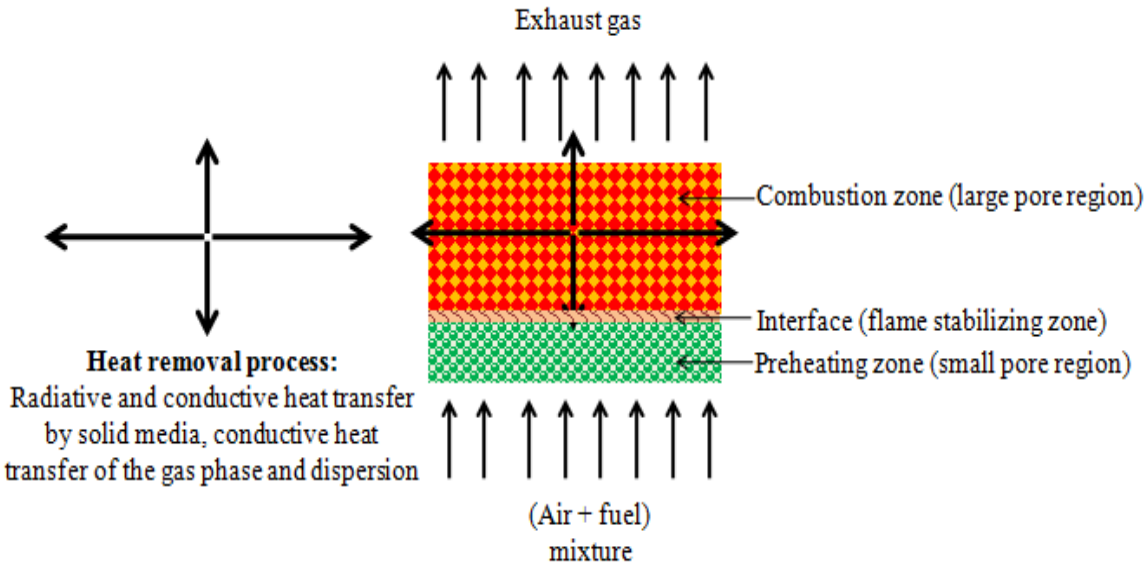

Fig. 2.6: Schematic of heat transfer mechanism in a bi-layered PB.

Generally, in the preheating zone, materials with pore sizes of the order of 1mm or less are used. Mathis and Ellzey (2003) tested two different thicknesses (2.5 and 5.1 cm) of preheating zones. They found that with the thicker preheating zone, the minimum stable firing rate was extended. Thus, the thickness of the preheating zone is important as it influences the burner performance.

Barra and Ellzey (2004) modelled the effects of the heat transport properties of the preheating zone in a bi-layered burner at an equivalence ratio (ϕ) of 0.65 and they found that a low thermal conductivity and convective heat transfer coefficient resulted in the largest stable operating range. They also reported that it was the properties of the preheat zone (upstream section) that significantly determined the minimum achievable flow velocity.

It is to be noted that the bi-layered design is not always employed either to act as flame holder or flashback arrestor. Some investigations have shown that the flame will propagate away from the interface, i.e, the combustion process establishes in some downstream location, when the flow velocity is increased or the equivalence ratio (ϕ) is decreased. Conversely, there are reports of the flame propagating into, and sometimes stabilizing within, the preheating region (Wood and Harris, 2008). Thus, depending upon the thermo-physical properties, in bi-layered PB also, combustion can occur in the preheating zone. Hsu et al. (1993) investigated the effect of pore size on the stable operating range of a bi-layered burner having three different pore densities (4, 12 and 18 ppcm) and reported that the largest pore size (4 ppcm) was the most effective in extending the lean limit. However, reduction of heat loss in the upstream, i.e., through the pre-heating zone is desirable. The next section discusses the materials that are used in PB and their thermo physic properties.

2.5 MATERIALS FOR PMC

In PMC, the selection of appropriate materials is important as heat recirculation is highly dependent on the properties of the solid materials being used. It is important to have the material capable of withstanding high operating temperature and having resistance to

oxidative or reductive atmospheres. For better durability, high thermal resistance and good mechanical strength under high temperature are also important. It should have low thermal expansion and high resistance to thermal shock. A high porosity and permeability are desirable in order to minimize the pressure drop across the burner, as well as to decrease the time required to preheat the porous bed during the start-up phase. Table 2.1 includes the some of the important parameters and features of the PM, reviewed by Weclas (2006) for design of PB. There are some features that are directly related to heat transfer and combustion process, while some are application specific.

The features that are directly related to the heat transfer and combustion process are specific surface area, heat capacity and transparency for fluid flow and flame propagation and heat transport properties viz., thermal conductivity, convective heat transfer coefficient, emissivity and optical thickness (or the radiative extinction coefficient,) etc (Weclas., 2006). Optical thickness affects the radiative heat transfer, contact surfaces affect the conductive heat transfer, and porosity, pore size, internal surface area and flow pattern influence the convective heat transport. The features that are directly related to the heat transfer and combustion process are specific surface area, heat capacity and transparency for fluid flow and flame propagation and heat transport properties viz., thermal conductivity, convective heat transfer coefficient, emissivity and optical thickness (or the radiative extinction coefficient,) etc. Optical thickness affects the radiative heat transfer, contact surfaces affect the conductive heat transfer, and porosity, pore size, internal surface area and flow pattern influence the convective heat transport. Form of the porous structure also affects the heat transport properties of solid materials. It is important to have the knowledge of form of the structures as they have strong influence on the overall heat transport properties.

Table 2.1: Basic requirements of porous materials (Weclas, 2006)

Parameters	:	Features
Specific surface area	:	Large (10^2-10^4/m^2): Permits enlargement of reaction zone owing to an effective heat transport between the gas phase and the solid-phase.
Heat transport properties	:	Excellent: High conductivity and good radiative properties of the PM allow better combustion and strong cooling of reaction zone which lowers formation of thermal NO_x.
Heat capacity	:	Large: Permits fast vaporization of liquid fuel and complete combustion.
Permeability to flow and flame propagation	:	High porosity: Large porosity provides transparency to gas, liquid flow and flame and this in turn permits low pressure losses in fluid (gas) flow. Preferable range of porosity should be 80-90%.
Pores size and size distribution	:	Typical pore density from 8-30 ppi.
Pore shape	:	Principally all available shapes are suitable.
Thermal shock and corrosion resistance	:	High.
Mechanical stability	:	Important under high temperature and pressure conditions.

2.5.1 Form of porous structure

Based on the form of the structure, PM are generally divided into 3 different types, viz., foams, packed beds and lamella. Foams are honeycomb type structure with non-uniform spherical-like cells connected to each other by ligaments, while packed bed are made of discite particles, and the lammela are gill-shaped structure with fine sheets of material

held adjacent to one another A brief description on each types structure as described in the review paper by Wood and Harris (2008) is presented below.

2.5.1.1Foams

Foams are the structures having open pores and made up of an interconnected passage of dodecahedral-like cells, with solid struts forming the cell edges (Figure 2.7 (a)). They are reticulated type and usually described in terms of volumetric porosity or as linear pore density (number of pores per centimetre or inch), defined as ppcm or ppi. The materials used for construction of foams are either metallic or ceramic. Typically foams have porosities in the range 70-90% and pore densities in the range 2-25 ppcm.

In PMC, they are found beneficial as they offer better radiative and conductive heat transports, and also exhibit good convective heat transport due to their large internal surface area. Besides, on account of large porosity, the pressure drop of air-fuel mixture is relatively low. They are light in weight and have good thermal resistance, high surface area to volume ratio, high stiffness to weight ratio and high thermal shock resistance. The only disadvantage with the foams is their short durability caused by the stresses of differential expansion experienced during start-up and shutdown (Howell, 1996).

2.5.1.2Packed beds

The next form of porous structure is the packed beds (Figure 2.7 (b)). They are made of discrete particles and are commonly used as an alternative to foams. Unlike foams, they have the advantage of increased durability as the particles are small and robust, and are

not constrained in a rigid matrix. However, they have relatively low porosities: in the range 30-50%, depending on bed size.

2.5.1.3Lamellae

The second alternative of reticulated foams is the lamella form (Figure 2.7 (c)). This structure is found in static mixers which are composed of several perforated ceramic sheets arranged side by side and twisted with respect to one another. These structures have a very high porosity of over 95%, and consequently, they offer a very low pressure drop and have a short start-up phase. They have good mechanical stability, thermal shock resistance and good convective and radiative heat transfer. However, the conductive heat transport is poor.

(a) (b) (c)

Fig. 2.7: Pictures of different forms of porous media (a) reticulated foam (b) packed bed of alumina sphere (c) lamella: static mixture

Having briefly reviewed the different form of porous structure, in the following pages, the types of porous materials are discussed.

2.5.2. Types of material

In the last decade, a few researchers (Mößbauer et al., 1999, Pickenäcker et al., 1999, Trmis and Durst, 1996) have identified some of the materials for construction of PB and they are: metal balls, metal foils, wires, pebbles to ceramic foams, ceramic pebbles, tiles etc. The research in the PMC started with metal balls. However, owing to higher melting temperature, oxidation resistance and superior creep resistance, ceramic foams have been found to yield better performance over metal balls. Metals are thermally unstable and they have poor response time because they have a high thermal mass per unit volume. The following paragarphs discuss the properties of ceramic and metals.

2.5.2.1 Ceramics

Ceramics are generally reticulated type (Figure 2.7(a)). However, they can also be in the form of packed bed and lamella (Figure 2.7(b) and Figure 2.7 (c)). A brief description of ceramic foam manufacturing process is presented in Annexure B.

Compraed to other materials ceramics are more prefferd as they can withstand very high temperatures and are chemically stable and resistant to erosion and wear. The most commonly used high temperature ceramics are alumina (Al_2O_3), silicon carbide (SiC) and zirconia (ZrO_2). Table 2.2 summarizes the relevant thermo-physical properties of these materials.

SiC is available either in reticulated foam or in packed beds. The reticulated one is the most common form. Compared to Al_2O_3, SiC has higher thermal conductivity, emissivity thermal shock resistance and mechanical strenghth. However the coefficient of thermal

expansion and the maximum usage temperature are lower than ZrO_2 and Al_2O_3. Xiong et al. (1995) reported that SiC provides more effective heat recirculation than Al_2O_3 and with SiC the combustion can be stabilized over a wider range of fuel concentrations. This is possible due to higher emissivity of SiC.

Table 2.2: Properties of ceramic materials usable for porous burner (Pickenäcker et al., 1999)

Material	Maximum allowable temperature in air (^oC)	Thermal expansion coefficient (20-1000 ^oC)	Thermal conductivity (1000^oC) (W/mK)	Total emissivity at 2000K
SiC	1600	4-5	20-50	0.9
ZrO_2	1800	10-13	2-4	0.31
Al_2O_3	1900	8	5-6	0.28

Al_2O_3 is employed either in a packed bed or as a lamella. Its uses are wide on account of high temperature and corrosion resistance. It is economical too. It has a moderate thermal conductivity and emissivity. However, the coefficient of thermal expansion is large and it has a poor thermal shock resistance.

ZrO_2 based ceramics generally have a very high application temperature but a low thermal conductivity, high coefficient of thermal expansion, and moderate thermal shock resistance and emissivity. Pure ZrO_2 undergoes a destructive phase change from tetragonal to monoclinic when cooled from the sintering temperature, and must be stabilised against this by the use of additives such as magnesia, yttria, calcium oxide or ceria (Wood and Harris, 2008). The resulting stabilized or partially stabilized ZrO_2 will typically have a lower application temperature (~1800 ^oC) than the pure solid. Other high

temperature ceramics previously employed in PB include lithium aluminium silicate (LAS) (Sathe et al., 1990), cordierite (Mital et al., 1997), silicon nitride (SiN) and mullite (Meng et al., 1991).

2.5.2.2 Metals and Alloys

The most commonly used material for metal burners is stainless steel (SS). It is generally used in the form of a mat composed of woven metal fibers. Packed beds with solid sphere are another common form. Metals have a short start-up phase, excellent radiation heat transport properties as well as a very low pressure drop. However, they show poor conduction heat transport and dispersion properties, due to their high porosity. Alloys can, however, be a good alternative of ceramic. Iron-chromium-aluminum alloy and nickel-base alloys are designed for oxidation resistance and high temperature use, up to 1400 ^{o}C. They are highly conductive in nature and have good resistance to thermal shock.

2.5.2.3 Carbon–carbon composites

Carbon-carbon (C-C) composite materials (carbon fibre reinforcement in a graphite matrix) are another alternative to reticulated foams. The strength of C-C composites with unidirectional reinforcement fibres is up to 700 MPa. C-C composites have excellent thermal shock resistance and thermal conductivity. Nevertheless, they have a major disadvantage that they oxidise rapidly at temperatures above 500 ^{o}C. This can however, be overcome by giving a protective coating of some materials like SiC, rhenium, hafnium, iridium etc. over the composite.

Having studied, the types and forms of material, next, a very brief discussion is presented on shape and orientation of combustion chamber in which PM are enclosed.

2.5.3 Shape and orientation of combustion chamber

The most commonly used configuration of the combustion chamber is the cylindrical type oriented vertically in which fuel/air mixture flows upwards or downwards through the porous bed (Kaplan, 1995, Takami et al., 1998, Jugjai et al., 2002,). The literature on usage of horizontally oriented burners are limited. Many researchers (Rumminger et al., 1996, Xiong et al., 1995, Brenner et al. 2000) used square or rectangular cross-sectional geometries. Trimis and Durst (1996) suggest that if the combustion chamber were surrounded by a heat exchanger for some applications, a rectangular design might be preferable, as in this case, the axial dimension (thickness) could then be kept reasonably small. Mößbauer et al. (1999) reported that a PB with a ring-shaped cross-section could also be designed as a burner. However, the shape of the cross-section of combustion chamber does not have much effect on the burner performance (Wood and Harris, 2008).

2.6 BURNER PERFORMANCE-GASEOUS FUELS

From the discussions presented in the previous section on PM, it is clear that the thermal and radiative properties of the PM viz., thermal conductivity, convective heat transfer coefficient, emissivity and optical thickness (or the radiative extinction coefficient), etc., have significant influence on the burner performance. Pore size (or the pore density) also influences the combustion process via its effect on heat transport. Typically, small-pored materials exhibit good conductive (more solid contact surfaces) and convective (larger internal surface area) but poor radiative (low optical thickness) heat transfer and vice versa. Furthermore, the pore size and geometry also influence the additional heat transfer i.e., the heat transfer through the thermal dispersion effects (Wood and Harris, 2008). In recent years there have been ample research on the performance of PB fired with gaseous

fuels in PM having different thermo-physical properties (Sathe et al., 1990, Leonardi et al., 2002, Barra and Ellzey, 2004).

Leonardi et al., 2002 measured the radiation and convection efficiencies of a burner made of woven metal alloy fibre pads (Fecralloy), firing methane-air, for a wide range of firing rates and equivalence ratios (ϕ). They found that the burner with thicker flame support pad (double Fecralloy layer) resulted in higher radiation efficiencies than the pad of single layer. It was also found that at higher firing firing rates, the radiation efficiencies (ratio of radiant output to total heat of reaction) remained constant in (18-26%). For radiant burner, radiant efficiency is one of the most important thermal performances (Qiu and Hayden, 2006). The radiant efficiecny increases with increase in heat recuperation.

Sathe et al. (1990) numerically studied the performance characteristics of porous radiant burner burning methane-air flame and reported they are affected by the solid phase conduction and scattering. For higher radiant efficiency, solids having low thermal conductivity and scattering albedo are desirable. With decrease in albedo, the radiation output also increases. Tong et al. (1990) studied the performance of porous radiant burner as a function of fire size. They found that the smaller fibre diameters resulted in smaller scattering albedo and hence higher radiant efficiency. Like radiant efficiency, thermal efficiency and emissions of pollutant are also dependent on burner materials. Higher emissive materials results in higher thermal efficiencies and lower emissions of CO.

2.7 POLLUTANT FORMATION AND CONTROL IN COMBUSTION

The control of pollutant emissions from the combustion devices is an issue that has gained significant importance in the last few decades as it poses a major threat to the

environment as well as human health. The pollutants can be of either primary or secondary types. The primary air pollutants are those which are emitted directly from the source and secondary pollutants are formed via reactions involving primary pollutants in the atmosphere. The primary pollutants of any combustion device includes oxides of nitrogen (NO_x combination of NO and NO_2) and carbon monoxide (CO). In PB, due to better heat transport, the formation of CO and NO_x are lower in comparison to the conventional burner (CB). CO and NO_x have severe impacts on health and environment. The following section discusses their various effects and their formation, which is important to know as the controlling is possible only if its combustion chemistry is known.

2.7.1 Oxides of nitrogen

The oxides of nitrogen are an important air pollutant which mostly originates in the combustion process. Nitric oxide (NO) and nitrogen dioxide (NO_2) belong to this category. Generally, these two species are together known as NO_x. NO is a precursor for the formation of NO_2 and other oxides of nitrogen. NO_x is harmful to human body. Contact with the skin or eyes can cause burns. Low levels of NO_x may also cause brief, non-specific symptoms such as cough, shortness of breath, tiredness and nausea. Exposure to massive concentrations can cause sudden death due to lung injury and suffocation or choking. The formation path of NO, NO_2, CO are discussed below.

a) Nitric oxide

In combustion process, NO is generally formed from molecular nitrogen (N_2) in air by breaking the triple bond between nitrogen atoms in N_2. Some fuels in which N_2 is present

at elemental level contribute extra NO on combination with air. The formation of NO from N_2 can take place through four different ways as illustrated in Figure 2.8. The difference in the route lies in the way by which the N_2 bond is broken.

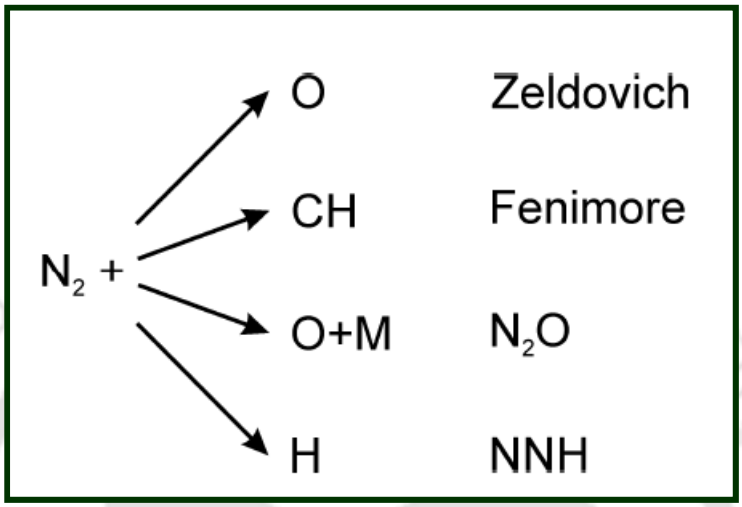

Fig. 2.8: Different NO forming path.

I. Zeldovich or thermal NO_x mechanism

In 1946, Zeldovich proposed a free radical chain mechanism for oxidation of atmospheric molecular N_2 at high temperature to produce NO. Zeldovich NO_x is also known as thermal NO_x. It is formed during the combustion of all fuels in the regions of peak flame temperature. The principal steps of Zeldovich NO_x are as follows.

$$O + N_2 \Leftrightarrow NO + N \quad (2.1)$$

$$O_2 + N \Leftrightarrow NO + O \quad (2.2)$$

$$OH + N \Leftrightarrow NO + H \quad (2.3)$$

This first reaction step i.e. the reaction between atomic oxygen with molecular N_2 is the rate determining step and has high activation energy. This reaction mechanism plays a role only at high temperatures (typically higher than 1580 °C). For this reason, NO

formed via the Zeldovich mechanism is referred to as "thermal NO". The reaction between OH and N, is important in fuel-rich flames in which [OH]>>[O]. In non-premixed combustion, the non-homogeneities in composition strongly influence NO_x emissions. Poor mixing substantially reduces the maximum NO formation rate but extends the domain of significant NO formation to lower equivalence ratios (ϕ).

II. Fennimore or prompt mechanism

In 1971, Fenimore suggested an additional NO formation mechanism known as Fenimore or prompt mechanism. The name prompt mechanism is given because of the early formation of NO by this mechanism, relative to that formed by the Zeldovich mechanism. The prompt NO occurs at low temperature, fuel-rich conditions and with short residence times. Fenimore suggested that the fast NO formation through this mechanism is due to the reaction of N_2 with hydrocarbon radicals, such as CH, CH_2. The CH radicals, important for Fenimore NO formation, are formed via the route: $CH_4 \rightarrow CH_3 \rightarrow CH_2 \rightarrow CH$. Once the CH radicals are formed, they react with N_2 and HCN and N are produced. They in turn give rise to NO. The prompt reaction mechanism is given below:

$$CH + N_2 \Leftrightarrow HCN + N \quad (2.4)$$

$$CH_2 + N_2 \Leftrightarrow HCN + NH \quad (2.5)$$

$$C + N_2 \Leftrightarrow CN + N \quad (2.6)$$

$$HCN + O \Leftrightarrow NCO + H \quad (2.7)$$

$$NCO + H \Leftrightarrow NH + CO \quad (2.8)$$

$$NH + H \Leftrightarrow N + H_2 \quad (2.9)$$

$$OH + N \Leftrightarrow NO + H \quad (2.10)$$

The reaction between CH radical and molecular N_2 is the rate-determining step. However, the oxidation of the fuel is usually sufficiently rapid that CH is at low concentrations. Under certain fuel-rich conditions, only such hydrocarbon radicals can reach high enough concentration levels and can react with N_2 and become responsible for significant NO formation.

III. N_2O mechanism

In the nitrous oxide (N_2O) mechanism, the process starts with the reaction of molecular nitrogen (N_2) and oxygen radical (O) in the presence of a third body, which could be walls of the combustor. Steps of the N_2O mechanism are the following.

$$N_2 + O + M \Leftrightarrow N_2O + M \quad (2.11)$$

$$N_2O + O \Leftrightarrow NO + NO \quad (2.12)$$

$$N_2O + H \Leftrightarrow NO + NH \quad (2.13)$$

The N_2O mechanism primarily appears under lean conditions, at low temperatures and elevated pressures. With the exception of lean premixed combustion in gas turbine engines, this mechanism has only a minor contribution to the total formation of NO in comparison with the Zeldovich and Fenimore mechanisms.

IV. NNH mechanism

This route for forming NO was suggested by Bozzelli and Dean (1995), where NO was formed by oxidation of NNH radicals. The NNH mechanism is suggested to be the dominant source of NO production in low temperature fuel rich premixed flame. The reactions involved in NNH mechanism are:

$$H + N_2 \Leftrightarrow NNH \tag{2.14}$$

$$NNH + O \Leftrightarrow NO + NH \tag{2.15}$$

b) Nitrogen Dioxide

NO is the precursor for NO_2. In the combustion zone, the amount of NO_2 is usually low, but in exhaust, at times, it can be significant. In this, the pertinent reaction is

$$NO + \frac{1}{2}O_2 \Leftrightarrow NO_2 \tag{2.16}$$

This reaction is exothermic. Hence, the formation of NO_2 is thermodynamically favoured at low temperatures. NO_2 formation is favoured by rapid cooling of combustion products in the presence of substantial O_2 concentrations.

2.7.2 Carbon Monoxide

CO is the most abundant air pollutant in the lower atmosphere and is hazardous for human health. For stoichiometric and slightly lean mixtures, CO is found in substantial quantities at typical combustion temperatures as a result of the dissociation of CO_2. The conversion of CO to CO_2 is a function of residence time. The oxidation of CO from fuel is very fast while the oxidation of CO leading to CO_2 needs more time. The reaction of CO with O_2 is as follows.

$$CO + \frac{1}{2}O_2 \Leftrightarrow CO_2 + O \tag{2.17}$$

This reaction does not contribute much to CO_2 formation due to its low reaction velocity.

With temperature the CO concentrations fall rapidly. Cold surfaces within the combustion chamber results in locally disappearance of flames and hence higher CO. Figure 2.9 shows the effect of CO exposure on human health. Its effect may start with headache and vomiting, and in adverse condition, it can lead to coma and finally to death.

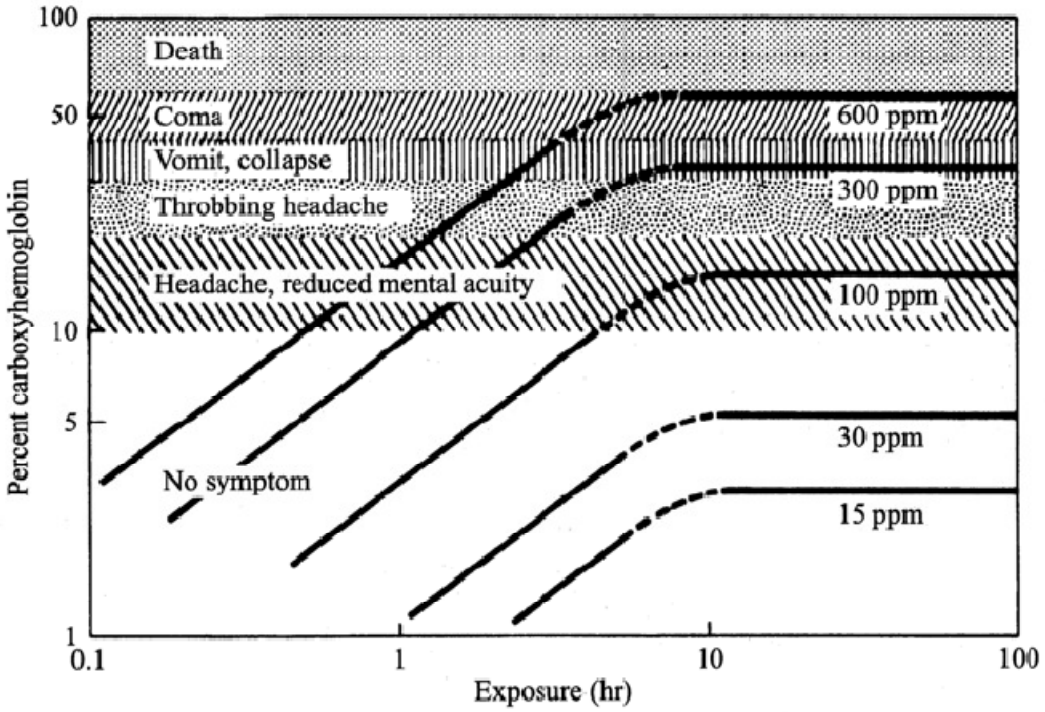

Fig. 2.9: Effect of CO exposure on human health (Avdic, 2004).

2.7.3 Control of pollutants

The most common technique adopted to control NO_x is to reduce flame temperature as the NO_x chemistry is highly temperature dependent. Lean premixed combustion can play a major role in lowering the temperature. It has the advantage of preventing local ‘‘hot spots’’ thereby avoiding the high temperature of stoichiometric combustion that increases thermal NO_x. Operating the burner at low equivalence ratio (ϕ) reduces the flame temperature by diluting the combustion gases with excess air. Depending on the time

required for combustion and the amount of heat rejected during the combustion process, various types of burners yield different NO_x emission levels.

Flame temperature can also be reduced by introducing diluents other than air which do not participate in the combustion reactions. The dilution is generally done with most readily available non-reactive gas which is mixed with air (Avdic, 2004). In utility boilers and other large stationary combustors this method is extensively used. The injection of other diluents such as water or steam can also be used to reduce the NO formation rates, but the at the cost of reduced system efficiency. Modifications of the combustion system design or operation are also used to control NO_x emissions.

PMC is an effective way of reducing NO_x as the combustion zone temperature encountered in it is low due to the effective heat removal by conduction and radiation. For instance, Suzukawa et al. (1997) and Goeckner et al. (1992) have found 50% and 30% lower level of NO_x in their PBs than the CBs. Besides, it is possible to run a PB even at low equivalence ratio (ϕ), without affecting the stability as there is preheating of the reactants. However, operating the burner at too lean condition is not favourable as it would lead to more CO.The conditions of CO and NO_x formations are opposite. CO is emitted at low process temperatures, while NO_x is produced at higher temperatures. Thus, it is essential to have an optimum burner temperature where CO and NO_x concentrations are both minimized.

The conventional methods for reduction of CO concentrations are (i) extension of residence time of the flue gases, (ii) use of high pressures where the equilibrium is shifted to a lower value and, at the same time, the conversion rate of CO to CO_2 reaches a higher

value, (iii) higher combustion temperatures and (iv) operation of the burner near stoichiometry.

In PMC, CO is low due to the increased residence times, as the air/fuel mixture has to pass through the porous matrix having tortuous path. For instance, Xiong et al. (1995) conducted an experimental study on 60 kW bench-scale porous matrix combustor heaters and reported NO_x and CO levels as less than 15 ppmv and total hydrocarbon (THC) less than 3 ppmv (parts per million by volume). Likewsie, Mital et al. (1998) measured the emission indices of CO, HC and NO_x and found CO: 0.1-3.6 g/kg, NO_x: 0.1-0.35 g/kg and HC: 0.1-1.2 g/kg.

Khanna et al. (1994) experimentally investigated the emissions and for methane/air combustion within a PM burner for various equivalence ratios (ϕ) and flow rates. Their results indicated that the CO and NO_x emissions increased with increasing equivalence ratio (ϕ) and the NO_x emissions are less than 36 ppm (corrected to 0% 0_2) over the entire range of experiments. Brennet et al. (2000) in their numerical study reported that CO emissions were as low as 24 ppm. Thus, reviewing the literature, it can be said that from emission reduction point of view, PMC is a very promising technology.

It is to be mentioned that although PMC offers several benefits, its research on liquid fuels had not started till 1995 (Kaplan, 1995), because of a misconception that the combustion of liquid fuels in PM would result clogging of pores. Additionally, the combustion of liquid fuel is complex compared to gases, owing to different modes of heat exchange including phase change; for instance, evaporation rate determines the intensity of heat transfer as well as burning.

2.8 LIQUID FUEL COMBUSTION

The first research activity in PMC of liquid fuel started in the year 1995 (Kaplan, 1995), and after that, a few researchers (Takami et al., 1998, Jugjai et al., 2002, Vijaykant and Agrawal, 2007) have come up with their innovative ideas and investigated the combustion behaviour of different fuels like heptanes, kerosene, ethanol, etc. However, the research on combustion of liquid fuels in PM is still in nascent state and in comparison to the reports on droplet combustion of liquid fuel in the free space, the literature on PMC of liquid fuel is sparse (Mujeebu et al., 2009c). Besides, most of the published reports focus on the basic combustion behaviour of fuel when burnt within the PM, rather than designing the burner for any specific application (Mujeebu et al., 2009d). The application oriented research is yet to take place. In the following section, a review of the various findings on PMC of liquid fuels that have been attempted so far is described.

Liquid fuel-fired PBs are classified into two types: (i) fuel-vaporizing type and (ii) fuel-spraying type. The spraying type is commonly used for industrial and civil applications such as boilers and furnaces. In this type, the flame is relatively large and the stability of the flame is affected by aerodynamics between air and fuel droplets. The combustion is homogeneous for a small range of load.

The vaporizing type, has many advantages over the former one viz., high turn-down ratio, compact in size, smaller flame, less soot and nearly homogeneous combustion. But the main disadvantage of this type is that it consumes higher electric power for fuel vaporization and have low overall efficiency. In recent years, both spraying and vaporizing type burners have been developed.

Kaplan and Hall (1995) examined the combustion of heptane within a PB. They constructed several burners with different configurations and with various types of ceramics viz. magnesia stabilized ZrO_2, SiC, and yttrium stabilized ZrO_2. Figure 2.10 shows their experimental setup. Heptane was impinged on the combustion section using an oil spray nozzle with a fixed flow rate of approximately 0.025 lpm. They established the suitable burner configuration (4ppcm–10ppcm–4 ppcm–4 ppcm–10 ppcm) supporting stable and complete combustion.

Among the three materials tested, they obtained the best performance in magnesia stabilized zirconia. Complete combustion was achieved for equivalence ratios (ϕ) 0.57-0.67. For fuel flow rates 0.025 lpm and 0.032 lpm, CO varied from 3 to 7 ppm and 1 to 4 ppm, respectively. For the same operating conditions, NO_x varied from 15 to 20 ppm and 15 to 25 ppm, respectively.

The experiments with two different insulations viz., alumina and quartz reveal that with quartz insulation, the CO and NO_x were lower owing to lower temperatures resulted from radiative heat loss than alumina. They also checked the emission characteristics of non-vaporized and pre-vaporized fuel and found similar performance.

A similar type of study was reported by Tseng and Howell (1996) who used a one-dimensional laminar flow model with multi-step combustion chemistry. They used ZrO_2 as PB and heptane as fuel and calculated the burning rates, temperature, and emissions. It was found that the combustion was stable even at very low equivalence ratio (ϕ) i.e., 0.3 with an average droplet diameter of about 10 µm. The emission levels were similar to those found by Kaplan and Hall (1995).

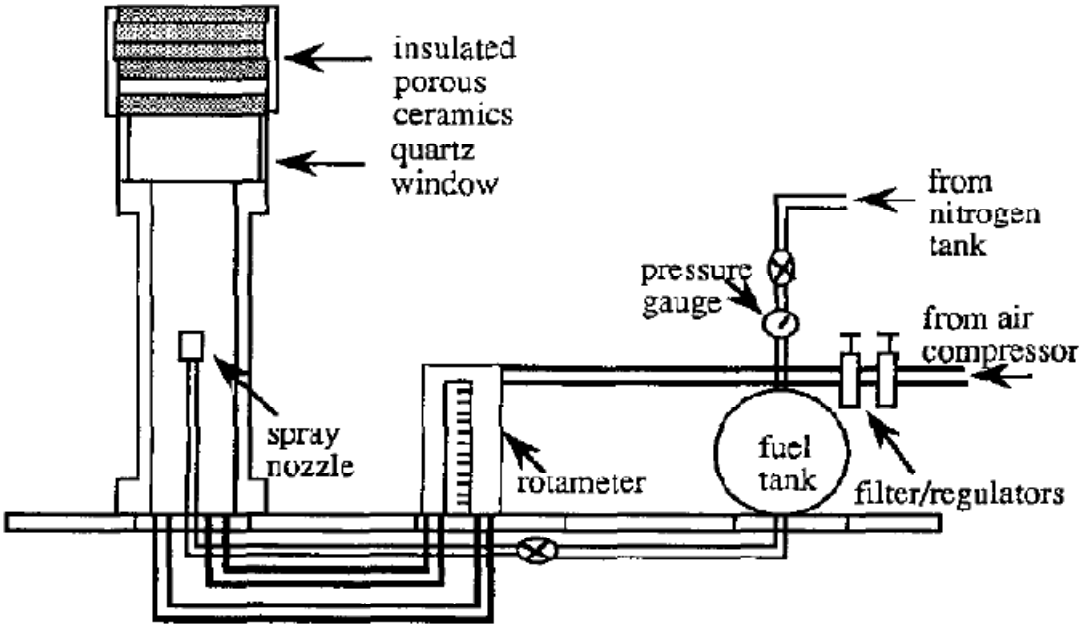

Fig. 2.10: Experimental set up of Kaplan and Hall (1995) for combustion of heptane in PB. (Figure reproduced with copyright permission, licence number: 2563020603416).

Another important observation of Tseng and Howell's research is that the liquid fuel droplets experienced early complete evaporation in the low temperature region before the flame front due to the small droplet size (< 25 μm) and high volatility of the fuel. This indicated the energy feedback mechanism through convection and thermal radiation was inadequate to effectively enhance the enthalpy required for droplet evaporation. They concluded that in order to have stable combustion, if the heat of vaporization of the fuel is higher, the droplet spray should be finer.

Takami et al. (1998) developed a PB made of mullite without a fuel atomizer. They use a vaporizing type burner and kerosene as fuel. Kerosene was supplied drop wise (instead

of spray) to the top surface of a PB through a steel wire net which served for uniform distribution of fuel over the surface of the burner. Figure 2.11 shows the burner setup.

In the set up of Takami et al. (1998) (Figure 2.11), air was supplied tangentially from the wall of the combustion chamber. It mixed with the fuel vapour and ignited at the lower surface of the porous plate. They analysed the combustion behaviour of the burner by measuring the profiles of temperature and composition of the combustion gas along the centreline in the chamber. A stable combustion flame, which is similar to a pool of fire, was realized.

Complete combustion was achieved for equivalence ratio (ϕ) in the range 0.5 to 0.9. The fuel-lean limit of the kerosene-air flame attained a lean equivalence ratio (ϕ) of 0.1. Corresponding to the input load ranging from 538-3879 kW/m^2, the turn down ratio of the burner was found to be 7.2. They reported that the porous ceramic was effective for vaporization of kerosene and clarified the effects of kerosene input and equivalence ratio (ϕ) on the thermal structures through the measurement of temperature profiles. However, the measurements were not taken within the PB, but in the combustion chamber.

Jugjai et al. (2002) studied the combustion of kerosene in a PB made of stainless steel wire net. They studied the heat transfer phenomena, the evaporation mechanism, and the combustion characteristics, which occur simultaneously in the burner system. Their experimental setup is shown in Figure 2.12. The design and operational function of the experimental apparatus are similar to that of Takami et al. (1998). However, the sizes of the combustion chambers, type of the PB, method of air entry and temperature

measurement points were different. Additionally, they used a porous emitter at the downstream of the burner.

They clarified the effect of various parameters such as thermal input, equivalence ratio (ϕ), downstream porous emitter and its optical thickness on the combustion temperatures and emission characteristics of the burner system. They reported that at an equivalence ratio (ϕ) 0.37-0.55 and thermal input of 2.62–3.49 kW, stable combustion with low emission of pollutants was achieved.

Jugjai and Polmart (2003) developed another PB made of Al_2O_3 spheres of diameter 5 mm for kerosene combustion. Figure 2.13 shows their experimental setup. This setup is similar to the previous one (Jugjai et al., 2002) except the length of the porous emitter. They studied the effects of various parameters such as heat input and equivalence ratio (ϕ) on the combustion characteristics. It was found that the introduction of the packed bed emitter was an efficient method for enhancement of evaporation and combustion of the liquid fuels without a spray atomizer. Stable combustion with low emission of pollutants was realized even though the combustion flame was confined between the PB and the packed bed emitter.

Fuse et al. (2003) developed a burner made of Al_2O_3 having 85% porosity as against the 36% porosity of Takami et al. (1998) for kerosene combustion. Their focus was on developing a burner without using electrical heater for vaporization, thereby saving a large amount of electricity. They introduced the concept of self-sustained combustion by the enhancement of fuel vaporization by the radiant heat flux from the flame, high

temperature walls and from the PM itself. An optically thin (highly porous) medium was found to achieve this goal compared with the optically thicker (low porous) one. Their experimental set up is shown in Figure 2.14.

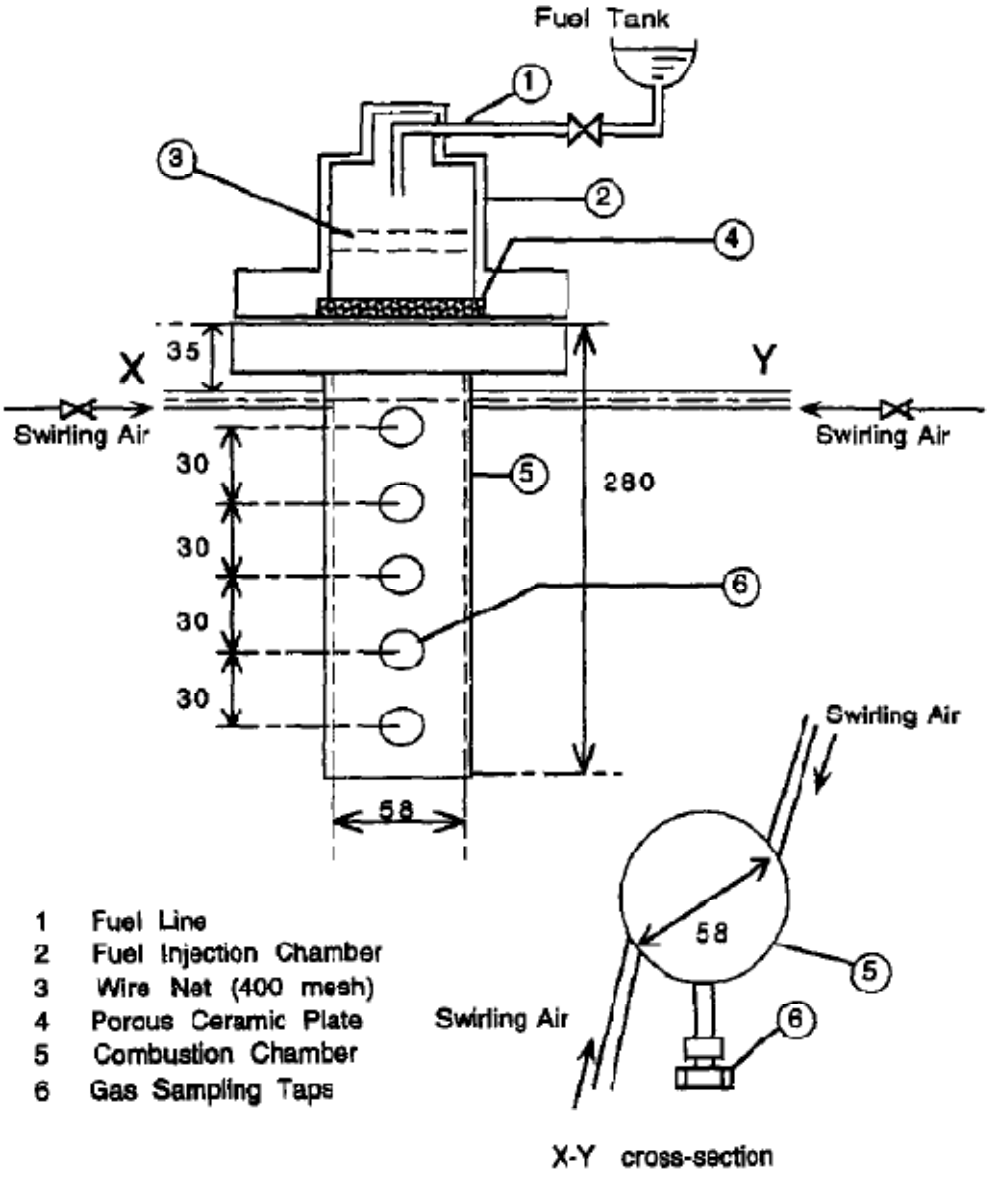

Fig. 2.11: Experimental set up of Takami et al.(1998) for combustion of kerosene in PB. (Figure reproduced with copyright permission, licence number: 2563020284185).

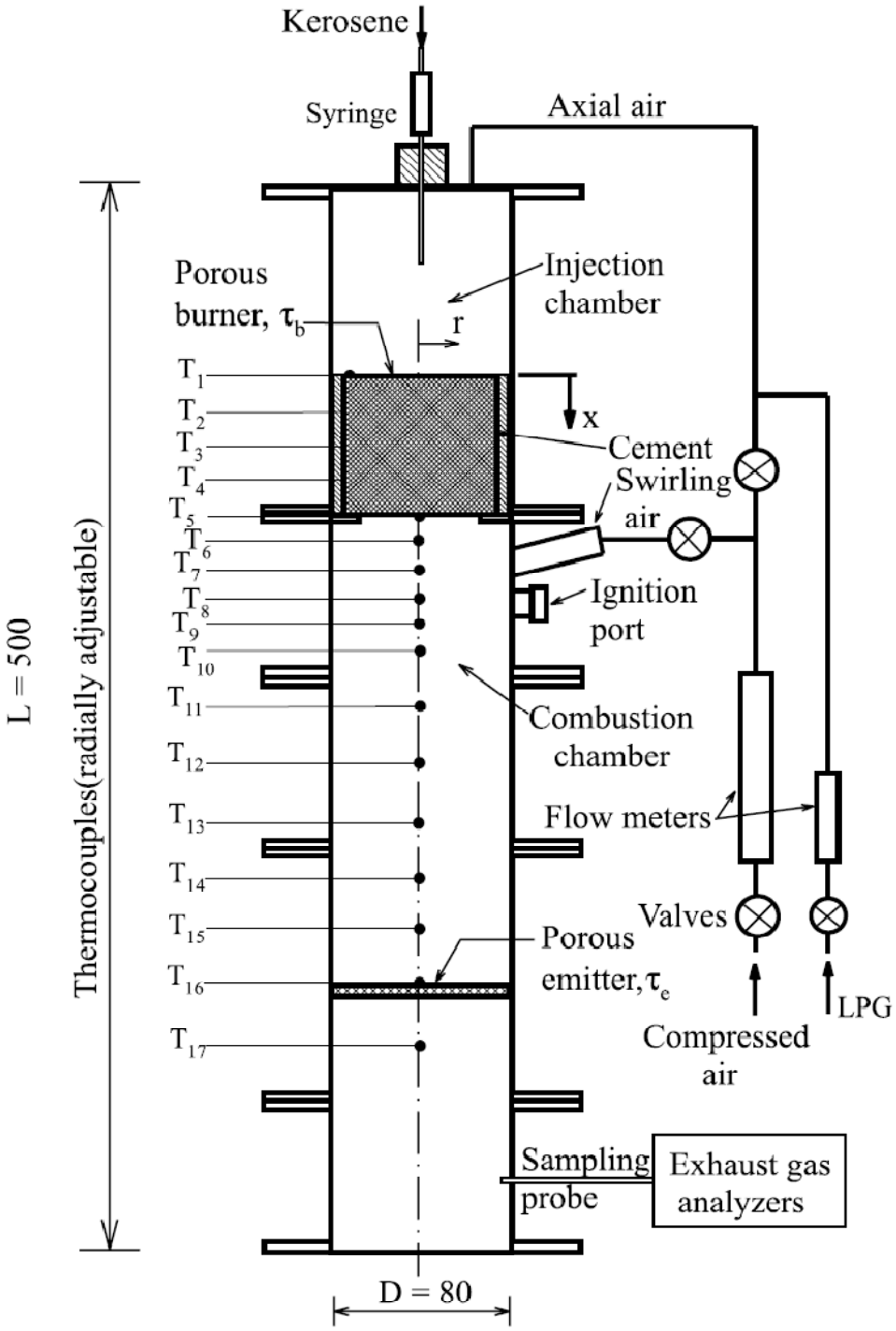

Fig. 2.12: Experimental set up of Jugjai et al. (2002) for combustion of kerosene in PB. (Figure reproduced with copyright permission, licence number: 2563010322329).

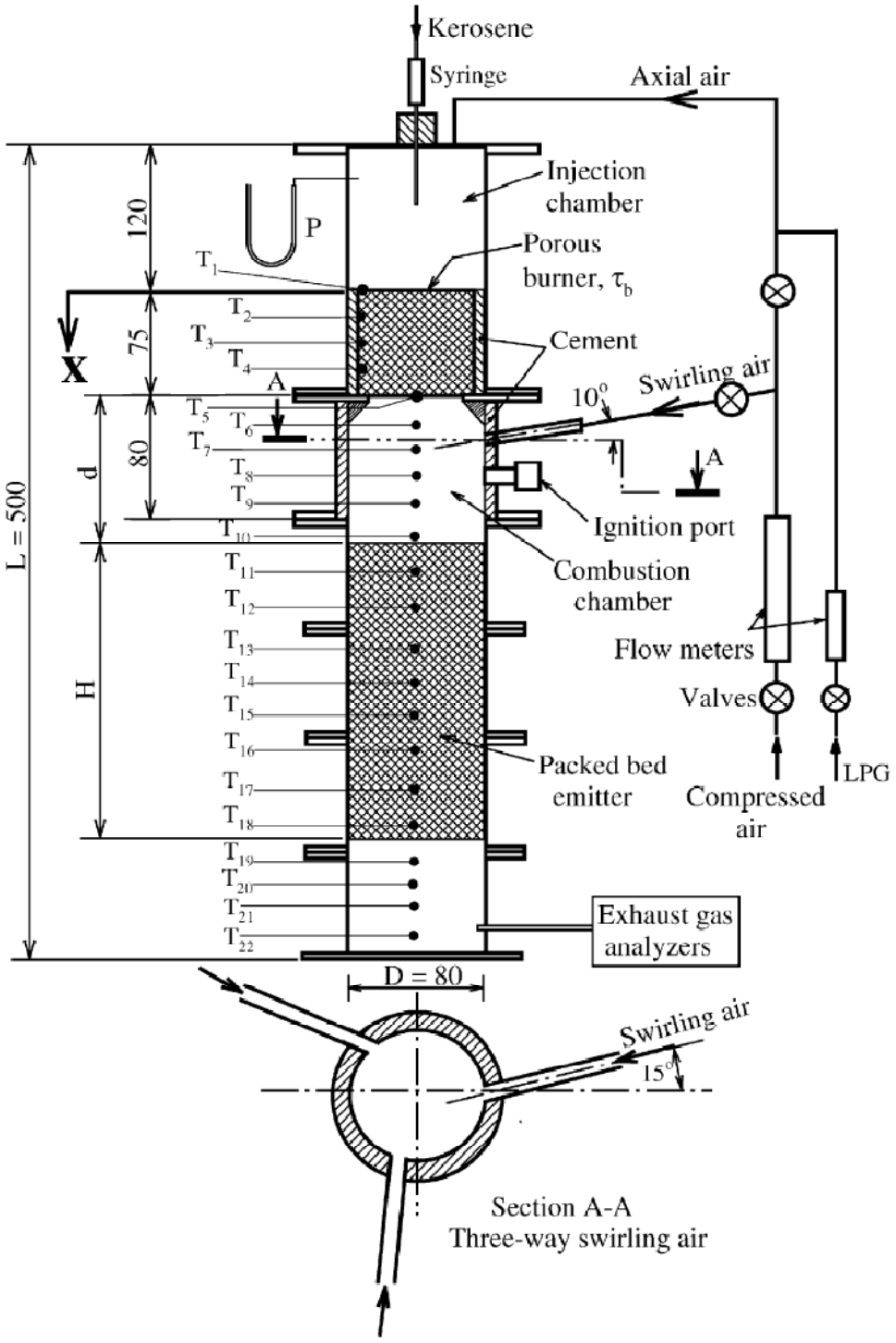

Fig. 2.13: Experimental set up of Jugjai and Polmart (2003) for combustion of kerosene in PB. (Figure reproduced with copyright permission, licence number: 2563021248189).

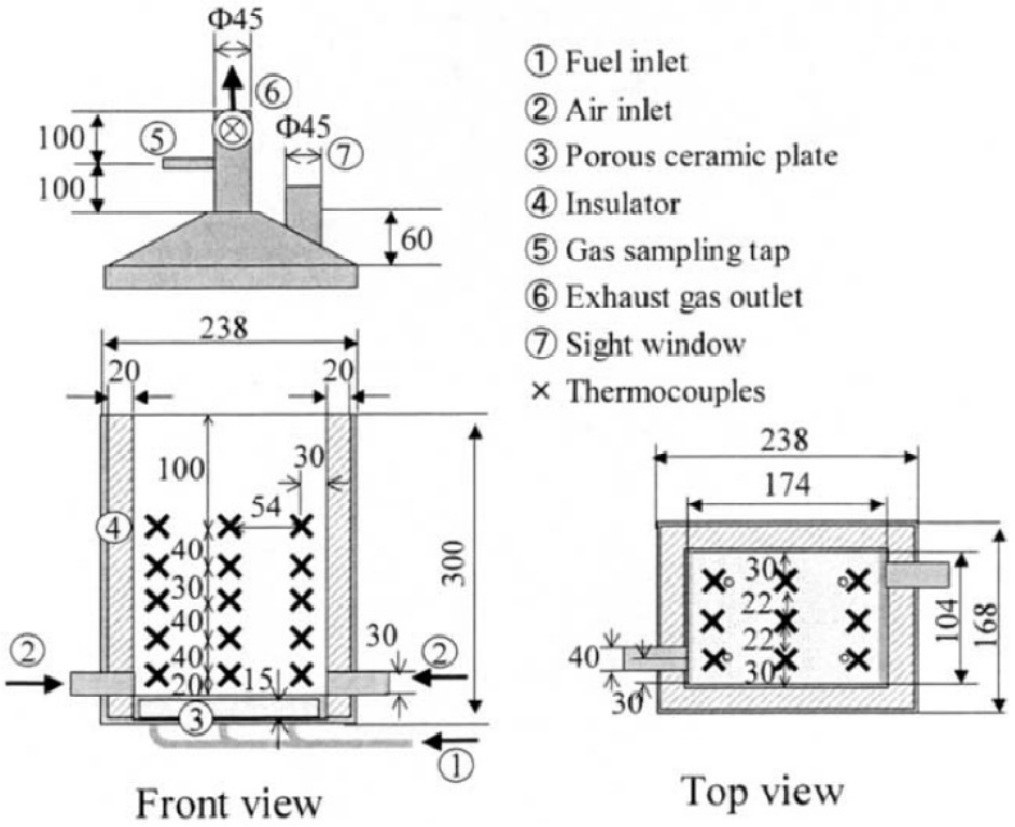

Fig. 2.14: Experimental set up of Fuse et al. (2003) for combustion of kerosene in PB. (Figure reproduced with copyright permission, licence number: 2563011014867).

Fuse et al. (2005) investigated the combustion behaviour of ethanol also. They used a porous ceramic burner made of Al_2O_3 equipped with an ultrasonic oscillator. The oscillator irradiation acted as ignition promoter. The complete combustion was achieved under the equivalence ratio (ϕ) ranging from 0.63-0.80, and in this region, the NO_x concentration was found comparatively high (59-97 ppm) because of high heat value per unit surface area of the flame.

Jugjai and Phothiya (2007) developed a liquid fuel-fired porous combustor heater (LPCH) without atomizer. The experimental setup is shown in Figure 2.15. It consists of two main cylindrical PM. The upstream media was made of a packed bed of metallic wire

screen with mesh size of 100 mesh/inch. The downstream media which acted as porous emitter was made of a packed bed of inert solid alumina spheres with average diameter of 19 mm. Water coil having diameter of 6 mm was embedded within the porous emitter for extracting heat.

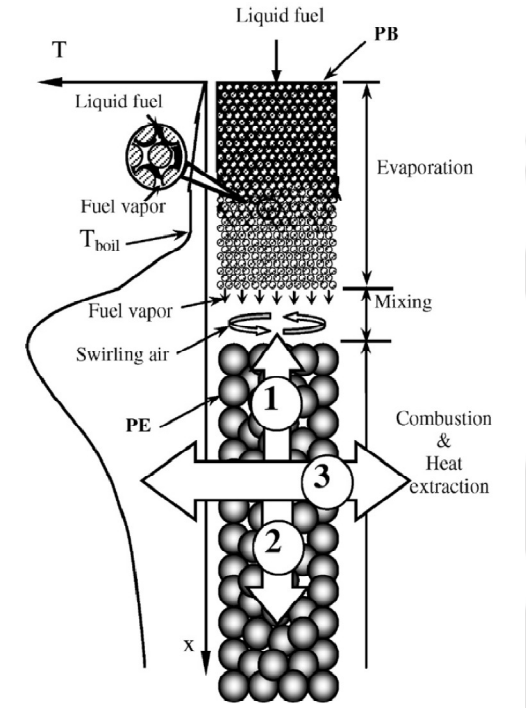

Fig. 2.15: Experimental set up of Jugjai and Phothiya (2007) for combustion of kerosene in PB. Figure reproduced with copyright permission, licence number: 2563020798538).

With kerosene, the LPCH was found very effective. In comparison of the conventional system, its thermal efficiency was found to be as high as 28%, and NO_x was low and CO was acceptable. They studied the effect of fuel flow rate, cooling water flow rate and equivalence ratio (ϕ) on thermal efficiency and pollutant emissions. These parameters were found to have a significant effect on the flame location, combustion temperature and pollutant emissions.

Wei et al. (2002) demonstrated that liquid fuels could be burnt under the condition of vaporized premixed lean (VPL) combustion. In the VPL, the fuel is first vaporized in an externally heated fuel vaporizer and then the mixture of vaporized fuel and air is homogenized in a static mixing device and finally it is burnt in a surface burner. It was found that in this type of burner, various fuels (diesel, kerosene, gasoline fractions and alcohols etc.) could be completely vaporized under pressure up to 30 bar. The unburned hydrocarbons (UHC) and CO were negligible and there was no soot formation.

Trimis et al. (2001) developed an experimental burner for combustion of liquid fuel (industrial gas oil) in which they introduced the concept of cool flame vaporization where a clear separation zone between the vaporization and the combustion was established. Their burner showed a high power modulation range (1:10) and a good emission characteristics over the entire power modulation range.

Vijayakant and Agrawal (2007) made an experimental study on combustion of kerosene in a PB made of SiC coated carbon foam. Figure 2.16 shows their experimental set up. They tested several burner configurations and used PM of different pore sizes. They observed that the stable combustion was dependent on the distance between the fuel injector and PM inlet. Depending upon the injector location, they identified three combustion regimes and reported that the best performance (in terms of homogenization of reaction mixture and lower level of emission) was observed when the injector was located far upstream of the PM. At an intermediate injector location, inhomogeneous air-fuel mixture was found. They found the emission slightly higher but reported that it could be reduced by a careful selection of the pore size and thickness of the PM section. In addition to this, they also found that the injection of swirling air and proper selection of

burner configurations had a significant effect on emission reduction as well as pressure drop. For the optimized configuration, the pressure drop in the PB was less than 0.7% of the total pressure.

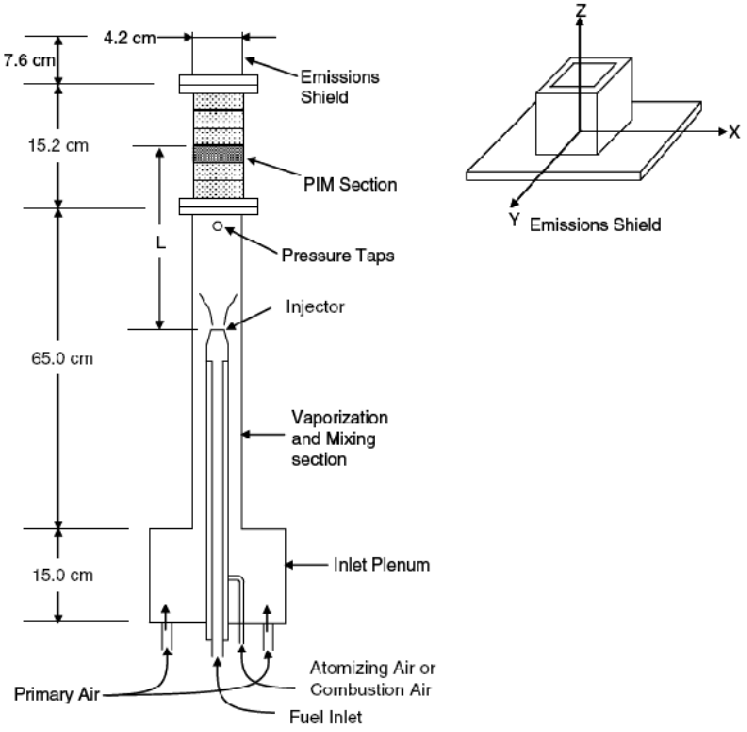

Fig. 2.16: Experimental set up of Vijaykant and Agarwal (2007) for combustion of kerosene in PB. (Figure reproduced with copyright permission, licence number 2563021033379).

Periasamy et al. (2007) studied kerosene (aviation-type) combustion in open-cell, SiC coated carbon–carbon ceramic foam. They sprayed kerosene into a co-flowing, preheated air environment using an air-blast atomizer and measured the minimum combustion heat feedback rate required for complete vaporization. They found that it increased with the decrease in distance between the PM and the injector. Complete vaporization was achieved at a co-flow air temperature of 400 K. Without PM,

however, a minimum co-flow air temperature of 500 K was required to achieve the same quality of evaporation.

Kamal and Mohamad (2006) employed a rotary swirl burner made of SiC with porosity 87% for combustion of natural gas in a cross-flow stream of air. The objective of their study was to analyze the effect of fuel spray orientation on mixing dynamics with the swirled air. Owing to improved mixing and increased kinetic rate, they found that CO and NO_x emissions were dominated by swirl. At high swirl numbers, a significant reduction in CO and UHC concentrations was obtained and the NO_x emission was decreased to a level below 10 ppm.

Kayal and Chakravarty (2005) did a numerical analysis of a one-dimensional combustion of kerosene in an inert PM in which the fuel droplets were assumed to suspend in air stream inside the PM. It was also assumed that the droplets vaporized completely prior to the entry of air into the flame. They investigated the effects of absorption coefficient, emissivity of the medium, flame position on radiative energy output, efficiency and optimum oil droplet size at the entry. The results showed that with increase in optical thickness of the PM, the radiative energy feedback from the post-flame region to reaction zone increased. It was also found that the radiative heat feedback was dependant on the peak gas temperature, burning velocity and effective upstream optical thickness. As emissivity of the solid increased, the radiative heat losses at the downstream and upstream ends were found to almost linearly decrease and increase, respectively. This proved that the emissivity of the PM had a profound effect on thermal performance of the system. With large droplet sizes, the PM with low absorption coefficient produced high downstream radiative output.

Kayal and Chakravarty (2006) made another numerical study where they assumed that the fuel oil was added drop-wise uniformly over the top surface of the porous matrix and allowed to trickle through the system. The vaporization was assumed to be completed in the pre-combustion zone of the PM. They found that for low optical thickness of the medium, combustion was efficient. Besides, they also found that the low emissivity ceramic material was desirable for maximum downstream and minimum upstream radiative heat loss.

Kayal and Chakravarty (2007) developed another two-dimensional numerical model in which they considered vaporization of liquid fuel on a wetted wall plate through indirect heat transfer from combustion. The vaporizing energy was provided through the radiative interaction between the vaporizing plate and an upstream end surface of the PM. They found that the combination of low emissivity of the vaporizing plate and high emissivities and low optical thickness of PM makes the system suitable over a wide range of power. They also concluded that the effect of optical thickness on the power output was significant, as with 50% increase in optical thickness, the power output increased by 450%.

Martynenco (1998) developed a physical model of self-sustaining combustion of the gaseous mixture with simultaneous evaporation of the fuel droplets in the PM. They considered the droplet behaviour and studied the self-sustaining combustion with the steady-state flame. They concluded that for a given thickness of the PM, the superficial velocity of gas, thermal conductivity of the solid, convective heat transfer coefficients among different phases (solid-gas, solid-liquid vapour) and initial diameter of liquid

droplets were the most important controlling parameters for self-sustaining combustion of the fuel vapour in an inert PM.

2.9 SUMMARY OF LITERATURE SURVEY AND SCOPE FOR PRESENT WORK

PMC is a century old technology; however, it has gained importance only in the last two decades when the concern for fuel conservation and clean combustion has been stressed. The PMC has become a suitable option now as it offers many advantages like homogenization of temperature field, extension of flammability limit, reduction of emissions from combustion devices, etc. So far, most of the studies on PMC have focussed on the basic understandings of the important phenomena like flame stabilization, heat recirculation, excess enthalpy combustion, etc. Few researchers have paid particular attentions on thermo-physical properties of material and prescribed various materials which could be used for PB construction. In recent years, the attention has also been paid on its possible applications, and as a result of that some burners have been designed. However, the application oriented studies are few.

Most of the studies are however, with gaseous fuels. The research with liquid fuel is relatively new. The liquid fuels which have been studied so far are kerosene, ethanol and heptanes. Out of these, kerosene has received greater attention as it is an important fuel in industrial as well as in domestic sectors. Its combustion behaviour was studied in different experimental setups and various important aspects like effect of bed height, emission characteristics, temperature homogeneity, radiation output, flame stability, emission, efficiency, etc. under different operating conditions were studied.

The reports on thermal efficiency are however, limited. Nevertheless, in case of cooking stove, measurement of thermal efficiency or first law efficiency is important as it gives the indication of percentage of heat utilized or the percentage of heat loss to the surroundings. However, thermal efficiency is sometimes misleading and the true performance can be achieved only with exergy efficiency from second law of thermodynamics (Ozturk, 2004, Petela 2005 and Kaushik and Gupta 2008). The exergy efficiency is more realistic than the efficiency based on the first law (Kaushik and Gupta, 2008). Exergy provides a better understanding of a system indicating energy degradation. The exergy efficiency is a true measure of performance of a thermal system (Bejan, 1988, Kaushik et al., 2000) and it helps to assess accurate utilization of energy.

During the past few decades, the exergy analysis has been used for different systems such as residential sector, transportation sector, thermal processes, solar cooker, etc. (Saidur et al., 2007, Dincer et al., 2004, Sahoo et al., 2009, Pope et al., 2010, Oztruk, 2004, Panwar et al., 2010). This analysis has not been done for any PM incorporated stove. In conventional cooking stoves also the same is not employed. Thus, there is a scope to employ this concept in newly developed PM incorporated kerosene pressure stove and study its performance.

The use of PM in other thermal system was found advantageous as it helped in reduction of pollutant emissions, which in the present time is of great concern. The higher levels of pollutants from combustion devices including domestic contrivances have posed threat to a sustainable environment. In this context, the reports on reduction of emissions from kerosene fired PM combustors has been a great motivation to adopt this technology in kerosene pressure stoves also.

The conventional kerosene pressure stoves that operate in free-flame combustion mode, produce higher CO emissions which is dangerous to environment and human health as well. Thus, a study on PB for kerosene was thought to be much useful as the levels of pollutants in PM are found lower. Hence, it is planned to develop an experimental setup to study the combustion behaviour of kerosene. The experimental setups which have been developed by different researchers cannot be used in the present study as they are meant for industrial applications. Besides, in all cases, for ignition either LPG or electric power is used which cannot be recommended when the application is aimed at domestic usage. Thus, it has become necessary to develop an indigenous setup for the study of kerosene within a PM and to optimize the various operating parameters for its best performance.

Besides, studies can also be made for a bi-layered PB each layer having different thermo-physical properties. A bi-layer PB for kerosene combustion has not been studied even for the industrial applications. Besides, it can be planed to undertake a preliminary study to know the advantages and disadvantages of using LPG for ignition and also the difficulties of operating the PM incorporated stove in natural draft mode. These have been described in following sections. The setup used for the detailed investigations is described in Chapter 3.

2.10 PRELIMINARY STUDIES

2.10.1 Stove with natural draft

The literature on liquid fuel combustion in PM reveals for smooth running of the systems, and also to study the performance of the system at different equivalence ratios (ϕ), air was supplied from an external source such as compressors. For the domestic applications,

the use of the compressed air is not always feasible. However, the use of a small fan or a blower to create the necessary draft is one of the viable options (Mukunda et al., 2010).

In this study, initially a simple attempt was made to evaluate if the burner works on natural draft. Trials were made on a BIS stove with minor modifications which basically includes a perforated cylindrical casing over the burner to enclose a PB within it. The holes were provided to draw secondary air. Several versions of the perforated cylinders with different aspect ratios (ratio of length to diameter) and hole sizes were constructed and tested for the combustion quality. Figure 2.17 (a) shows a schematic of the casing and Figure 2.17 (b) shows the picture of the burner operating in radiant mode.

A combination of SiC having pore density 10 ppi and Al_2O_3 balls having diameter 7 mm were used as PM. The thickness of the SiC piece was 20 mm and that of the porous bed Al_2O_3 balls was 15 mm. They were housed insides a perforated cylinder. Air flow into the casing was by free convection, which was due to the hot porous bed and the hot gases. The operational procedure of the system was similar to that of the conventional stove which is described in Chapter 3. It was found that the initial mode of combustion was convection, however, once the PM was sufficiently heated, it gradually shifted to radiant mode, without any visible flame.

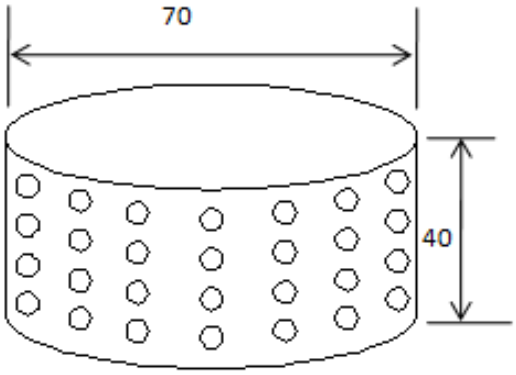

(a)

(b)

Fig. 2.17: (a) Schematic of perforated cylindrical casing (b) Picture of burner operating in radiant mode.

Although there was no difficulty in ignition and combustion was stable, this configuration was not satisfactory as CO emission was very high (~500 ppm, corrected to 3% O_2). There was also soot formation in the interior and surface of the burner. This might be due to the insufficient draft causing a fuel rich combustion. Thus, the amount of air drawn by the free convection was not large. It was observed that CO emission peaked (~1000 ppm) in the initial stage of the operation and once the thermal profile was established, its concentrations reduced. Nevertheless, in comparison to a conventional stove, the values were high. This limits the scope for using the natural draft stove with PM, unless some major modification is attempted.

2.10.2 Stove with LPG preheater

It is evident from the literature survey of various PM systems that the usual way of starting a PB is to preheat it either by electric heating or by combustion of high calorific fuel. Jugjai et al (2002) used LPG as preheater. This is necessary if fuel is directly sprayed in the PB and allowed to vaporize by the radiant heat emitted by PM. Without sufficient heating of PM, it is not possible to retain flame within the PB without being quenched. In this work also initially, an attempt was made to initiate the process by LPG for which a separate experimental setup was developed. The following paragraph outlines the setup and summarizes the experimental findings.

Figure 2.18 and Figure 2.19 show a schematic and a picture of the experimental set up with LPG preheater respectively. The setup was based on the design of Kaplan and Hall (1994) and Vijaykant and Agrawal (2007) who studied combustion of heptane and kerosene, respectively. It consisted of a kerosene tank, a kerosene duct with a spray nozzle, two air ducts, a LPG duct, a compressor, two rotameters, a PB (SiC+ Al_2O_3) and casing. The compressor was used to supply an undisturbed supply of air and the rotameters were used for the measurement of air and kerosene flow rates.

The PM used were a combination of SiC having pore density 10 ppi and Al_2O_3 balls having diameter 7 mm were used. The thickness of the SiC piece was 20 mm and that of the porous bed Al_2O_3 balls was 15 mm. They were housed insides a cylinder/casing having diameter 70 mm and length 110 mm. The casing diameter was chosen according the size of the PM and the length was fixed based on several experimentations with various distances between the PM and the air duct and the PM and the spray nozzle.

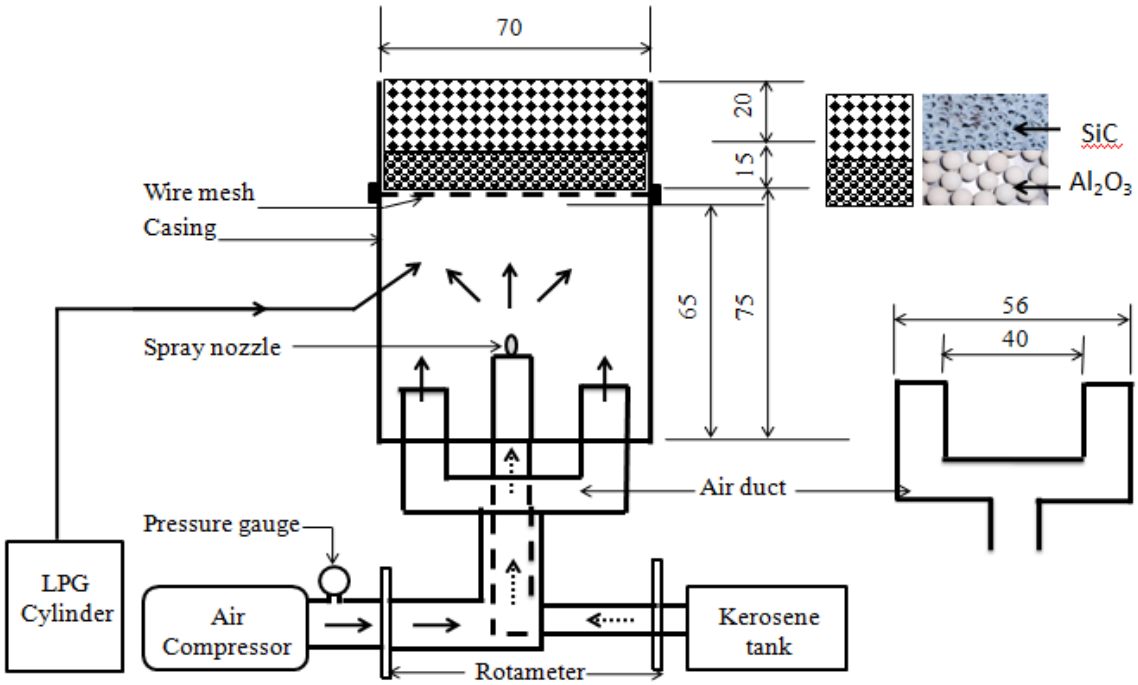

Fig. 2.18: Schematic of the experimental set up with LPG preheater.

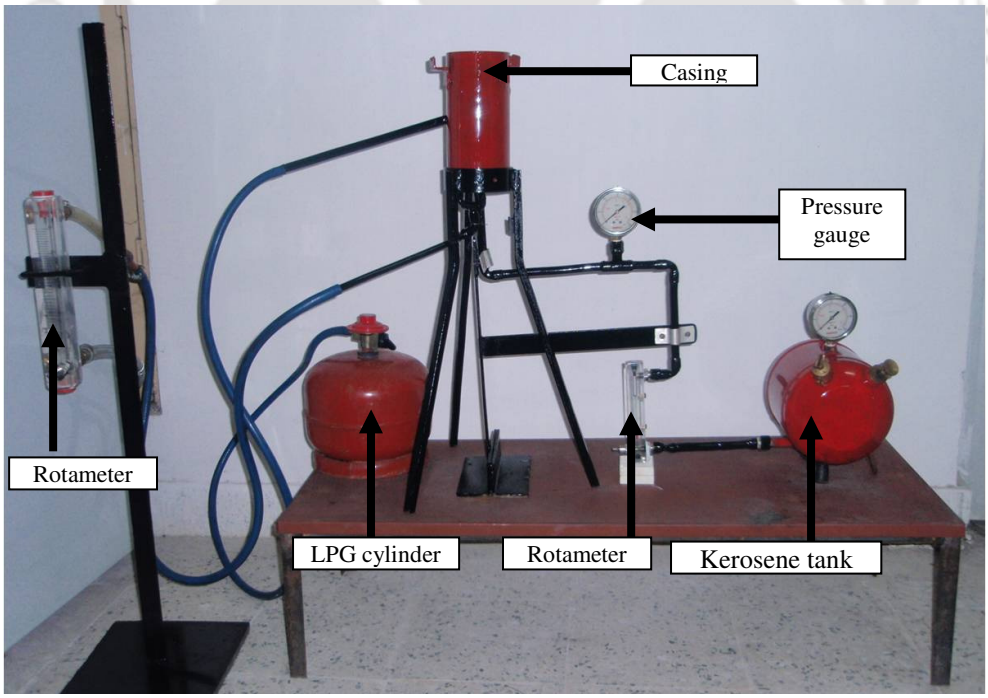

Fig. 2.19: Picture of the experimental set up with LPG preheater.

The operating procedure of the setup is as follows. Initially, the PB is preheated with a LPG/air premixed flame with an appropriate equivalence ratio (ϕ) of 0.9 and once the burner is sufficiently heated, kerosene is sprayed to the PB and the LPG connection is turned off. Kerosene is vaporized owing to the radiative flux emitted from the PB and mixes with air and burnt. Experiments were conducted at different levels of air pressure and also different flow rates so as to find out the actual requirement to create the necessary draft. It was found that the air pressure just above the atmospheric would suffice the requirement. On further increase in pressure, the flame structure got distorted. Minimum air flow rates required to retain the flame within PM was found to be 60 lpm which corresponds to 80% excess air.

At the stated before, air pressure (1.2 bar), the flame quality was better than the previous case i.e., the stove with the natural draft arrangement, owing to the sufficient air draft. Excess air supply avoided the chances of rich combustion. The burning was however, in diffusion mode; a long flame was seen at the top of the burner. The droplet burning in diffusion is the indication of inefficient vaporization. The evaporation process of liquid is governed by combustion heat release and also the heat transport properties. In the present case, the radiant heat transfer from PB to upstream might not be sufficient ~~enough~~ to vaporize the fuel completely. Besides, the heating period with LPG was found sufficiently long (~30 minute). This makes the overall efficiency of the system low. Thus, the scope of using LPG as preheater in kerosene stove is negligible.

भारतीय प्रौद्योगिकी संस्थान गुवाहाटी
Indian Institute of Technology Guwahati

CHAPTER 3

EXPERIMENTAL SETUP AND PROCEDURE

3.1 INTRODUCTION

The research on combustion of liquid fuel in the PM is relatively new. Aimed at industrial applications, in the last two decades, some studies have been devoted to understand the combustion characteristics of liquid fuels like kerosene, heptane, ethanol, etc. However, for the domestic cooking applications, no such study has been reported. In a developing country, a good share of kerosene consumption goes to domestic cooking, and for that, mostly kerosene pressure stoves are used. These kerosene pressure stoves operate in free-flame mode. To harness the benefits and also to see the suitability of the PM in improving the thermal performance, in this work a kerosene pressure stove with PB has been developed. This chapter first discusses the development criterion and description of the experimental setup. Following this, a discussion on various experimental tools and techniques used in the present study are elaborated. Finally, the formulations used for the calculations of the efficiencies of the burners based on both the first and the second law of thermodynamics are presented.

3.2 DESIGN CRITERIA OF COOKING STOVE

The basic design criteria of a cooking stove is based on the output power requirement. For domestic cooking, the required output power range is 0.6-2 kW_{th} (Mukunda et al., 1988). The other parameters to be considered for the design of a stove are: low ignition time, high combustion efficiency i.e., low emission of NO_x and CO and better flame stability. The commercially available kerosene cook stoves are designed to operate at ~ 2 kW_{th}. In the present study, a BIS specified kerosene pressure stove was used with a specified fuel

consumption rate of (190 g/hr ± 15%), yielding an output power of ~1.3 kW_{th}. In the following pages, the experimental setup fabricated from the BIS stove to study its performance with PM is described.

3.3 DESCRIPTION OF THE EXPERIMENTAL SET UP

The experimental setup was developed from a BIS stove keeping most of the components similar to the original stove, however, the main component, i.e., the burner was designed in an entirely different fashion. In this section, first, the construction and operation details of the BIS stove that was used in the present study is described. Figure 3.1(a) shows a schematic of the BIS stove. Its principal components are a fuel tank with a hand operated plunger, a spirit cup, a vapour burner, a fuel regulator, a flame holder, a heat shield and a pot holder. The vapour burner (Figure 3.1 (b)) consists of one rising tube, two ascending and two descending tubes and a flat circular chamber called vaporizer. A spray nozzle is attached to the descending tubes. The function of the spray nozzle is to spray kerosene vapour on application of pressure in the kerosene tank. When fuel tank is pressurized, kerosene flows to the vapour burner and gets vaporized in the vaporizer. The vapour then sprayed through the nozzle mixes with air and burns, giving rise to a blue flame. Thus, the combustion takes place in the gaseous environment. This type of combustion is dominated by convection and is known as free-flame combustion.

The free-flame combustion is different from the PMC, in which the flame is submerged within the porous matrix and radiation becomes the dominant mode of heat transfer. In the modified stove, the burner utilizes the concept of the PMC and operates on radiant mode, giving rise to a flameless combustion. Figure 3.2 shows a schematic of the experimental setup used for development of the modified stove.

1: Fuel tank, **2**: Hand operated plunger pump, **3**: Fuel regulator, **4**: Rising tube, **5**: Spirit cup, **6**: Heat shield, **7**: Vapour burner with flame holder, **8**: Pot holder.

(a)

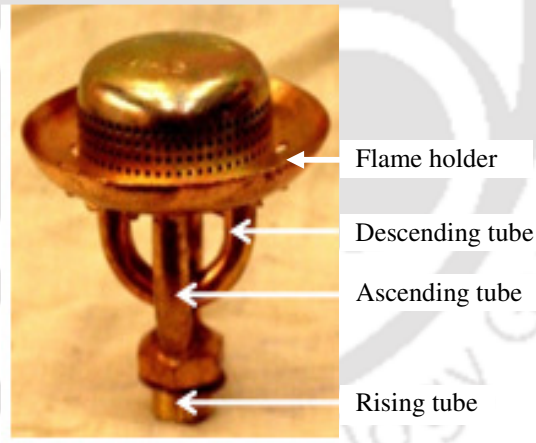

(b)

Fig. 3.1: Picture of (a) conventional kerosene pressure stove (b) vapour burner.

The experimental setup consists of a fuel tank with a hand operated plunger, two air ducts, a fuel duct attached to a vapour burner, an air compressor with pressure regulator, a heat shield, a PB enclosed in a metal casing, a wire mesh supporting PM and an spirit cup/oil

plate. The role of vapour burner is to assist in the vaporization process. The fuel duct is centrally located while the air ducts are positioned from the sides of the casing. Air supply is given from a compressor. The compressor was used to create an undisturbed flow of air and to study the effects of equivalence ratios on efficiencies and emissions. A heat shield is provided across the top surface of the casing to restrict heat transfer to the sides and direct the same to the load.

The operating principle of the stove is as follows. Initially, as in the conventional stove, a small amount of kerosene is burnt in the spirit cup/oil plate and the vaporizer receives heat from it. The ignition is initiated by burning a wick which is inserted into the casing through a 30 mm × 30 mm slot (Fig. 3.2(b)). Once the vaporizer is sufficiently heated, kerosene gets vaporized and the hot vapour mixed with air moves up to the PM. The hot mixture then burns within the media and it receives heat through convection. The media becomes hot and it starts radiating heat in all directions. The vaporizer continues to receive heat from the PM and transfers it to kerosene and the cycle continues. At this stage, the burning wick is taken out and the slot is covered with a small window. On attainment of steady-state, various measurements were taken.

Figure 3.3 shows a picture of the experimental setup. This picture gives a better comparison with the conventional stove shown in Figure 3.1 (a). The two major components of this stove which are not present in the conventional stove are: the air ducts and the casing with PM. Additionally, in the modified stove, the flame holder as shown in Figure 3.1 (b) is not present instead, the PM itself acts as a flame holder. Due to the porous nature of the material, the flame is trapped within the PM and stabilizes there. Besides, the pot holder is also fixed at different heights.

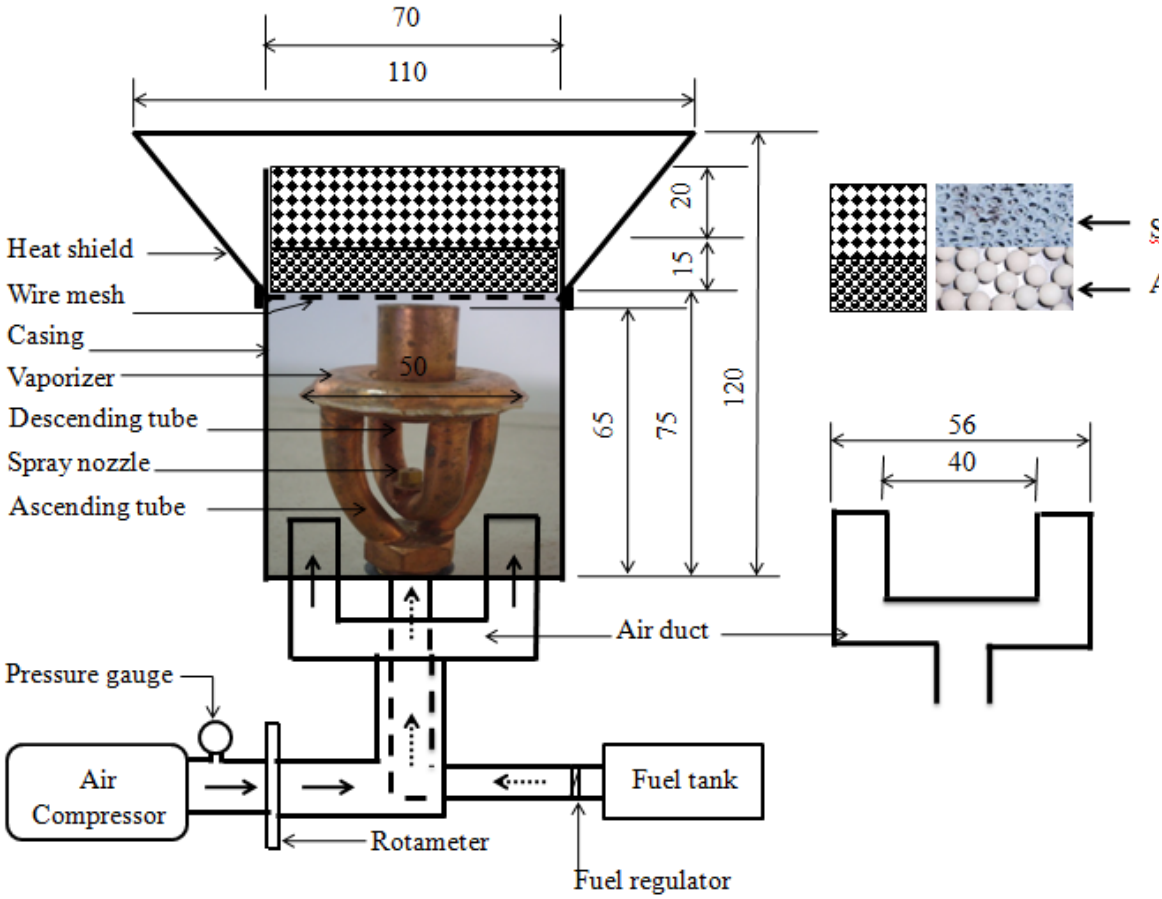

(a)

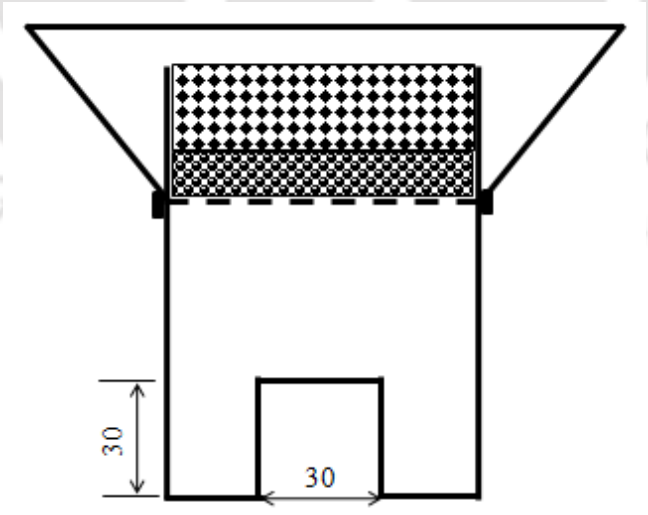

(b)

Fig.3.2: (a) Schematic of the experimental setup and (b) view of the setup showing ignition slot.

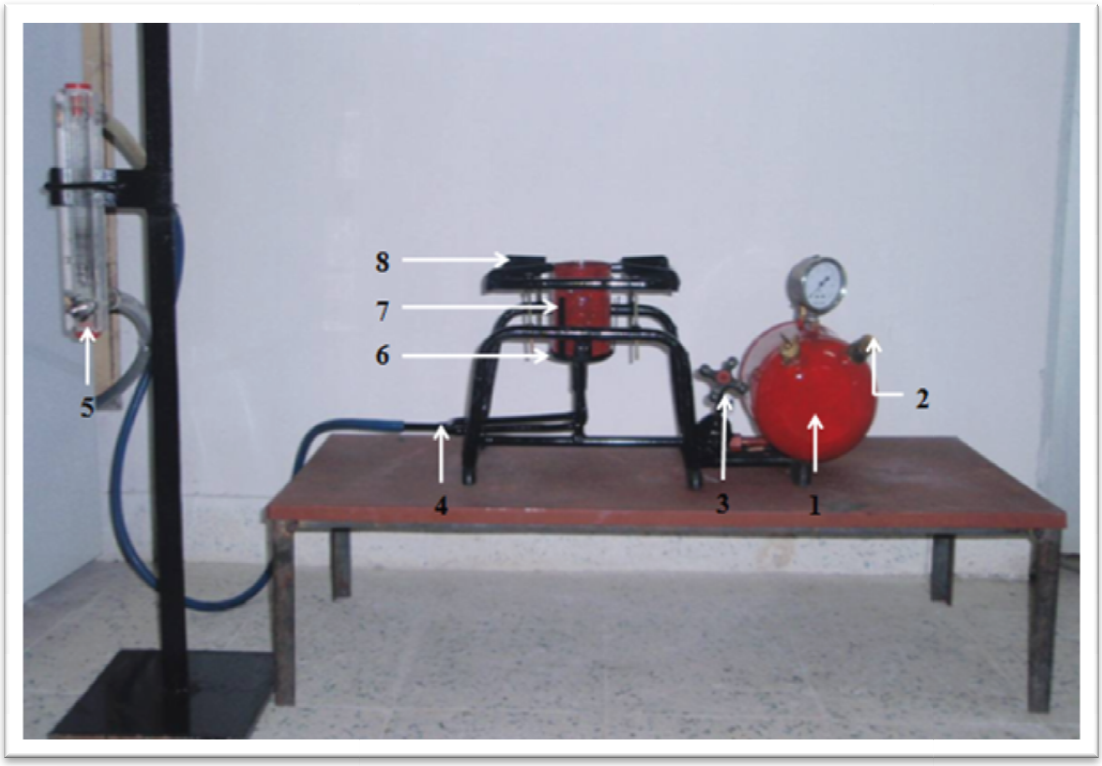

1: Fuel tank, **2:** Hand operated plunger pump, **3:** Fuel regulator, **4:** Air duct, **5:** Rotameter **6:** Oil plate, **7:** Casing containing porous burner, **8:** Pot holder

Fig. 3.3: Picture of the experimental setup.

3.4 DESIGN CRITERIA AND SELECTION OF POROUS BURNER

The most important design criterion for PB construction is the material with good thermo-physical properties as it helps in improving heat transport from the burned gases to the unburned reactants. Besides this, the other factors to be considered are the length of the porous bed, the length of the preheat and the combustion zones (in case of a bi-layered PB), the shape and orientation of the combustion chamber etc. (Mujeebu et al., 2009a). Proper selection of PM with good thermo-physical properties helps in stabilization of flame within PB. The flame stabilization process is very complex as it involves an intimate coupling of combustion, heat transfer and fluid dynamics (Xiong, 1995).

The materials used in the current study for construction of PBs are SiC, Al_2O_3 balls, ZrO_2 and metal (stainless steel) balls. Most of the experiments were however, conducted with the combination of SiC and Al_2O_3 due to their abundance and easy availability. ZrO_2 was largely avoided due to their higher cost compared to SiC and metal balls were not preferred, although they are cheap and easily available, as at elevated temperature, their thermal degradation is high (Pickenäcker et. al., 1999). Thus, the choices were restricted between SiC and Al_2O_3 as they are relatively cheap and, they exhibit good thermal and radiative properties. These materials were obtained from Mica industries, Pune, while the metal balls were procured in local shops. Table 3.1 summarizes the sizes of the PM used in the present study and Figure 3.4 shows their pictures.

Table 3.1: List of materials used for PB construction

Materials	Pore size (ppi)	Diameter (mm)	Thickness (mm)	Porosity (%)
SiC plate	10, 20	70, 80, 90	20	90
ZrO_2 plate	10, 20	70	20	90
Al_2O_3 ball	-	5,7	-	30,40
Metal ball	-	7	-	30

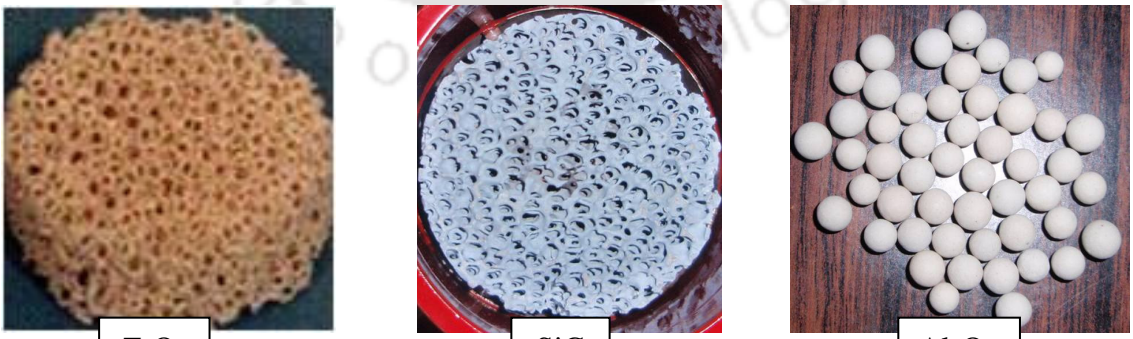

Fig. 3.4: Pictures of different types of ceramics used for PB construction.

As evident from Figure 3.4, SiC and ZrO_2 are honeycomb type, while Al_2O_3 are in the form of spheres. Initially, these materials (SiC+ Al_2O_3) were stacked together in different combinations and the baseline combination was identified based on the ability to retain flame completely within the PM. Figure 3.5 illustrates the schematic of various combinations of the PM tried, and this is followed by a discussion on their performances.

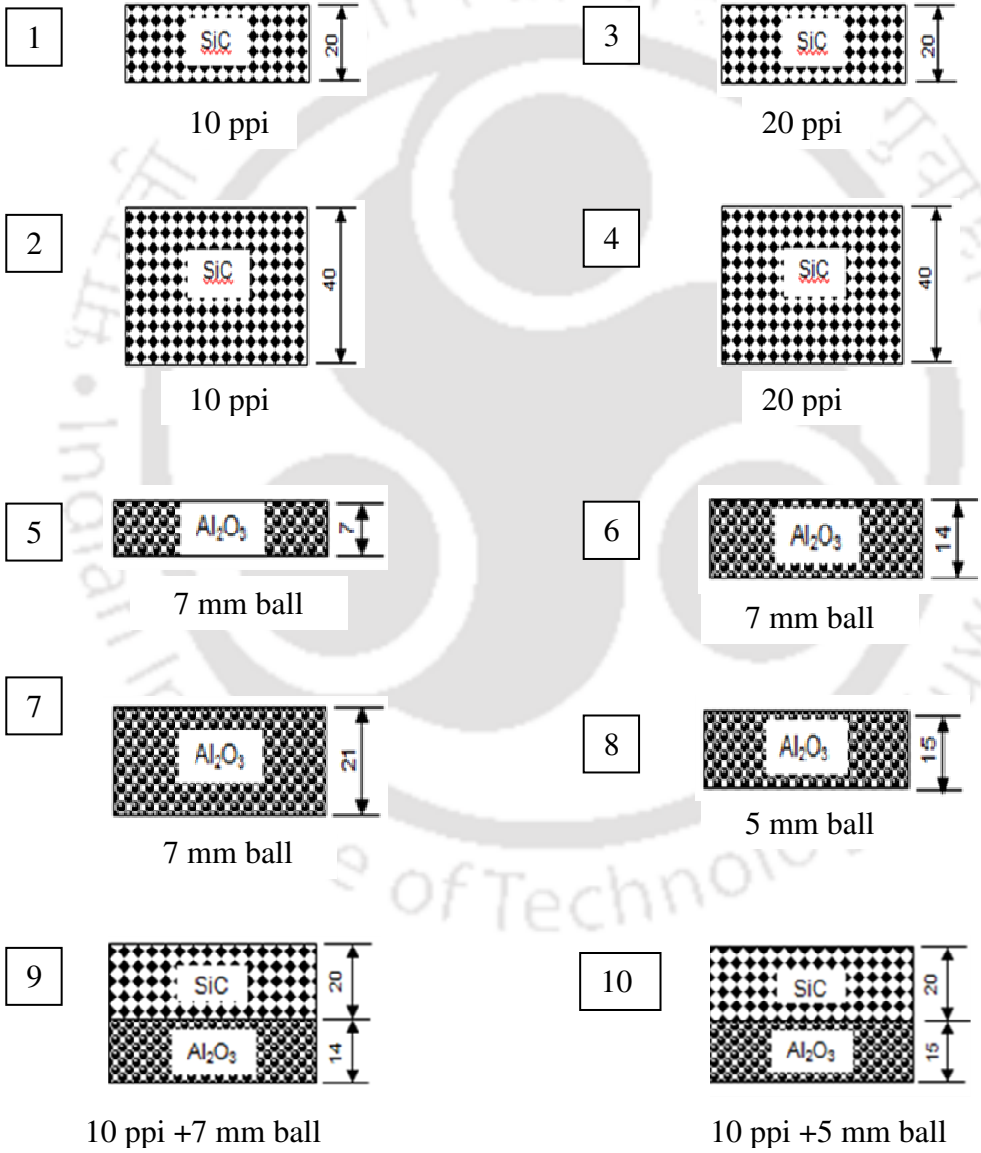

Fig. 3.5: Schematic of different combinations of the porous media configurations.

Configuration 1: In configuration 1, a single piece of 20 mm thick, 70 mm diameter SiC having pore density 10 ppi was used as the porous bed, and the behavior of the stove with this combination was observed for varying air flow rates. At all air flow rates, a short blue flame was found to hover over the top surface of the media, and this confirmed the bed thickness was not sufficient enough to entrain the flame completely. Hence, in the next configuration i.e., configuration 2, the thickness was increased to 40 mm.

Configuration 2: In configuration 2, no flame was seen over the top surface of the PM. Rather, it became red hot as the enthalpy of combustion released in the gas phase heated it up to incandescence. It emitted thermal radiation in both upstream and downstream directions. High upstream temperature was however not desirable, as the objective was to achieve higher heat flux in the downstream. Hence, this configuration was not considered.

Configuration 3: In configuration 3, a single piece of 70 mm diameter, 20 ppi SiC was used as porous bed and it was observed that like, configuration 1, in this configuration also, flame was not completely entrained within the porous bed. A short blue flame was seen over the surface. This confirmed that for complete retention of the flame within the porous bed, the bed thickness should be greater than 20 mm.

Configuration 4: In configuration 4, two pieces of 70 mm diameter, 20 ppi SiC were stacked together. In this configuration, flame was completely retained within the porous bed. The solid matrix was heated to incandescence and like configuration 2, the flameless combustion was achieved. However, within the pores of the matrix, deposition of soot was observed. Thus, between 10 ppi and 20 ppi, 10 ppi was preferred.

Configuration 5: In configuration 5, a packed bed of single layer of 7 mm diameter, Al_2O_3 balls (porosity: 40%) were used. In this configuration, balls were heated to incandescence, but a long blue flame was seen over the porous bed. This was due to insufficient porous bed thickness as observed in configurations 1 and 3.

Configuration 6: In configuration 6, a packed bed of 2 layers of 7 mm diameter, Al_2O_3 balls (porosity: 40%) were used. In this configuration also flame was not completely retained within the porous bed; a small blue flame was seen at the top of the PM. The reason is again the same as for the configuration 5.

Configuration 7: In configuration 7, a packed bed of 3 layers of 7 mm diameter Al_2O_3 balls with porosity 40% were used. In this configuration, combustion was successfully initiated, however, the air/fuel mixture did not move up, instead the burning took place below the bottom ceramic. This was owing to higher pressure drop on account of the tortuous bed. It was realized that increased bed thickness of Al_2O_3 balls posed difficulty in overcoming the resistance offered by the porous bed to the moving fluid. This observation helped to arrive at a conclusion that for undisturbed fluid propagation, it is important to have Al_2O_3 bed thickness less than 21 mm.

Configuration 8: In configuration 8, the porous bed was composed of 3 layers of Al_2O_3 balls having 5 mm diameter and porosity 40%. In this combination also, air-fuel mixture did not move up, and burning took place below the bottom layer. This was due to large pressure drop resulted on account of increased in solid porous layer. Thus, this observation confirmed that the number of Al_2O_3 ball layer should be less than 3 as with increase in ball layer the pressure drop increases.

Configuration 9: In configuration 9, a packed bed of 2 layers of 7 mm diameter, Al_2O_3 balls (porosity: 40%) and a single piece of 70 mm diameter, 10 ppi SiC were used to construct the porous bed. SiC was placed over Al_2O_3 balls. The idea of putting Al_2O_3 at the bottom and SiC at the top was to minimize upstream heat loss and to maximize heat transfer in the downstream. Al_2O_3 being low emissive material was expected to provide maximum downstream and minimum upstream radiative heat loss. Upstream radiative loss is undesirable because it is a waste of energy, while the downstream radiative loss is used for thermal applications.

Kayal et al. (2005) reported that the downstream heat transfer is important, as the heat is used for thermal load, while the upstream heat transfer is undesirable because it is a waste of energy. The maximum downstream radiative heat transfer through high surface temperature can be achieved by the use of high PM in the downstream section (Kaplan and Hall, 1995). Besides, the small pore material at the upstream and the larger pore at the downstream increase the stability of the combustion zone, due to the change in turbulence intensity and optical path length of the materials (Kaplan and Hall, 1995). Further, the small porosity material acts as a radiation shield between the high temperature side and the fuel vaporization zone, as it has shorter optical path length (Wei et al., 2002).

Experiments were conducted at different air and fuel flow rates and the combustion behaviour was observed. It was revealed that combustion in this configuration was much better than any other configuration tried. The burning characteristics were very much closer to the expected one. The flame was completely retained within the porous bed and there was no soot deposition. Fluid motion was undisturbed. The upstream heat transfer through convection and radiation was lower than the downstream owing to the low

emissive nature of Al_2O_3. The bottom temperature i.e., the temperature below the porous matrix was found to lower by ~200 ^oC when compared with the combination of SiC and SiC (configuration 2).

Configuration 10: In configuration 10, a packed bed of 3 layers of 5 mm diameter, Al_2O_3 balls (porosity 30%) and a single piece of 70 mm diameter, 10 ppi SiC were used as porous bed. In this configuration, like configuration 9, flame was embedded within the porous bed, the solid matrix became red hot and emitted radiation. However, there was soot deposition within the porous bed as there was increased pressure drop owing to increase in Al_2O_3 layer. Besides, smaller pore diameter led to local extinguishment of the flame.

Thus, among all the configurations considered, the configuration 9 was the optimal one as in this configuration, the combustion was soot free and combustion took place within the PM. Besides, it helped to restrict the heat transfer from the PM to the vaporizer through use of Al_2O_3 at the bottom.

Al_2O_3 and SiC were housed in a metal casing and the experiments were conducted with their different types. Figure 3.6 shows the schematic of the different casings tested. The symbolic representations of the casing are as follows. 70SCC: 70 mm straight cylindrical casing; 60SCC: 60 mm straight cylindrical casing; 80SCC: 80 mm straight cylindrical casing; 70SCCWHS:70 mm diameter straight cylindrical casing with heat shield; 70TCWHS: 70 mm conical casing with heat shield; 70CCWHS: 70 mm taper casing with heat shield. The dimensions of the casings were fixed based on several experiments with different aspect ratios (ratio of length to diameter). The distances between the vaporizer

and the air ducts and also the vaporizer and the PB were varied and based on the results of emission yielding lower CO and NO_x, the optimum length was fixed.

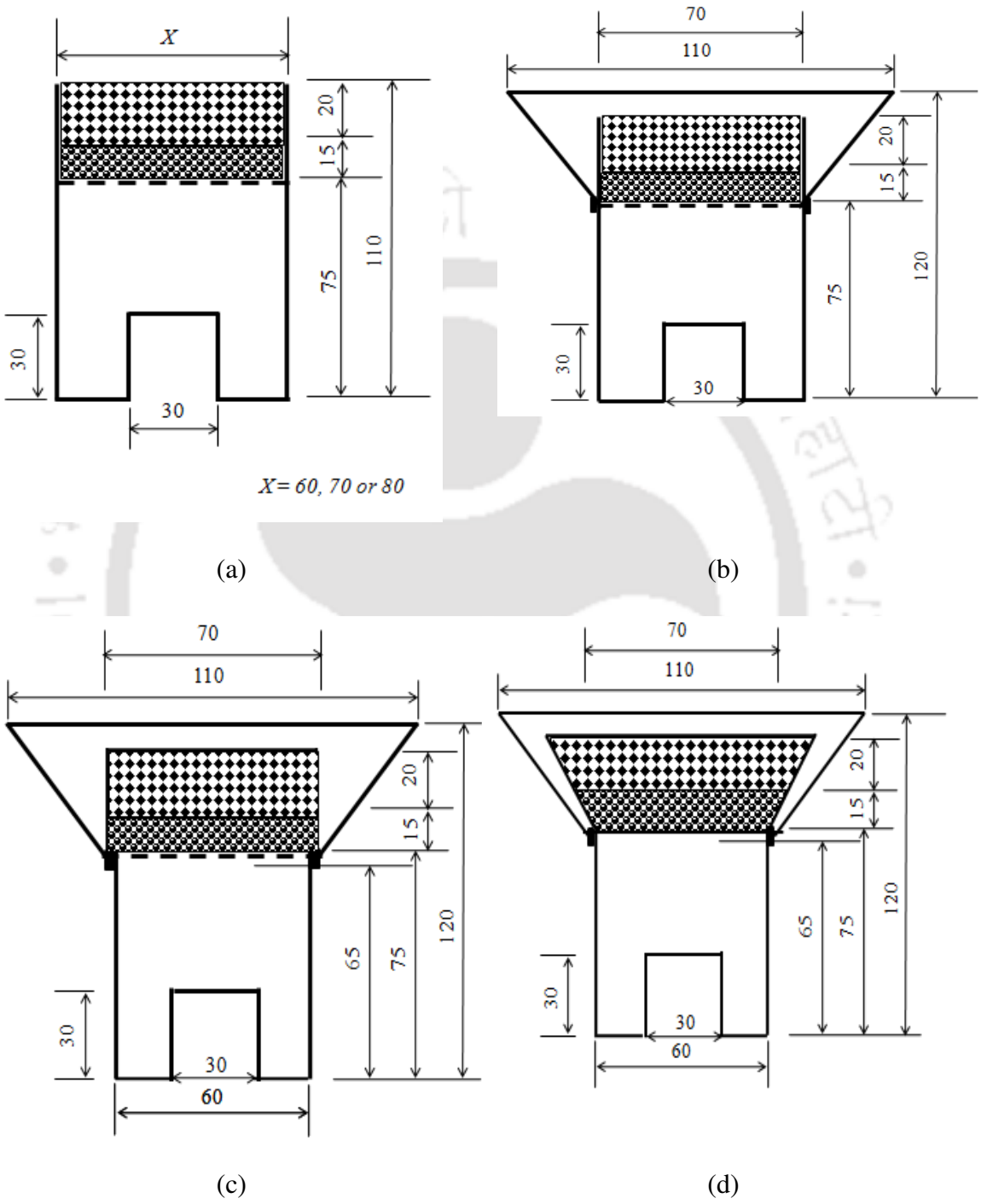

Fig. 3.6: Schematic of the different types of casings (a) 60SCC, 70SCC, 80SCC (b) 70SCCWHS (c) 70TCWHS and (d) 70CCWHS.

Different diameters were chosen starting from 60 mm to 80 mm so as to find out the optimum one in terms of better temperature distributions. Initial 60 mm was fixed considering the diameter of the vaporiser (50 mm, shown in Figure 3.2 (a)) and the minimum allowable passage for air flow through the air ducts. Diameter beyond 80 mm was not chosen since the radial temperature distribution in 80 mm was found non uniform when compared to 60 or 70 mm burner (results discussed in Chapter 4, section 4.2.1). Further, a heat shield was added around the casing efficiencies with an aim of increasing efficiency thereby delaying the flue gas dispersion to surroundings. Lucky and Hossain (2001) demonstrated the useful of heat shield in their study on different cook stoves.

The following paragraphs describe the various measurement tools and techniques that were adopted for performance evaluation of the burner. The detail specifications of various instruments are presented in the Annexure C.

3.5 MEASUREMENT TOOLS AND TECHNIQUES

A strain gauge based weighing balance (Figure 3.7) (least count: 1 g and range: 30 kg) with digital display was used for the measurement of fuel consumption during the thermal efficiency test. The thermal efficiency defined as the ratio of heat absorbed by the load to the heat given by fuel. It is estimated using the standard water boiling test (WBT). In WBT, the stove is first placed over the platform (size: 400 mm × 300 mm) of the weighing. The ignition is carried out with a burning wick as per the procedure described in section 3.3. Upon attainment of the steady-state, a flat aluminium vessel with a known quantity of water is placed over the stove. Water is then allowed to heat up by the thermal power of the stove and the heating continues till it attains a temperature of 90 ^{o}C. The initial temperature of water is measured with a mercury thermometer having a range of -1

to 100 ^{o}C. The time required to bring the water from room temperature to 90 ^{o}C is noted and also, the mass of the fuel consumed during this period is recorded by the difference in mass before and after heating. This gives information about the fuel consumption rate and on combining this data, with the calorific value of the fuel, the heat input is found out. The calorific value is taken from the BIS standard (IS 10109:2002) and also verified with a bomb calorimeter using the ASTM standard: 240D. The detail calculation of the calorific value is presented in Annexure D.

(a) (b)

Fig. 3.7: Picture of (a) weighing balance (Make: SARTORIUS) and (b) Bomb calorimeter (Make:IKA).

Heat output is the combination of the water, the vessel and the water vapour. The sensible heat taken by water and the vessel is calculated considering the mass, specific heat and the temperature rise from the room temperature to 90 ^{o}C. The heat carried away by the water vapour that is formed when it is heated from the room temperature to 90 ^{o}C is calculated by multiplying its latent heat of vaporization with the mass of water vapour, obtained by measuring the difference in the weight of the water before and after heating.

The ratio of heat output to the heat input gives the information of thermal efficiency of the burner. The formula used for efficiency calculation is presented in the latter part of this chapter.

For emission analysis, specified standard hood method specified by BIS standard: IS 10109: 2002 was used. An extraction hood was constructed according to the specifications and placed above the stove through which flue gases were allowed to pass. Figure 3.8 (a) and (b) show the schematic (IS: 10109, 2002) and picture of the hood used, respectively. The sampling was done by a flue gas analyzer (TESTO 350 XL) (Figure 3.9) incorporated with electrochemical sensors having accuracy of ±5%. Emission data are reported on dry basis corrected to 3% O_2 with the measurement uncertainty of ±5%. NO_x (NO and NO_2) and CO were measured experimentally, while CO_2 was calculated from stoichiometry.

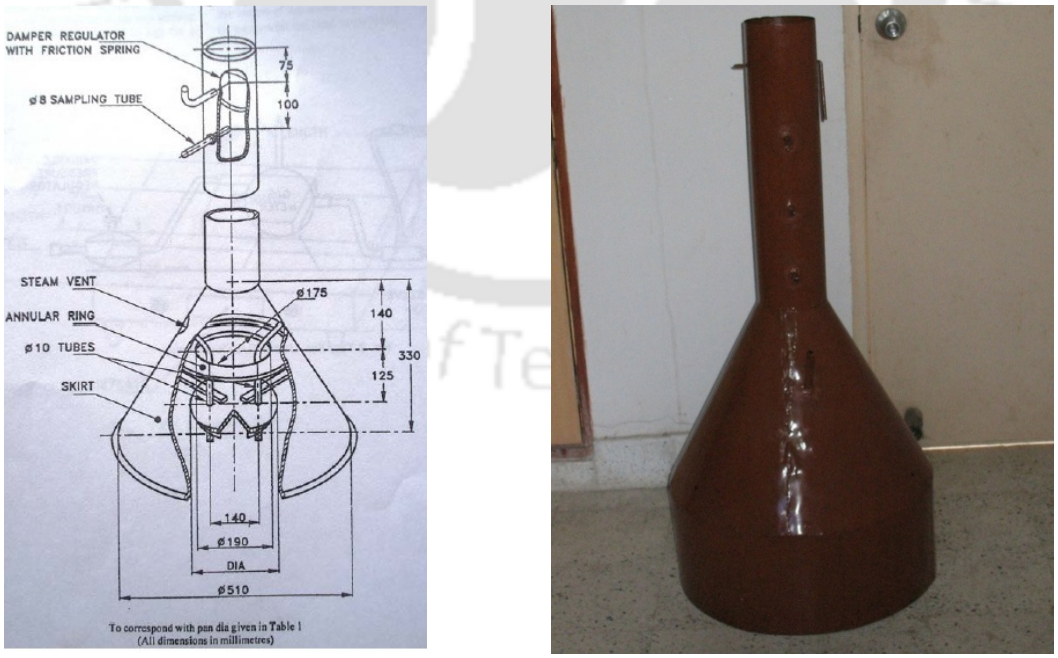

(a) (b)

Fig. 3.8: (a) Schematic (IS10109, 2002) and (b) picture of extraction hood used in

emission measurements.

Temperature measurements of the PB were taken with some specially made metal sheathed K-type thermocouples with two different varieties: one with grounded junction and the other with exposed junction, as shown in Figure 3.10 (a) and (b). The grounded junction thermocouple was used to measure temperature at the interface of the two media SiC and Al_2O_3 while, the exposed junction type was used to measure the temperature at the surface. The readings from both these thermocouple were interpreted with a data acquisition system Agilent 34970A (Figure 3.10 (c)) which converts the electrical output into the corresponding temperature.

Fig. 3.9: Picture of the gas analyser (Make: TESTO 350XL).

For radial temperature measurements at the surface of 60SCC, 70SCC and 80SCC burner (Figure 3.5 (a)), the diameters of the PM were divided into a number of equidistant divisions (6 for 60SCC and 70SCC burner and 8 for 80SCC burner) and the measurements were taken at specified locations as shown in Figure 3.11. The distance

between the two adjacent measurement locations is 10 mm. In the temperature plot, the distance between the centre and first sets of points viz., pt. 3, in 60SCC and 70SCC burner and pt. 4, in the 80SCC burner are marked as "+10" and the similar sets on the other sides i.e., pt. 4 for 60SCC and 70SCC, and pt. 5 for 80SCC burners are marked as "-10". Likewise, the second sets of points are marked "+20,-20", the third sets are labelled as "+30,-30" and the fourth sets in case of 80SCC burner, are marked as "+40,-40".

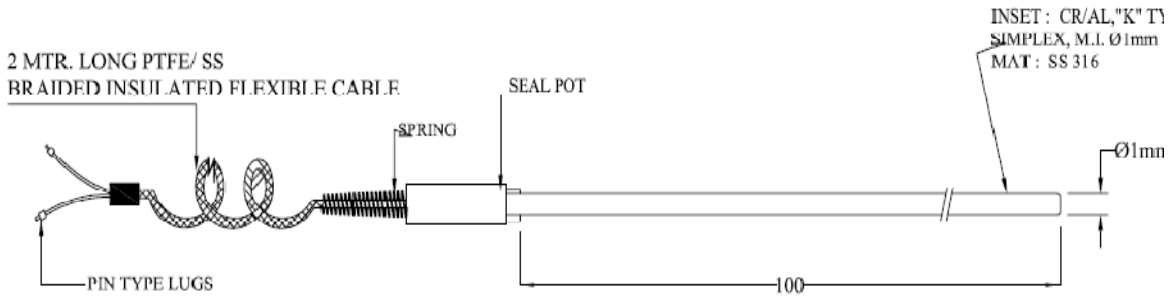

(a)

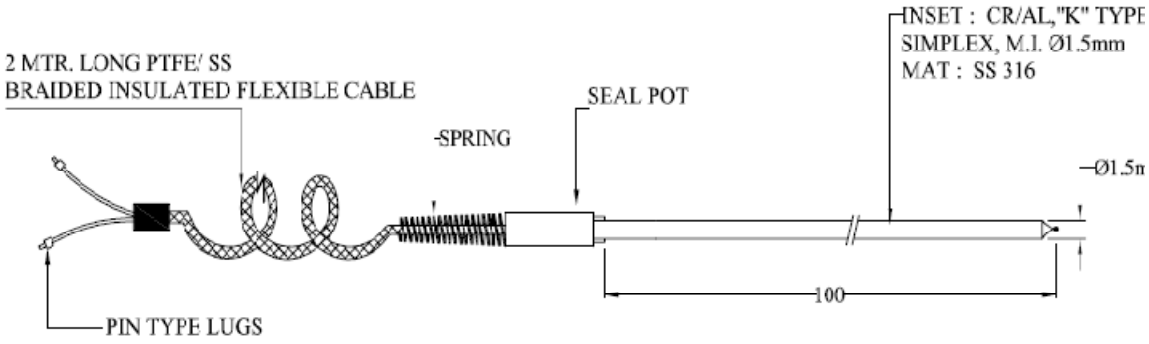

(b)

(c)

Fig. 3.10: Specifications of the metal sheathed (a) grounded K- type thermocouple (b)

exposed K- type thermocouple (c) Agilent data acquisition system.

Based on the temperature distributions and also, considering a few other parameters like thermal efficiencies and emissions, the optimum diameter casing was selected and the temperature measurements were further taken to ascertain maximum accuracy. Figure 3.12 (a) shows the radial temperature measurement points (pt. 1, pt. 2, …..pt. 12) at the surface of 70SCCWHS, 70TCWHS and 70CCWHS burners.

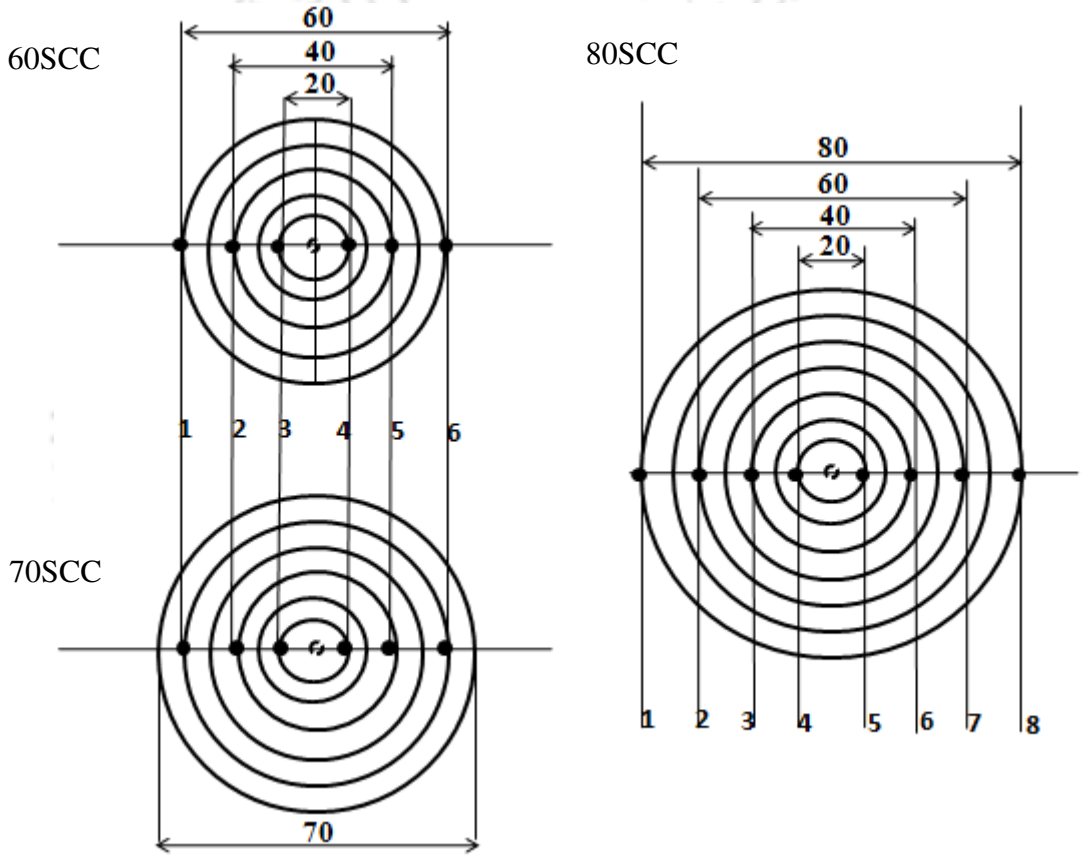

Fig. 3.11: Radial surface temperature measurement points for 60SCC, 70SCC, 80SCC burner.

As seen, temperatures were recorded along the diameter of the PB in two perpendicular directions. The top surface of the PM is divided into 6 equidistant divisions (Fig. 3.12(a)) and the distance between the two divisions is 10 mm. The first and the last divisions along

a given direction are 5 mm away from the outer edge of the PM. Measurements were taken at the specified positions and values are reported.

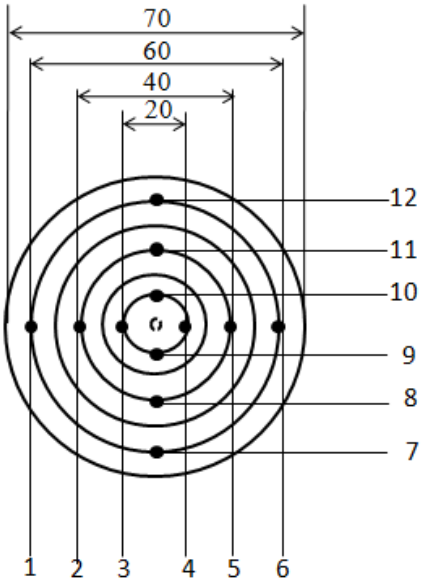

(a)

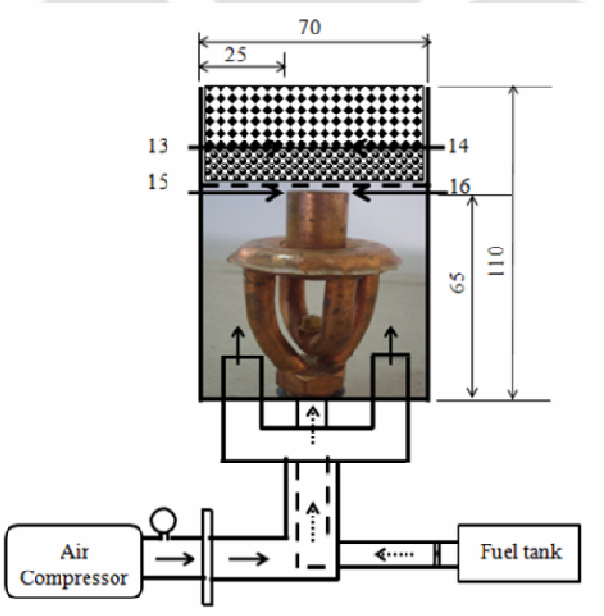

(b)

Fig. 3.12: (a) Radial locations of thermocouples on the burner surface for temperature measurement and (b) axial locations of thermocouples for temperature of measurement.

As shown in Fig. 3.12(b), axial temperature measurements were taken at 4 different locations, marked as points 13, 14, 15 and 16. Therein, two (13 and 14) thermocouples were inserted at the interface between Al_2O_3 balls and SiC, and two (15 and 16) were inserted 10 mm below the wire mesh.

Air flow rate was measured by a rotameter (make: Flow tech engineers) having range 0-400 litres per minute (lpm) and pressure by a dial type pressure gauge (make: Waree instruments) of 0-2 bar capacity. Another pressure gauge having same range was used to measure the kerosene tank pressure.

3.6 EXPERIMENTAL REPEATABILITY AND UNCERTAINTY ANALYSIS

All experiments were repeated thrice and the average values are reported. The error associated with the efficiency of the stove is estimated using sequential perturbation technique (Kline and McClintok, 1953). It was found to be within ± 2.1%. The details of the calculation procedure are given in Annexure E.

3.7 FORMULATIONS FOR ENERGY AND EXERGY ANALYSES

In the present work, the performance of the stove is analysed from the view points of both energy and exergy analyses. The convention way of performance evaluation of thermal system is based on energy analysis. However, exergy analysis provides a better understanding of a system indicating energy degradation. The exergy efficiency is a true measure of performance of a thermal system, and it helps to assess accurate utilization of energy. To evaluate the exergy flows associated with a cooking device, the standard atmosphere is taken as the reference environment. The following are the formulae used in

energy and exergy (available energy) analyses for estimation of energy and exergy efficiencies.

The energy or heat input $Q_i\,(kW)$ to the cooking stove is given as

$$Q_i = \dot{m} \times \text{LCV} \tag{3.1}$$

where $\dot{m}$ is the mass flow rate (kg/s) and LCV is the lower calorific value of fuel (kJ/kgK)

For smooth operation, air supply was from a compressor. The compressor work $W_c\,(kW)$ is also considered as an input parameter to the system. It is calculated from the following equation.

$$W_c = \frac{1}{0.80 \times 0.90}\left[\dot{m}_a \times R \times T_1\left[\left(\frac{n}{n-1}\right)\left(\frac{P_2}{P_1}\right)^{\frac{n-1}{n}} - 1\right]\right] \tag{3.2}$$

where $\dot{m}_a$ is the mass flow rate (kg/s) and $R = 0.287$ (kJ/kgK) is characteristics gas constant, $n = 1.2$ is the index of compression, $P_2 = 1.2$ bar is the final pressure and $P_1 = 1.013$ bar is the initial pressure. The mechanical and that of the motor transmission efficiencies of the compressor are assumed to be 80% and 90%, respectively. With these date the compressor is found to be 0.035 kW. The calculation for compressor power is shown in Annexure F.

Thus, $Q_i + W_c$ is the heat input to the burner. For calculation of heat output, 3 parameters are to be considered. They are heat gained by the water, water vapour and vessel. The following formulae are used for calculation of the same.

Heat taken by water,

$$Q_1 = m_w \times c_{pw} \times \left(T_f - T_i\right),\ (kJ) \tag{3.3}$$

where m_w is the mass of water (kg), c_{pw} is the specific heat of water (kJ/kgK), T_f is the final temperature of water and T_i is the initial temperature of water.

Heat taken by water vapour

$$Q_2 = m_{wvp} \times L,\ (kJ) \tag{3.4}$$

where m_{wvp} is the mass of water vapour (kg), L is the latent heat of vapour (kJ/kg)

Heat taken by vessel

$$Q_3 = m_v \times c_{pv} \times \left(T_f - T_i\right),\ (kJ) \tag{3.5}$$

where m_v is the mass of vessel (kg), c_{pv} is the specific heat of water (kJ/kgK), T_f is the final temperature of vessel and T_i is the initial temperature of vessel.

Total output is given as

$$Q_1 + Q_2 + Q_3 \Big/ t,\ (kW) \tag{3.6}$$

where t is the time (s) taken by water to reach 90 ^{o}C when brought from room temperature

First law efficiency or thermal efficiency is

$$\eta_I = \left(\frac{Q_1 + Q_2 + Q_3}{Q_i + W_c}\right)\frac{1}{t} \tag{3.7}$$

A part of heat released from fuel is lost to the surrounding through convection and radiation and thus the available heat energy at the exit of the burner is lower than the chemical availability. The available energy or exergy of the hot gases at the exit of the burner can be calculated in the following manner.

The heat energy of the hot gases at the exit of the burner is given as

$$Q_g = \dot{m}_g \times c_{pg} \times \left(T_g - T_o\right),\ (kW) \tag{3.8}$$

where $\dot{m}_g$ is the mass flow rate of gas (kg/s), c_{pg} is the specific heat of gas (kJ/kgK), T_g is the gas temperature (K) and T_o is the ambient temperature (K).

Available energy with hot gases at the exit of the burner

$$A_g = \dot{m}_g \times c_{pg} \times \left(T_g - T_o\right)\left(1 - \frac{T_o}{T_g}\right),\ (kW) \tag{3.9}$$

The available energy of the hot gas is destroyed during heat transfer to the water, water vapour and vessel, and this causes changes in entropies of each of the components. These losses are calculated from the following;

Change of entropy of water can be given as

$$\Delta S_w = \int_{T_i}^{T_f} m_w c_w \frac{dT}{T} = \left(m_w c_{pw} \ln \frac{T_f}{T_i}\right),\ (kJ) \tag{3.10}$$

Non-available energy of water

$$\begin{aligned} T_o \Delta S_w &= T_o \left(m_w c_{pw} \ln \frac{T_f}{T_i}\right),\ (kJ) \\ &= \left(T_o \left(m_w c_{pw} \ln \frac{T_f}{T_i}\right) / t\right),\ (kW) \end{aligned} \tag{3.11}$$

Available energy of water

$$\begin{aligned} A_1 &= \left(m_w \times c_{pw} \times \left(T_f - T_i\right) - \left(T_o \Delta S_w\right)\right),\ (kJ) \\ &= \left(\left(\left(m_w \times c_{pw} \times \left(T_f - T_i\right)\right) - \left(T_o \Delta S_w\right)\right) / t\right),\ (kW) \end{aligned} \tag{3.12}$$

Change of entropy of water vapour (3.13)

$$\Delta S_{wvp} = \left(\frac{m_{wvp} L}{T_f} \right), \ (kJ/K)$$

Non available energy of water vapour

$$\begin{aligned} T_o \Delta S_{Wvp} &= T_o \left(\frac{m_{wvp} L}{T_f} \right), \ (kJ) \\ &= \left(T_o \left(\frac{m_{wvp} L}{T_f} \right) / t \right), \ (kW) \end{aligned} \tag{3.14}$$

Available energy of water vapour

$$A_2 = \left(\left(\left(m_{wvp} L \right) - T_o \Delta S_{wvp} \right) / t \right), \ (kW) \tag{3.15}$$

Change of entropy of vessel

$$\begin{aligned} \Delta S_v &= \int_{T_i}^{T_f} m_v c_{pv} \frac{dT}{T} \\ &= \left(m_v c_{pv} \ln \frac{T_f}{T_i} \right), \ (kJ) \end{aligned} \tag{3.16}$$

Non available energy of vessel

$$T_o \Delta S_v = \left(T_o \left(m_v c_{pv} \ln \frac{T_f}{T_i} \right) / t \right), \ (kW) \tag{3.17}$$

Available energy vessel

$$A_3 = \left(\left(m_v \times c_{pv} \times \left(T_f - T_i \right) - T_o \Delta S_v \right) / t \right), \ (kW) \tag{3.18}$$

Total available energy is

$$= \left(A_1 + A_2 + A_3 \right), \ (kW) \tag{3.19}$$

Exergy efficiency or second law efficiency or is thus given by

$$\eta_{II} = \frac{A_1 + A_2 + A_3}{A_g} \tag{3.20}$$

3.8. SUMMARY

In this chapter, the experimental setup as well as different tools and materials that have been used during the course of experimental study are introduced. Different combinations and configurations of the PM used to evaluate the burner performance are described. Details of experimental procedure and measurement techniques employed during the experimentation are also discussed. In addition, the formulation used for various calculations of the first law and the second law efficiencies are discussed.

In the next chapter, results of the energy analysis are presented.

भारतीय प्रौद्योगिकी संस्थान गुवाहाटी
Indian Institute of Technology Guwahati

CHAPTER 4

ENERGY ANALYSIS

4.1 INTRODUCTION

For a sustainable environment, two issues, viz., energy saving and environmental protection need to be stressed. In recent times, many new technologies have been developed, and the use of PM in combustor is one of them having potential to address the above concern. Towards above goal, this study reports the usefulness of PM in kerosene pressure stoves. This chapter includes the results of the energy analysis done on the stove with different casings under different operating conditions by varying air and fuel flow rates. Within the stable range, radial surface temperatures, axial temperatures, emissions and thermal efficiencies were examined. Through several sets of experiments, for a given burner, the optimum air flow rate, the fuel flow rate, the vessel size and the distance between the burner surface and the bottom surface of the vessel were identified. Results of the preliminary experiments conducted to establish the performance of the stove under two different conditions are addressed.

4.2 PARAMETRIC STUDIES ON PERFORMANCE OF KEROSENE PRESSURE STOVE INCORPORATED WITH POROUS MEDIA HAVING 3 DIFFERENT DIAMTERS

Thermal performance of the stove was judged from three different aspects, viz., (1) combustion stability, (2) emission and (3) thermal efficiency. For assessment of the combustion stability, the air and fuel flow rates were varied and the conditions where there is no flash back or blow off were noted. Flash back occurs when flame propagates

upstream and blow off occurs when flame propagates downstream beyond the topmost layer of the PM. These two conditions are considered as the stability criteria.

Initially, experiments were conducted at different air pressures, and the minimum pressure that keeps the flame attached to the PM was found to be 1.2 bar. This pressure was maintained for the entire series of experiments. Next, air and fuel flow rates were varied and it was found that at stoichiometric (air flow rate: 30 lpm and fuel flow rate: 160 g/hr) or near stoichiometric condition, the air/fuel mixture did not find its way through the PM, but it burnt below the Al_2O_3 layer in diffusion mode. This happened because, at lower air flow rates, the air draft was not sufficient enough to overcome the resistance offered by the PM. When the air flow rate was increased from 30-60 lpm, a sufficient draft was generated to push the air/fuel mixture into the PM. Thus, 60 lpm of air flow rate was found to be the minimum flow rate to prevent the flash back from the stove. Blow off occurred even at 1.2 bar, when the stove was operated beyond 180 lpm. Thus, the stable range was identified between the air flow rates of 60-180 lpm. Table 4.1 shows air and fuel flow rates with their corresponding equivalence ratios. The calculation procedure is shown in Annexure G. Annexure H shows sample efficiency calculation.

The equivalence ratio has a strong influence on burner performance (Jugjai and Rungsimuntuchart, 2002). It affects efficiency, emission and also the temperature profiles. The equivalence ratio can be changed either by changing the fuel flow rate or the air flow rate. In the conventional stove, since air is drawn through natural draft, the equivalence ratio is varied by changing only fuel flow rate. In the present experimental set up, since it is intended to study the effect of equivalence ratio on thermal performance of the burner, a provision was made to vary both the air flow rate and the fuel flow rate.

Table 4.1: Air and fuel flow rates with corresponding equivalence ratios.

Air flow rate (lpm)	Fuel flow rate (g/hr)	Equivalence ratio $\phi = \frac{\text{Stoichiometric air-fuel ratio (=14.8)}}{\text{actual air- fuel ratio}}$
60-180	160	0.18-0.55
60-180	170	0.19-0.58
60-180	180	0.21-0.62
60-180	190	0.22-0.65
60-180	200	0.23-0.69
60-180	210	0.24-0.72
60-180	220	0.25-0.75

In a conventional combustion system, due to poor heat transfer, the operation of the burner at very lean equivalence ratio is difficult. However, in a PM incorporated system, this problem is not experienced as there is a process of self-organized internal heat recirculation which allows the reactants to be preheated and the combustion to start at low temperature (Huang et al., 2002). Preheating plays a major role in sustaining the combustion reaction without being quenched. The lowest equivalence ratio at which the present setup operated was 0.18, representing a very lean condition. At such condition, the flame in CB does not sustain. In the present case it was possible because there was heat transfer from the SiC matrix to the incoming air-fuel mixture primarily through conduction and radiation as it is a highly conductive and radiative material. However, the operation at such a lean condition is not useful as the emission levels were found high and the thermal efficiencies were low. Figure 4.1 shows the variations of CO concentration with air flow rate (60-180 lpm) for 4 different fuel flow rates.

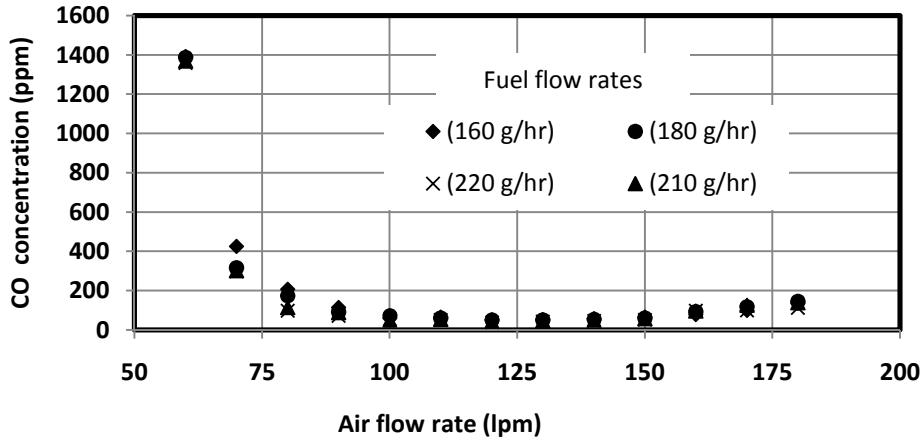

Fig. 4.1: Variations of CO concentrations with air flow rate for 4 different fuel flow rates.

It is evident from Figure 4.1 that with increase in air flow rate, the CO emission first decreases fast and then increases slowly. The highest emission (1400 ppm) is observed at 60 lpm which is attributed to incomplete combustion as it took place below the first layer, i.e., Al_2O_3 due to insufficient draft. As the air flow rate increases, the sufficient air draft improves the mixing of air and fuel within the PM, and this leads to lower CO emissions. The satisfactory air flow rate range, resulting lower emission was found to be 90-160 lpm. Beyond this range, CO concentration again increases.

In order to ascertain the reason for variations of emissions and thermal efficiencies at different air flow rates, the surface temperature profile of the burner was measured for different flow rates of air and fuel. The surface temperature of the burner is the indication of the amount of heat transferred from the burner surface to the load. The following paragraph describes the effect of air and fuel flow rates on surface temperature of the PM enclosed in straight cylindrical casings having 3 different diameters viz., 60 mm, 70 mm and 80 mm (60SCC, 70SCC, 80SCC).

4.2.1 Effects of air and fuel flow rates on surface temperatures of 60SCC, 70SCC, 80SCC burners

In a radiant burner, the measurement of surface temperature is important. It is a direct measure of transferrable heat flux which decides the thermal efficiency of the system. A surface with higher temperature is preferable as the radiant heat transfer is proportional to the fourth power of the temperature. Besides, with increase in surface temperature, the convective heat transfer also increases as the temperature differential with respect to the surroundings is high. Thus, herein, for the burner enclosed in 60 mm, 70 mm and 80 mm diameters casings viz., 60SCC, 70SCC and 80SCC, the surface temperatures were measured at different radial locations (Fig. 3.11). Further, the study of temperature distribution has relevance, since non-uniformity may result in local "hot spots" which will increase the NO_x level. Figures 4.2 (a)-(c) represent the variations of surface temperatures with radial distances. The measurements were carried out at an air flow rate of 120 lpm. The selection of air flow rate of 120 lpm is supported by the fact that at this particular air flow rate, the emissions of CO were found low (Fig. 4.1).

It is observed from Figure 4.2 (a)-(c) that the trends of temperature profiles in all the selected casings are the same. In all cases, the surface temperature decreases radially. The maximum temperature is observed at a distance of 10 mm from the centre of the PM, and the minimum is observed at 30 mm from the central point. However, the difference between the maximum and the minimum temperatures, in case of 60 mm diameter and 70 mm diameter casing is not very large. For the 60SCC burner, it is 5% and, for the 70SCC it is 7%. This indicates, the temperature distribution is radially uniform which is a desirable feature of the radiant burner, as non-uniformity results in greater amount of thermal NO_x.

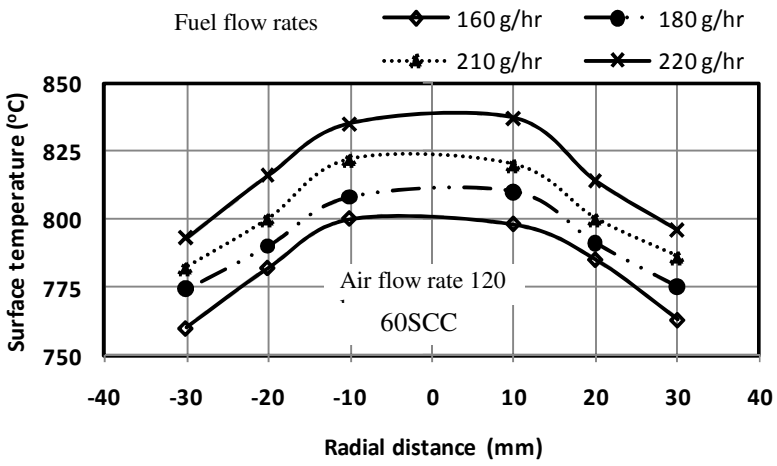

(a)

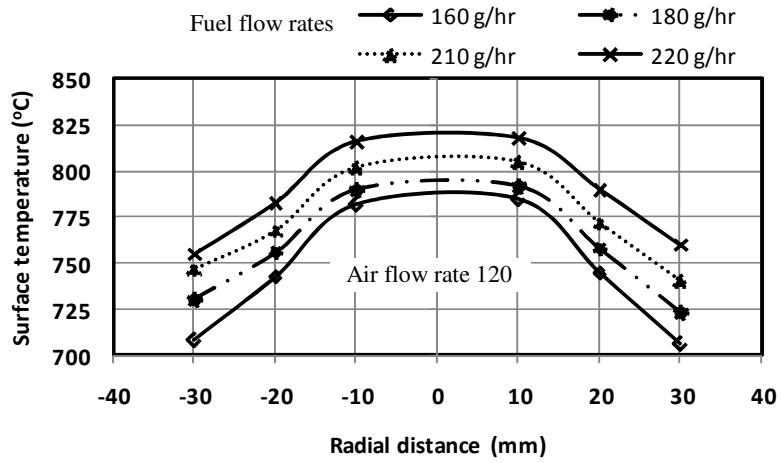

(b)

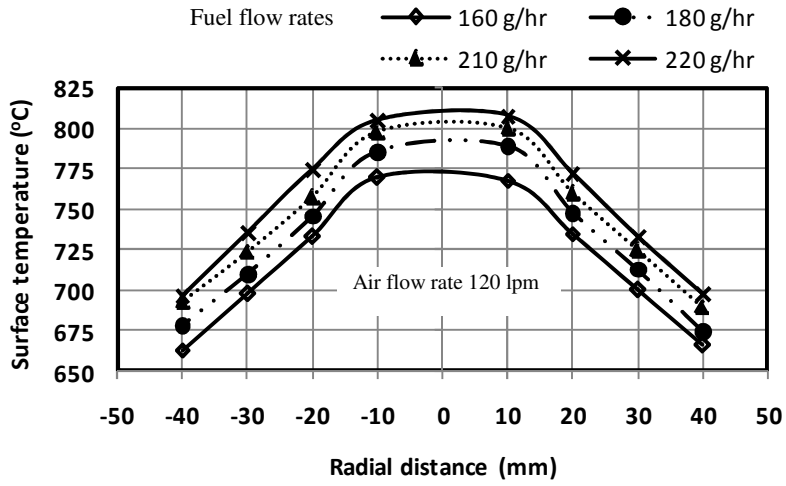

(c)

Fig. 4.2: Variations of surface temperatures of (a) 60SCC (b) 70SCC and (c) 80SCC with air flow rates for the 4 selected fuel flow rates.

For 80 mm burner, however, the difference in the maximum and the minimum temperatures is slightly higher (15%). The reason for this non-uniformity is attributed to the larger diameter of PM in comparison to the spray angle which led to a condition that the vapour coming out from the spray nozzle could not wet the entire surface of the PM.

Besides, the maximum temperature, in case of 80 mm diameter burner is lower (~810 ^{o}C). Among the 3 casings, the 60 mm diameter burner exhibits the highest temperature (~835^{o}C). Further, it is observed that the surface temperature increases with increase in fuel flow rates. The highest temperature is recorded for the fuel flow rate of 220 g/hr and the lowest for 160 g/hr. These variations in surface temperature with the fuel flow rates results variation in emissions and thermal efficiency of the system which is described in the following few pages.

4.2.2 Effects of air and fuel flow rates on emissions of 60SCC, 70SCC, 80SCC burners

The emission measurements were taken for 4 different fuel flow rates viz., 160 g/hr, 180 g/hr, 210 g/hr, 220 g/hr and air flow rate in the range of 100-150 lpm. CO was found to be dependent on both air and fuel flow rates while NO_x was found non typical, independent of fuel flow rate (heat input). With air flow rate also, the variation of NO_x is not significant, although there is a slight improvement at higher air flow rates. However, it remained low (between 1-2 ppm) for the whole operating range studied. This low value is due to homogenized temperature field and also, due to lower combustion temperature as there is recirculation of heat from the hot combustion products to the reactants. Figure 4.3(a)-(c) shows the variations of NO_x concentration with air flow rates for the 4 selected fuel flow rates.

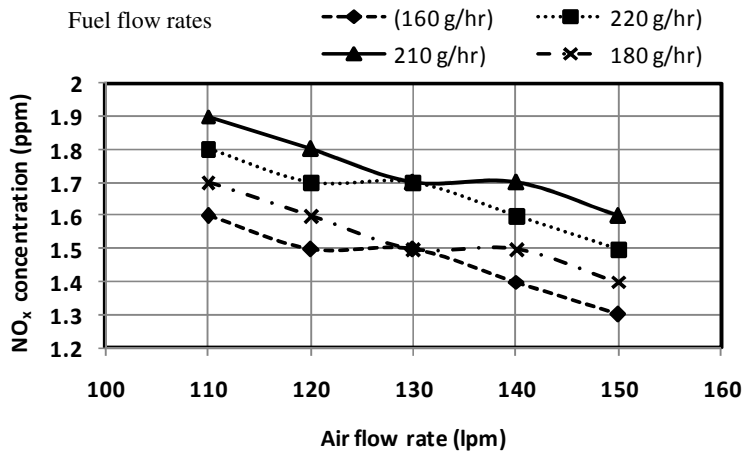

(a)

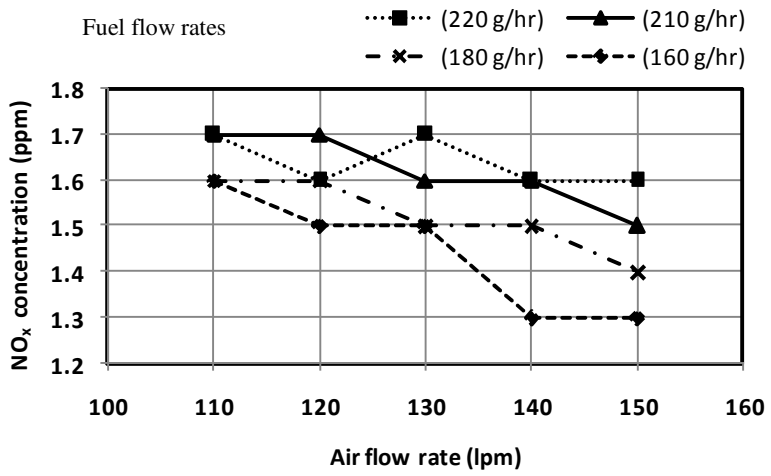

(b)

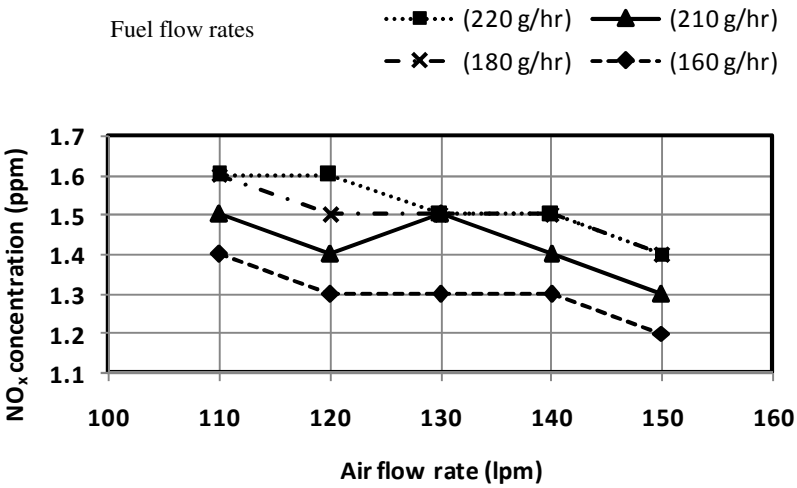

(c)

Fig. 4.3: Variations of NO_x emissions of (a) 60SCC (b) 70SCC and (c) 80SCC burner with air flow rates for the 4 selected fuel flow rates.

In lean combustion, NO_x is formed mainly through the thermal route; the contribution of prompt mechanism is not significant. Thermal NO_x is formed in the region of high localised temperature and the best way to reduce this is to lower the combustion temperature. In most of the PM incorporated thermal systems, this is found lower as the recirculation of heat lowers the combustion temperature (Delalic et al., 2004). In the present case also, the NO_x emission is low due to reduction of combustion temperature through supply of excess air, unlike a conventional stove which operates near stoichiometric condition having combustion temperature of 1500 ^oC (Mukunda et al., 1988). High combustion temperature is however, beneficial for reduction of CO. Figures 4.4 (a)-(c) shows the variation of CO concentration with air and fuel flow rates.

It is evident from Figures 4.4(a)-(c) that with increase in air flow rates, CO emission first decreases and then again increases. For all the casings, the lowest value is observed at 120 lpm. Beyond this flow rate, it increases and reaches the maximum at 150 lpm. This increase is attributed to lower residence time. At high air flow rates, the mixing of fuel and air is not adequate and this gives rise to increase in CO concentration. Similarly, at lower air flow rates, the mixing is influenced by insufficient air draft which again causes improper mixing. At higher fuel flow rates, CO concentration decreases due to higher combustion temperature. The lowest concentration of CO is found at the fuel flow rate of 220 g/hr. Among the 3 casings considered, the lowest CO concentration is observed in 70 mm diameter burner. Higher CO concentration in 80 mm burner is attributed to non uniformity of temperature. It is found that the combination of 70 mm diameter media with air flow rate of 120 lpm and fuel flow rate 220 g/hr results the lowest CO concentration, i.e., 45 ppm. This value is very much lower than that reported `by Kakati et al. (2007) for the conventional kerosene stove.

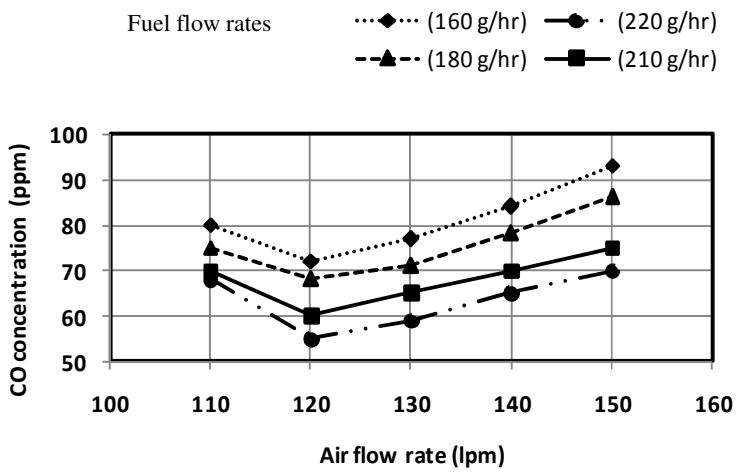

(a)

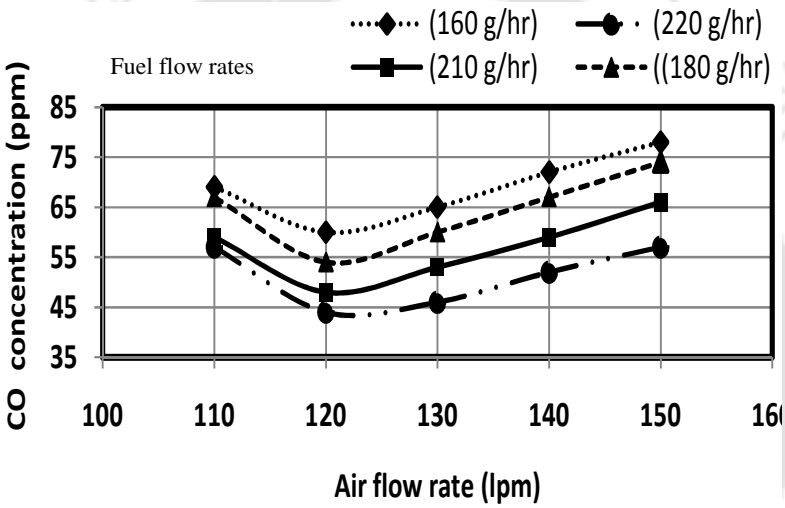

(b)

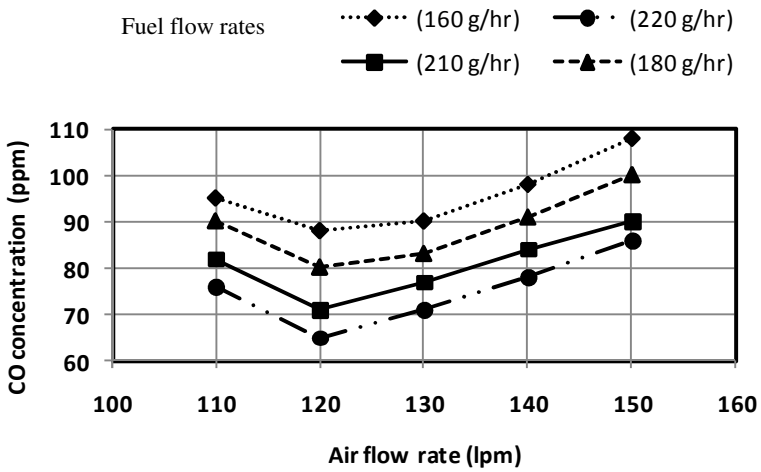

(c)

Fig. 4.4: Variations of CO emissions of (a) 60SCC (b) 70SCC and (c) 80SCC burner with air flow rates for the 4 selected fuel flow rates.

At different air and fuel flow rates, having studied the emission characteristics of three different sizes of the burners, next, the thermal efficiencies of the burners are investigated. The thermal efficiency of a stove is defined as the percentage of the thermal input transferred to the load. The detail of the test procedure (WBT) for investigation of the thermal efficiency has been discussed in Chapter 3. The following section describes the effect of air and fuel flow rates on thermal efficiencies of 60SCC, 70SCC and 80SCC burners.

4.2.3 Effects of air and fuel flow rates on thermal efficiencies of 60SCC, 70SCC, 80SCC burners

The WBT for thermal efficiency was conducted on an aluminium vessel having diameter 260 mm with a water carrying capacity of 6 kg. The experiments were conducted for 3 different sizes of the burners with 4 different fuel flow rates viz., 160 g/hr, 180 g/hr, 210 g/hr and 220 g/hr. The air flow rate was varied between 110-150 lpm. The results are presented in Figures 4.5 (a)-(c). Figure 4.5 (a) represents the variations of thermal efficiencies of the 60 mm diameter burner (60SCC) with air flow rates for the 4 selected fuel flow rates.

It is seen from Figure 4.5 (a) that for a fixed fuel flow rate, with increase in air flow rates from 110 lpm to 150 lpm, the thermal efficiency increases by 1-2%. This increase is considered minimal when compared to the variations of thermal efficiencies with fuel flow rates for a particular air flow rate. With increase in fuel flow rate from 160 g/hr to 220 g/hr, the thermal efficiency decreases by ~7%. This decrease in thermal efficiency at higher fuel flow rate is attributed to increased convective and radiative losses as observed by Lucky and Hossain (2001) who studied the performance of Bangladeshi cook stoves.

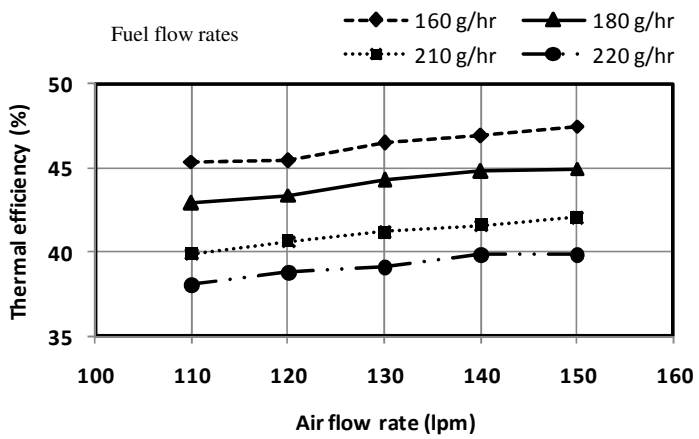

(a)

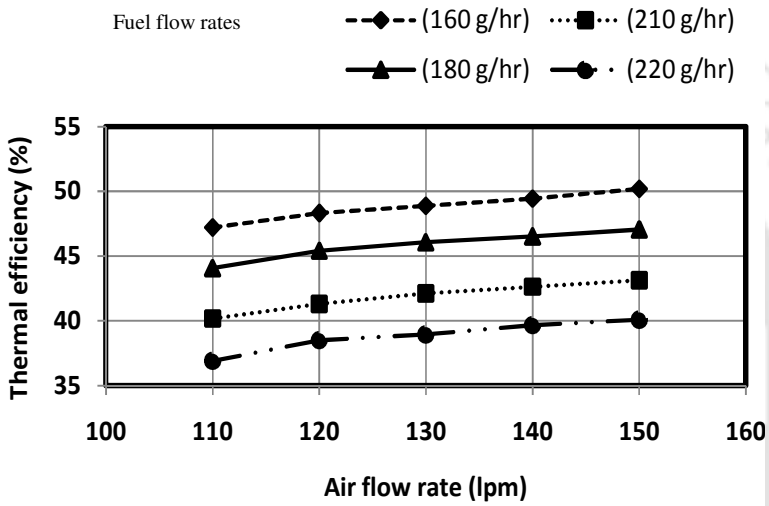

(b)

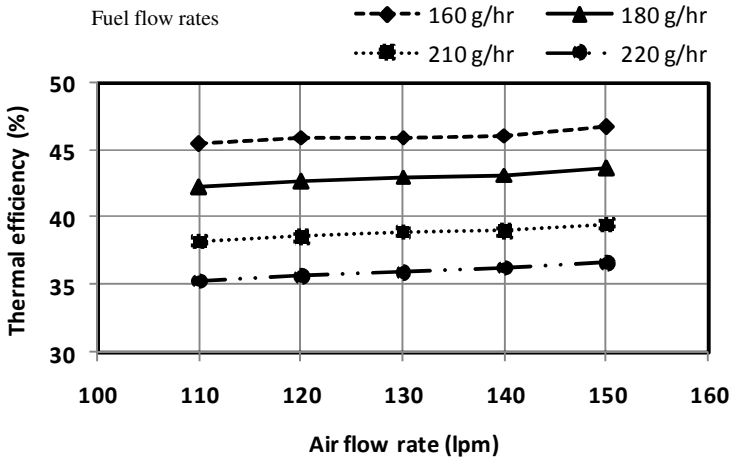

(c)

Fig. 4.5: Variations of thermal efficiencies of (a) 60SCC (b) 70SCC and (c) 80SCC burner with air flow rates for the 4 selected fuel flow rates.

The increase in thermal efficiency with decrease in fuel flow rates and increase in air flow rate is common for all the burners considered. It is to be noted that although at higher heat input, the surface temperature of the burner was high, and this high surface temperature should have resulted in higher thermal efficiency, however, the increased surface temperature was offset by the increased radiant and convective losses. Thus, the extra energy supplied did not contribute much to bring the water from room temperature to 90 ^{o}C at a faster rate. Among the 3 selected casings, the 70 mm diameter burner (70SCC) shows the highest thermal efficiencies (~50%). The thermal efficiency of the 60SCC lies between 70SCC and 80SCC. The highest thermal efficiency in 60SCC is found to be 48%. This was obtained for the air flow rate of 150 lpm and fuel flow rate of 160 g/hr.

In comparison to 60SCC and 70SCC, at all air and fuel flow rates, the 80SCC burner shows lower thermal efficiencies. This is due to less radiative heat transfer at lower average surface temperature. The non-uniform distribution of the surface temperature results in a sharp temperature gradient across the media and this influences the radiant heat transfer to the load and thus, the efficiencies. However, it is to be noted that the efficiency of this particular configuration (80SCC) is comparable, and the thermal efficiencies of 70SCC is 5% higher than the average thermal efficiencies (~45%) of the stoves available in the Indian market. Thus, the use of PM is beneficial not only in reducing emissions but also in increasing thermal efficiencies. Further, improvement in thermal performance of the stove is brought about by the use of a heat shield (Figure 3.6(b)-(d)) across the casing. The idea of using the heat shield is in conformity with the findings of Lucky and Hossain (2001) who demonstrated the usefulness of using a heat shield which helped in improving the efficiencies thereby delaying the flue gas dispersion to surroundings.

4.3 PARAMETRIC STUDIES ON PERFORMANCE OF KEROSENE PRESSURE STOVE INCORPORATED WITH POROUS MEDIA ENCLOSED IN 3 DIFFERENT CASINGS WITH HEAT SHIELD

The study on performances of the burners enclosed in casings of 3 different diameters have shown that the burner in 70 mm casing (70SCC) offer the best thermal performance in terms of thermal efficiencies and emissions. However, it was felt that the performance of this burner can be further improved with inclusion of a heat shield around the casing and also, through incorporation of different casing geometries. Flow field will be different for different casings geometries (Figures 3.5 (b)-(d)), and this changed flow field affects the thermal performance. Thus, accordingly 3 different casings viz., 70SCCWHS (Figure: 3.5(b)), 70TCWHS and 70CCWHS with heat shield were constructed and the thermal performances were checked. The experiments were conducted for different air flow rates (range: 90 - 160 lpm) and fuel flow rates (160 g/hr, 180 g/hr, 210 g/hr and 220 g/hr). In the subsequent pages, the effects of air and fuel flow rates on temperature distributions, emissions and efficiencies of 70SCCWHS burner are reported.

4.3.1 Effects of air and fuel flow rates on temperatures of 70SCCWHS burner

In a radiant burner, higher is the surface temperature, more is the heat transferred to the load. Surface temperature is influenced by the location of the flame/combustion zone (Leonardi et al., 2002, Takami et al., 1998) which in turn is dependent on air and fuel flow rates, flame speed and heat recirculation. With increase in air and fuel flow rate, the combustion zone shifts downstream. Further, the knowledge of temperature distribution on the surface is important, as the higher spatial non-uniformity will lead to higher NO_x and CO emissions. Figure 4.6 (a) shows the variations of surface temperatures taken at 12 different locations viz., (pt.1, pt. 2, …..pt. 12) with air flow rates. The details of the

measuring points are shown in Figure 3.12(a). In this experiment, the fuel flow rate was maintained at160 g/hr while the air flow rates varied from 90-160 lpm.

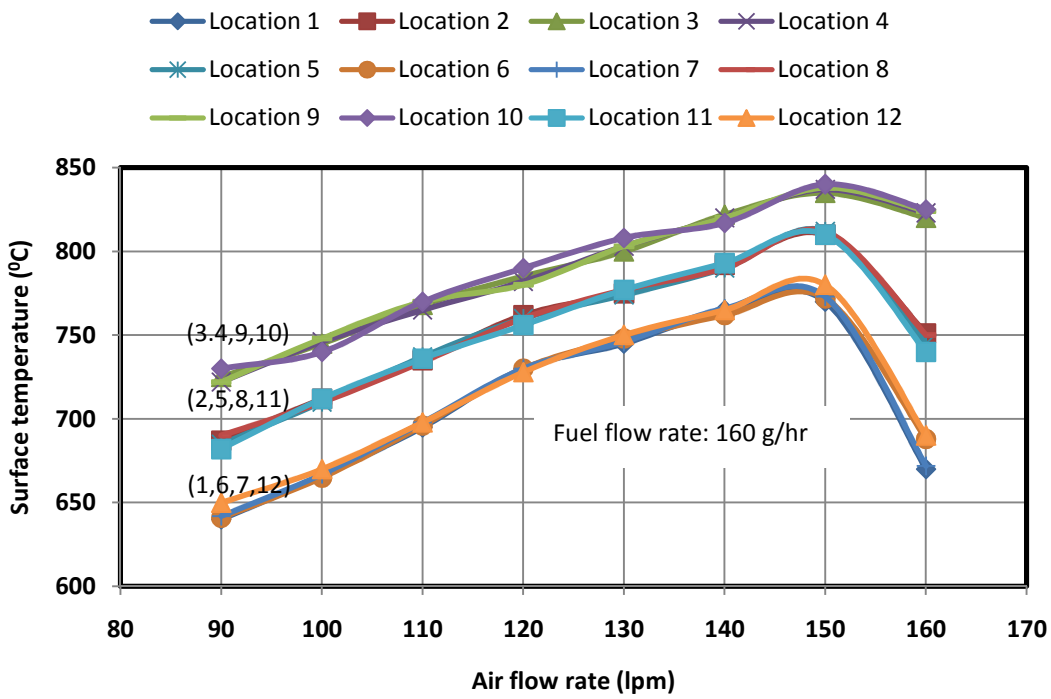

(a)

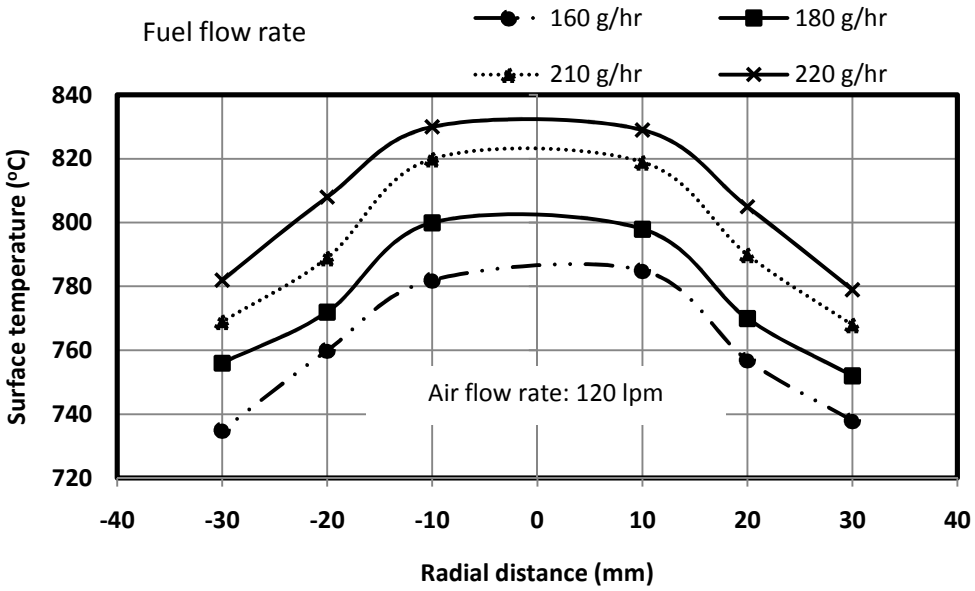

(b)

Fig. 4.6: (a) At 12 radial locations, variations of surface temperature with air flow rates and (b) for 4 fuel flow rates, variations of surface temperature with radial locations.

It is seen from Figure 4.6(a) that between the two identical points, temperatures are almost the same. Besides, it is also observed that at locations 3, 4, 9 and 10 (Figure 3.12(a)), which are closest (10 mm) to the centre, at all air flow rates, the temperature is the maximum, while at locations 1, 6, 7 and 12 which are the farthest (30 mm) from the centre, the temperature is the minimum. For the three sets of points (1, 6), (2, 5) and (3, 4), the difference in temperature is the lowest at the air flow rate of 120 lpm, and for this flow rate, at these [(3, 4) and (1, 6)] locations, this variation is ~6% of the minimum temperature at (1, 6). At 150 lpm, a maximum of ~830 ^{o}C is recorded at locations 3 and 4 (Figure 3.12(a)) which are 10 mm away from the centre. For these (3, 4) points, at 90 lpm of air flow rate, the same is ~725^{o}C. With increase in the air flow rate, the combustion zone moves downstream, and hence is observed increase in temperature with increase in air flow rate. Further, for a fixed fuel flow rate (160 g/hr), when the air flow rate increases from 90-150 lpm, temperature increases by ~12%. At 160 lpm, because of high turbulence, the combustion zone partially recedes from the surface of the PM and hence is the drop in temperature.

Drawing conclusions from the results presented in Figure 4.6(a) that the maximum uniformity in surface temperature of the burner is obtained with 120 lpm air flow rate, keeping this air flow rate constant, next the effect of fuel flow rates was studied. For this, 4 different fuel flow rates, viz., 160 g/hr, 180 g/hr, 210 gm/hr and 220 g/hr, were chosen and the variations of surface temperature with radial distance (pt. 1, pt. 2,….pt. 6 in Figure 3.12(a)) are analysed. Results are shown in Figure 4.6(b). It is observed from the figure that at higher fuel flow rate or heat input, the surface temperature is higher. This increase in temperature is attributed to stabilization of the combustion zone near the surface. Mital et al. (1997) reported that at higher fuel flow rate, flame zone shifts

downstream as the rate at which the unburnt mixture is supplied to the PM exceeds the rate at which the mixture can be consumed.

Among many other parameters, the flame location in the PM depends on air flow rate (Mital et al., 1997). For instance, with increase in excess air the flame shifts downstream. Thus, flame location affects the surface temperature of the burner, and hence the heat output and emissions. The upstream radiant losses can be quite high depending upon the flame location.

With air supply pressure (1.2 bar) and fuel flow rate 160 g/hr fixed, in Figure 4.7, the variations of gas temperatures at the interface (locations: 13 and 14, Figure 3.11(b) and below the Al_2O_3 layer (locations: 15 and 16, Figure 3.11(b) are shown. It is to be noted that the interface temperature in Figure 4.7 is the average of temperatures at points 13 and 14 (Figure 3.11(b)) and the gas temperature below the Al_2O_3 layer is the average of the temperatures at points 15 and 16.

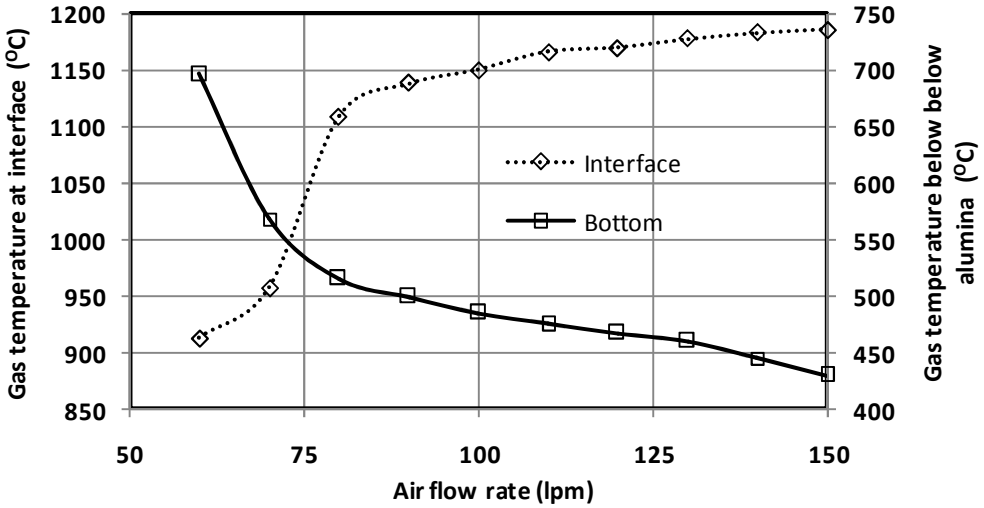

Fig. 4.7: At axial locations 13 and 15, in the steady-state, variation of gas temperature with air flow rate.

It is observed from Figure 4.7 that as the air flow rate increases, the gas temperature at the interface increases while its temperature that below the Al_2O_3 layer decreases. Up to 80 lpm of air, the rise in the interface temperature is very sharp. However, beyond this flow rate, the increase is gradual. This increase in interface temperature at higher flow rate is attributed to shifting of the combustion zone. At higher air flow rate, the air draft was sufficient enough to carry the air-fuel mixture into PM where the combustion took place. Conversely, at lower air flow rate, the combustion zone stabilized just upstream of the PM which is indicated by high bottom temperature.

At 120 lpm of the air flow rate, the gas temperature at the interface is as high as 1160 ^oC, which indicates the occurrence of combustion reaction within it. However, it was realized that for the same air flow rate, the bottom temperature i.e., the temperature of the air-fuel mixture just upstream of the PM is ~480 ^oC which is higher than the auto ignition temperature of kerosene (210 ^oC). This means the combustion reaction is initiated below the first layer of the PM. Thus, in the present burner, Al_2O_3 balls acted as a flame supporting layer, unlike, the conventional bi-layered PB in which the first layer acts as the preheating zone, inhibiting flame propagation. This observation is similar to that of Liu and Hsieh (2004) who studied the combustion characteristics of LPG in a PB. In their setup also, the burning took place in entire the PM, indicated by high preheat temperature. They however, reported that the high preheat temperature had a good implications on CO emissions, as a significant portion of the energy generated through combustion was transferred to upstream to preheat the reactants. Reduction of CO emission is very much desirable as there is a greater concern for the environmental protection. Next, the emissions from the modified stove at different air and fuel flow rates are studied. The results are presented in the following pages.

4.3.2 Effects of air and fuel flow rates on emissions of 70SCCWHS burner

Low residence time and low combustion temperature cause incomplete combustion and the CO emission is its consequence. CO emission depends on equivalence ratios and heat input (Xiong et al., 1995). Figure 4.8(a) shows the variation of CO emissions with air flow rates for 4 different fuel flow rates viz., 160 g/hr, 180 g/hr, 210 g/hr and 220 g/hr. It is observed that, as the air flow rate increases, initially the CO concentration decreases and then it increases. The lowest CO (40 ppm) emission is observed at the air flow rate of 120 lpm and fuel flow rate 220 g/hr. This corresponds to the equivalence ratio of 0.38. This low value is attributed to better mixing of air and fuel. At high air flow rate, due to low residence time, the combustion is incomplete and this gives rise to higher CO emission. At higher fuel flow rate, CO emission decreases due to higher combustion temperature and enhanced combustion intensity. Similar observations were reported by other researchers (Vijaykant and Agrawal (2007), Tseng and Howell, (1996), Jugjai et al. (2002)) who studied combustion of kerosene in PM for applications other than that of the kerosene cooking stove.

Apart from the lower emissions of CO, reduced emissions of NO_x is also a desirable feature of any combustion device. The important parameters affecting NO_x formation are flame temperature, temperature uniformity and residence time in the combustion chamber. Higher combustion temperature promotes thermal NO_x. Similarly, temperature non-uniformity and low residence time also increase NO_x due to local rise in equivalence ratio. The reduction of thermal NO_x involves elimination of high temperature region and better mixing of fuel and air (Fuse et al., 2003). In the PMC the lower NO_x is due to better heat transfer (Howell et al., 1996). Figure 4.8(b) shows the variations of NO_x emissions with air flow rates for the 4 different fuel flow rates.

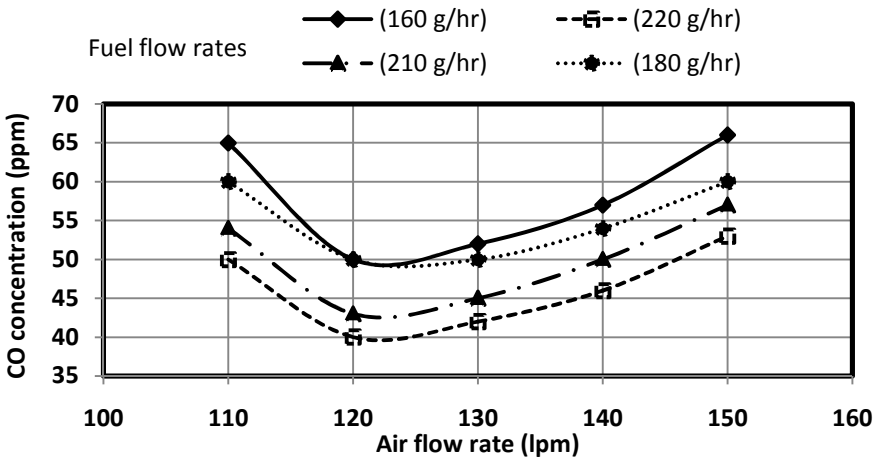

(a)

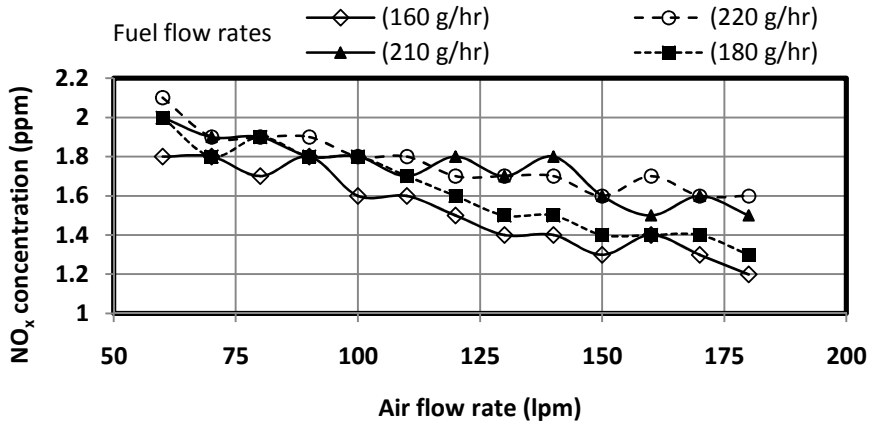

(b)

Fig. 4.8: For 4 different fuel flow rates, (a) variations of CO concentrations with air flow rate and (b) variations of NO_x concentration with air flow rates.

It is seen from Figure 4.8(b) that for a given air flow rate, the NO_x emissions do not change much with the change in fuel flow rates. But, at lower air flow rate, it is higher. This is for the reason that at lower air flow rate, the mixing of air and fuel is poor, and this leads to incomplete combustion. This is also the reason for higher CO emissions (Figure 4.8(a)). For all 4 values of the fuel flow rates, values of NO_x emission are low, and even its maximum value, 2.2 ppm at air flow rate 60 lpm and fuel flow rate 220 g/hr, is much lower than that (4.0 ppm) reported for the conventional stove (Kakati et al., 2007). The lower CO is attributed to fuel preheating and increased residence time of the

exhaust gases as they pass through a convoluted path of hot PM after combustion. Preheating also improves thermal efficiency of the system. Next, the dependence of thermal efficiencies of the burner on different operating parameter is discussed.

4.3.3 Effects of various parameters on thermal efficiencies of 70SCCWHS burner

Thermal efficiency of any stove is an important aspect as it is related to fuel consumption rate, which means cost, and in some way, to the emissions, as higher fuel consumption per unit wattage of the stove will lead to more emissions. Having studied the effects of air and fuel flow rates on radial and axial temperature distributions, and CO and NO_x emissions, next for different fuel flow rates, the variations of thermal efficiency with air flow rates are studied. Besides, the effect of vessel size is also considered, since, the thermal efficiency of a stove is vessel specific (Sharma et al., 2009), and for radiant burner no standard has yet been established that prescribes the appropriate vessel.

Lucky and Hossain (2001) reported that with burner size and other parameters fixed, the heat received by the vessel depends on the diameter and also on the shape of the bottom surface of the vessel. Improper vessel size would result in lower thermal efficiency due to unwanted losses. With smaller vessel, the convective loss to the surrounding is higher, while with bigger vessel, the heating time could be notably higher. Hence, it is important to find out the optimum vessel size giving the best thermal efficiency. Apart from that, the distance between the burner surface and bottom surface of the vessel also affects the thermal efficiency. Hence, it is necessary to identify the optimum distance. Keeping this in mind a experiments were conducted with 3 different vessel sizes and also with varied distance between burner and vessel. Figures 4.9 (a)-(c) show the dependence of thermal efficiencies on air flow rate, vessel size and distance between burner and vessel.

For the 4 values of fuel flow rates, viz., 160, 180, 210 and 220 g/hr, considered before, with a vessel of 260 mm diameter and a distance 10 mm between the burner surface and the bottom of the vessel, variations of thermal efficiency with air flow rate are given in Figure 4.9(a).

It is observed that for any fuel flow rate, efficiency increases with increase in air flow rate. The maximum efficiency 53% is found for air flow rate 150 lpm and fuel flow rate 160 g/hr. The increase in thermal efficiency at higher air flow rate is attributed to higher surface temperature. The maximum efficiency obtained in the present stove is higher than the efficiency of the conventional BIS stove (~48%) measured under similar conditions (same heat input). This increase is due to the additional heat transfer through radiation. However, in the strictest sense, these efficiency values are not comparable as the equivalence ratio for both the stoves are different since the methods of air drawing are different.

At higher fuel flow rate, the efficiency is found to decrease (Figure 4.9(a)), although the surface temperature increases (Figure 4.6(b)). The increase in surface temperature is compensated by increased energy loss to the environment. When the air flow rate was increased from 150 g/hr to 160 g/hr, for any fuel flow rate, the efficiency was found ~6% lower than that of the maximum value. This is due to the drop in surface temperature. For higher thermal efficiency, it is desirable to have a high combustion temperature (Mukunda et al., 1988). However, higher combustion temperature leads to an increase in the formation of NO_x. Thus, in order to have better emission, one needs to have a compromise on thermal efficiency. Trimis and Durst (1996) reported that for a better emission, the process temperature should be between 1100-1400 ^{o}C.

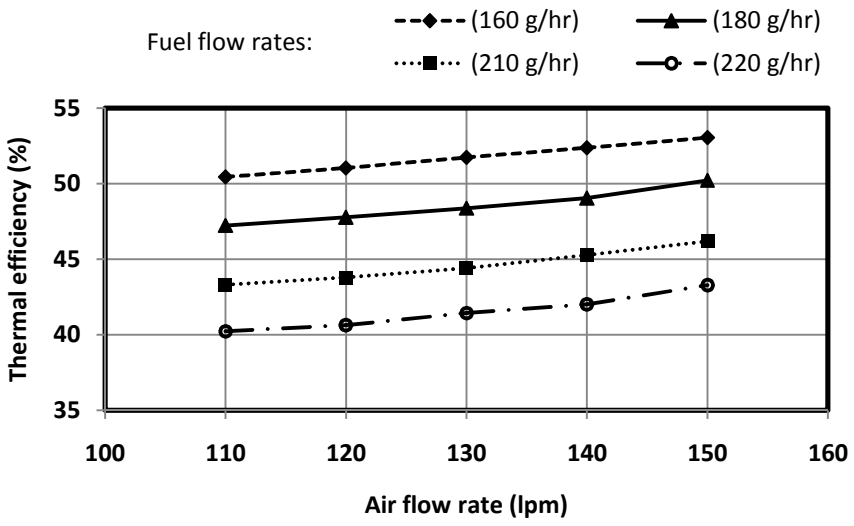

(a)

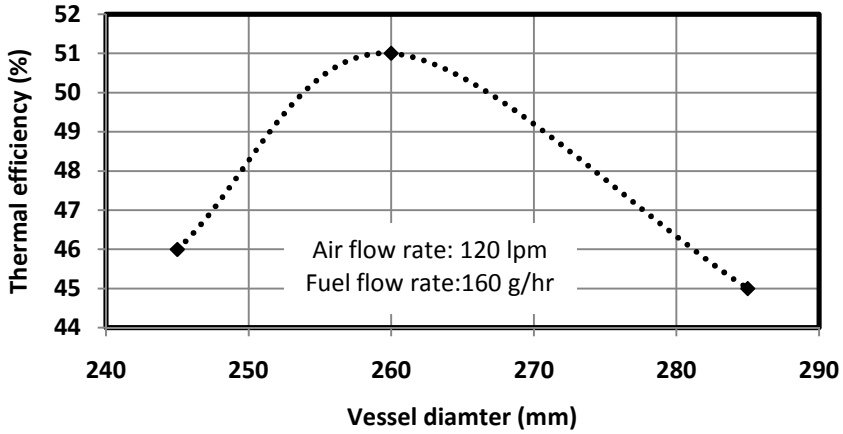

(b)

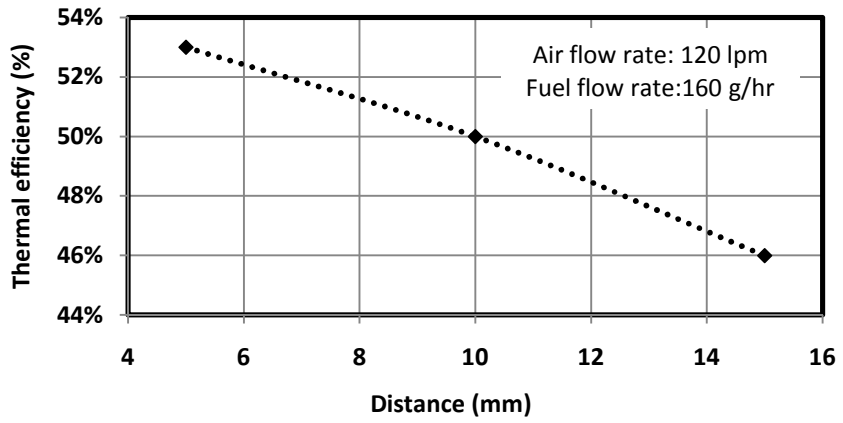

(c)

Fig. 4.9: (a) For 4 values of fuel flow rates, variation of thermal efficiency with air flow rate, (b) variation of thermal efficiency with vessel diameter for 160 g/hr fuel flow rate and (c) variation of thermal efficiency with distance between vessel and burner for 160 g/hr fuel flow rate.

Apart from air-fuel flow rates, types and sizes of PM, the thermal efficiency of a burner is dependent on many other factors, viz., burner head design, shape and size of the cooking vessel, distance between the top surface of the burner and the bottom surface of the vessel, etc. (Lucky and Hossain, 2001, Ko and Lin, 2003). In this work, the effect of vessel size was studied for three vessels diameters, viz., 245 mm, 260 mm and 285 mm. The water carrying capacities of these vessels were 4 kg, 6 kg and 9 kg, respectively. With air flow rate 120 lpm and fuel flow rate 160 g/hr and distance 10 mm, the effect of the vessel diameter on thermal efficiency is shown in Figure 4.9(b). For a given air flow rate, the efficiency is seen to first increase until a maximum value is reached and then it decreases. Due to proper matching of vessel diameter with the burner diameter, the highest efficiency was noted for the 260 mm diameter vessel. When the vessel diameter increases from 245 mm to 260 mm, there is 5% improvement in thermal efficiency. But with further increase in vessel diameter i.e., from 260 mm to 285 mm, the efficiency decreases by 6%. This trend of increase and decrease in efficiency with vessel diameter can be explained in the following manner.

With smaller vessel, the convective and radiative heat losses to the environment are more and thus, the heat received by the vessel is less. On the other hand, with a bigger vessel, the heat loss from the vessel is more. The larger surface of the vessel results in more heat losses to the surrounding and this affects the thermal efficiency. Thus, for the best thermal efficiency, it is important to have an optimum vessel size. In the present case, 260 mm diameter vessel gave the highest thermal efficiency, and hence it was selected for the next experiment in which the distance between the bottom of the vessel and burner surface was varied. Readings were taken at 3 different distances. The results are shown in Figure 4.9(c).

To study the effect of distance between burner surface and the bottom surface of the vessel, experiment was conducted for fuel flow rate 160 g/hr and air flow rate 120 lpm. As shown in Figure 4.9(c), the thermal efficiency is found to increase when the vessel is close to the PM. The highest efficiency is observed when the vessel was placed at a distance of 5 mm. When the vessel was placed at a distance of 15 mm, the drop in efficiency for the same air and fuel flow rate was 7%. At 15 mm, the efficiency was 47% and at 10 mm distance, the same was 50%. The increase in efficiency at a closer distance is attributed to the lower heat losses to the surroundings. Next, for the same operating conditions, the emission results are presented.

4.3.4 Effect of distance between vessel bottom and burner surface on emissions

Figure 4.10 shows the variations of CO and NO_x emissions with the distance between the vessel bottom and the burner surface. The lowest CO and NO_x are observed when vessel was placed at a distance of 15 mm. Nearly 50% drop in CO emission was observed when the vessel was placed at a distance of 10 mm compared to 5 mm in the previous case. This increase in CO emission at a closer distance is attributed to the quenching effect of the flue gases on impingement of the vessel, ceasing the post flame combustion (Lucky and Hossain, 2001).

Summarizing the results of efficiency and emission from Figure 4.9(c) and Figure 4.10, it is inferred that the best thermal efficiency is obtained when the vessel is placed at a distance of 5 mm from the burner, while the best emission characteristics are shown when the vessel is placed at 15 mm distance. Thus, the conditions for higher thermal efficiency and lower emission are contradictory, and hence it is essential to provide a baseline to

trade off, considering the quantitative data of emissions and efficiencies at different distances. A distance of 10 mm is considered optimal. The drop in efficiency by 4% at 10 mm compared to 5 mm distance is considered a reasonable sacrifice for lowering the emission which in the present time is a prime concern for a sustainable environment.

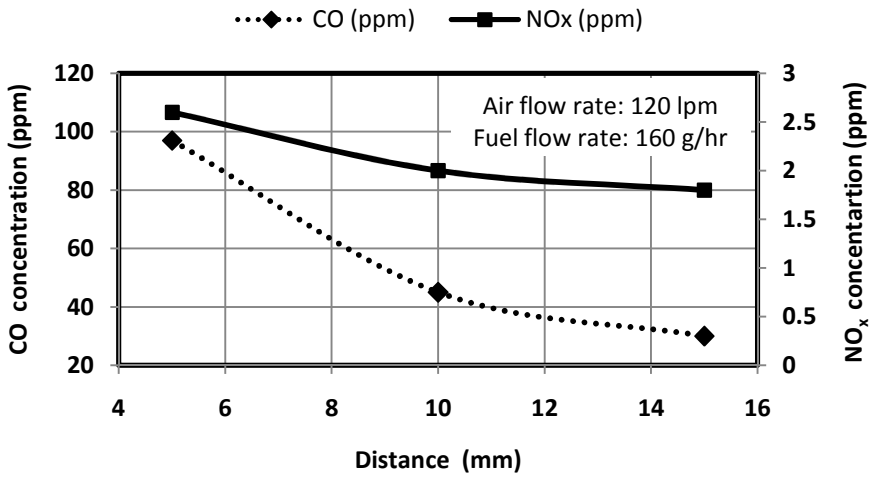

Figure 4.10: Variation of CO and NO_x concentrations with distance between vessel bottom surface and burner surface; fuel flow rate 160 g/hr air flow rate 120 lpm.

4.3.5 Effects of air and fuel flow rates on surface temperatures of 70TCWHS burners and 70CCWHS burners

After evaluating the thermal performance of the 70 mm diameter PB enclosed in a straight cylindrical casing, similar sets of experiments were conducted on 70 mm diameter PB enclosed in taper and conical casing (Figures 3.6(c)-(d)). This was done to study the effects of casing geometry on emission and efficiency since with change in geometry, the flow field changes. Figures 4.11 and 4.12 show the variations of surface temperatures of the PM enclosed under two different casings viz., taper (Figure 3.6(c)) and conical (Figure 3.6(d)) casings, with their radial distances. The trend of the temperature variation is similar to 70SCC (Figures 4.6(b)). The maximum temperature is

observed at the centre and then it radially decreases. The variation in temperature is found to be 6% and 4%, respectively, for the taper and conical casings. Thus, the temperature distribution of taper and conical casing burner is better than the burner in straight cylindrical casing i.e., 70SCC. The tapered and conical geometries improve the mixing and hence the non-uniformity in temperature decreases.

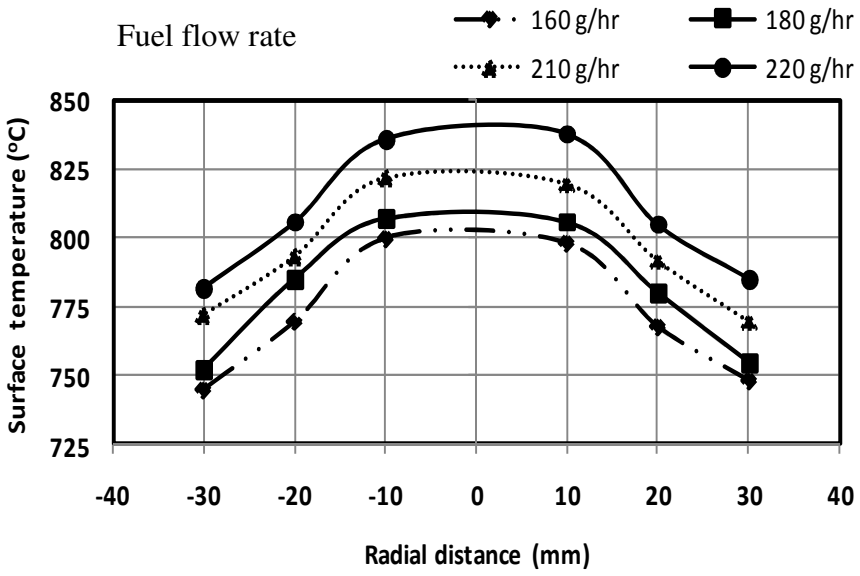

Fig. 4.11: Variation of gas temperature with air flow rate of 70TCWHS burner.

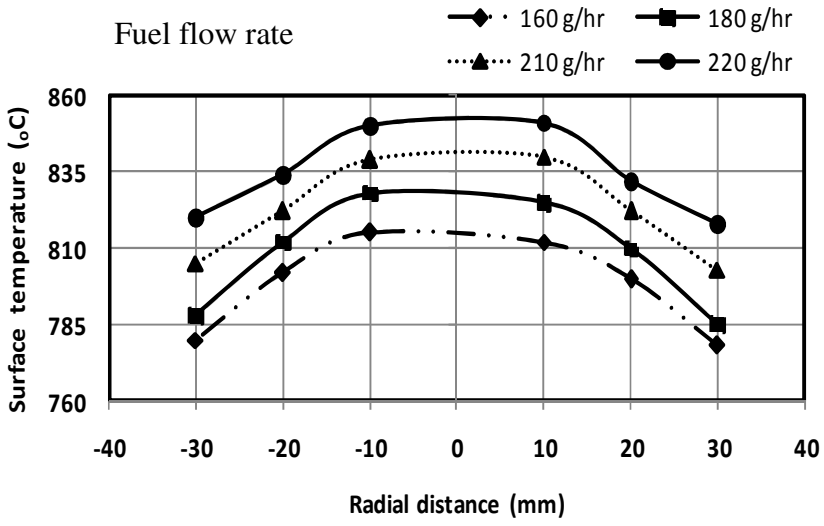

Fig. 4.12: Variation of gas temperature with air flow rate of 70CCWHS burner.

4.3.6 Effects of air and fuel flow rates on thermal efficiencies of 70TCWHS burners and 70CCWHS burners

After evaluating temperature profiles, the thermal efficiencies were evaluated for the PB enclosed in taper and conical casings. Air flow rates were varied from 110-150 lpm and the fuel flow rates were maintained at 160 g/hr, 180 g/hr, 210 g/hr and 220 g/hr. Figures 4.13 and 4.14 show the variation of thermal efficiency with air flow rates for 4 different fuel flow rates viz., 160 g/hr, 180 g/hr, 210 g/hr and 220 g/hr of the PB enclosed in taper (Figure 3.5(c)) and conical (Figure 3.5(d)) casings, respectively.

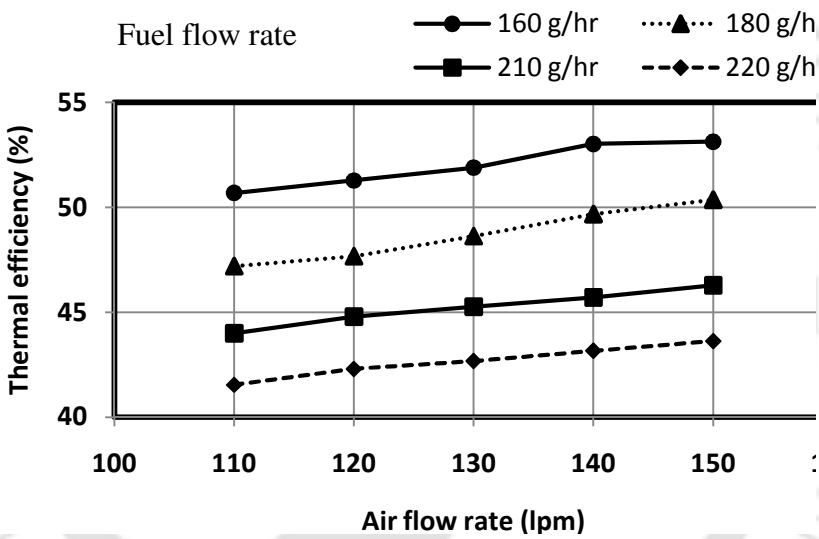

Fig. 4.13: Variations of thermal efficiencies with air flow rate of 70TCWHS burner.

It is observed from Figures 4.13 and 4.14, the conical casing burner (70CCWHS) exhibited higher thermal efficiencies than the taper casing. The highest thermal efficiency obtained in the conical casing is 57.5%. It is obtained for the fuel flow rate of 160 g/hr and the air flow rate of 150 lpm. This efficiency is the highest among all the configurations considered. The highest thermal efficiency of 70TCWHS is 54.2% and is comparable to the thermal efficiencies of 70SCCWHS. Thus, the conical geometry is found effective in raising thermal efficiency of the stove. Having established this, next the

emission characteristics were investigated for the burner enclosed in taper and conical casings viz., 70TCWHS and 70CCWHS. The results are shown in Figure 4.15.

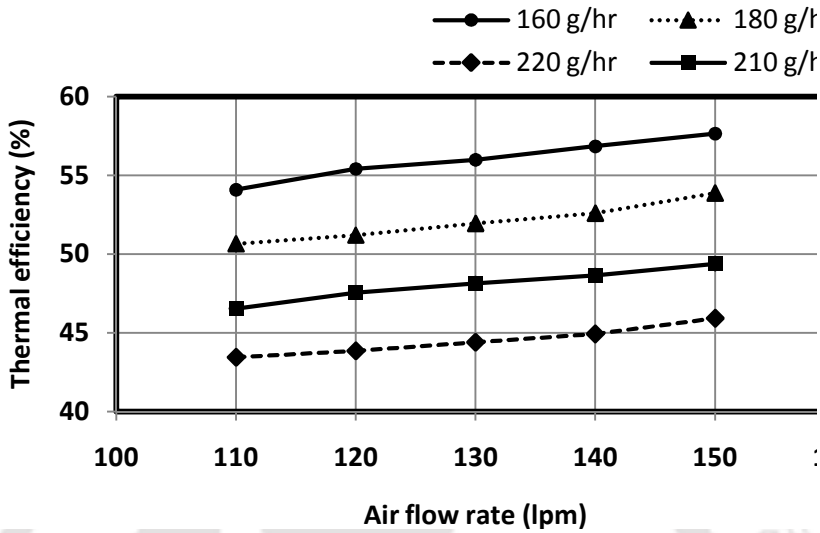

Fig. 4.14: Variations of thermal efficiencies with air flow rate of 70CCWHS burner.

4.3.7 Effects of air and fuel flow rates on emissions of 70TCWHS burners and 70SCCWHS burners

Fuel stoichiometry has a significant effect on combustion emissions (Xiong et al., 1995). At higher excess air i.e., for lean conditions, CO and NO_x vary widely. The typical emission curves for CO of PB enclosed in taper and conical casings are shown in Figures 4.15 and 4.16. Like before, the measurements were taken for 4 different fuel flow rates, viz., 160, 180, 210 and 220 g/hr and air flow rate in the range 100-150 lpm. At higher air flow rate, CO increased due to lower residence time. Likewise, at lower flow rate also CO increased. This was due to improper mixing of fuel and air owing to lower air draft. Minimum CO is observed at air flow rate 130 lpm. The lowest values were obtained for the largest fuel flow rate i.e., 220 g/hr. This was due to higher temperature. The trend of decrease in the CO with an increase in heat input is consistent with the observations of Jugjai et al. (2002) and Trimis and Durst (1996) for the combustion of liquid fuel in PM.

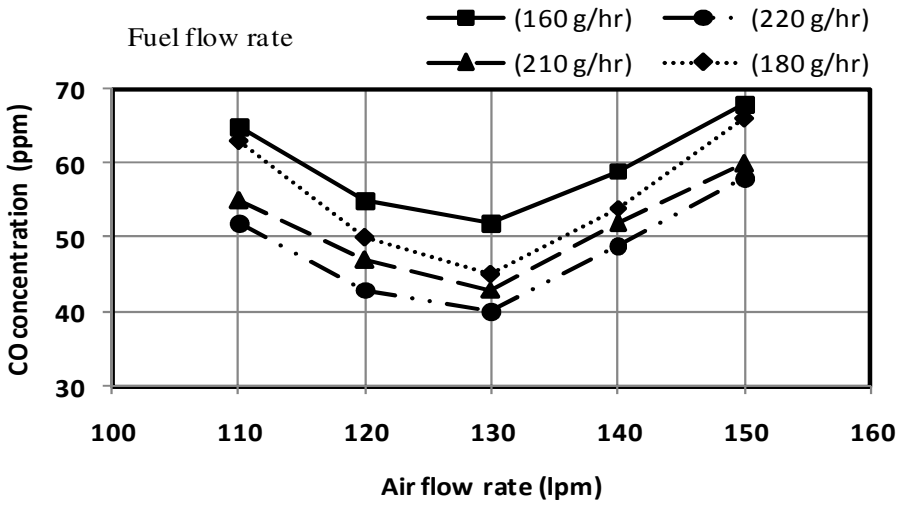

Fig. 4.15: Variations of CO concentration with air flow rate of 70TCWHS burner.

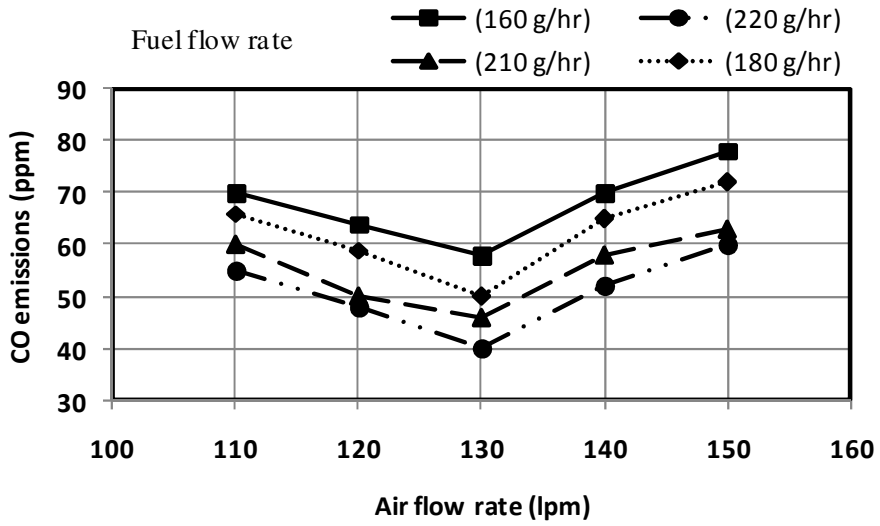

Fig. 4.16: Variations of CO concentration with air flow rate of 70CCWHS burner.

Between the 2 selected configurations, the lower CO (38 ppm) was observed for the taper casing at fuel flow rate 220 g/hr. In comparison to 70SCCWHS burner, the CO emission in 70CCWHS is however slightly higher. This is due to an increased gap between the walls of the casing with the porous bed, leading to escape of fuel without mixing with air.

The residence time for mixing was also low in 70CCWHS and 70TCWHS burners in comparison to 70SCC.

The residence time has a strong influence on NO_x emissions (Xiong et al., 1995, Trimis and Durst, 1996). With increase in excess air, the residence time decreases and this has direct effect on the NO_x emissions. Thus, it is important to evaluate the NO_x concentrations at different air flow rates. Figures 4.17 and 4.18 show the NO_x concentration of the selected configuration for 4 different fuel flow rates viz., 160, 180, 210 and 220 g/hr and air flow rate 100 -150 lpm.

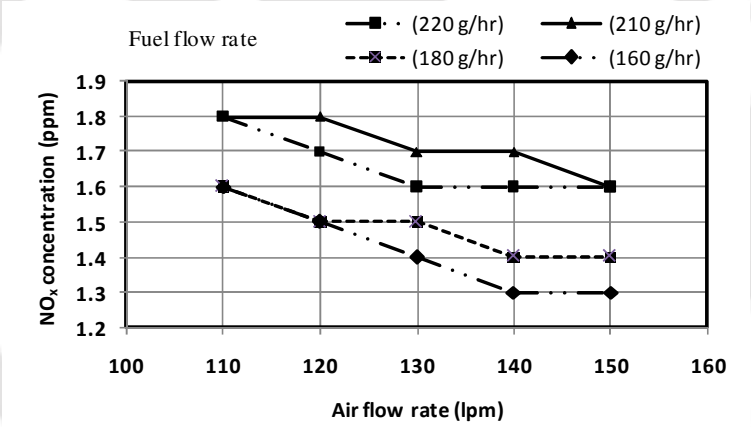

Fig. 4.17: Variations of NO_x concentration with air flow rate of 70TCWHS burner.

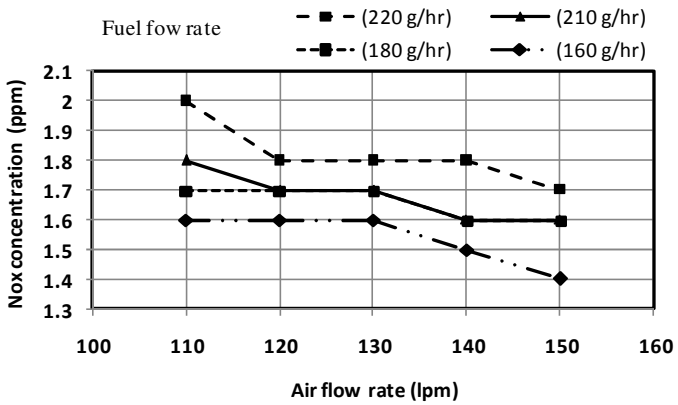

Fig. 4.18: Variation of NO_x concentration with air flow rate of 70CCWHS burner.

It is observed from Figures 4.17 and 4.18 that the trends of the variations of NO_x concentration with air flow rates for all the configurations considered are the same. With change in air and fuel flow rates, no significant change is NO_x concentrations are observed. Due to internal heat recirculation, this is attributed to the lower combustion temperature. Conventional burner exhibit relatively higher NO_x. The following paragraph describes the comparative performance of conventional burner with the present PB.

4.4 PERFORMANCE COMPARISONS OF BIS STOVE WITH POROUS MEDIA INCORPORATED STOVE

To see how the efficiency and emissions of the PB compares with that of the conventional stoves, experiments were performed on a BIS specified kerosene pressure stove. Table 4.2 shows results of the efficiency test carried at 2 different fuel flow rates viz., 160 g/hr and 180 g/hr. The comparison was made with PB having conical shape casing (Figure 3.5(d)). The conical shape was chosen because it showed the best performance in terms of efficiency. The tests were conducted for fuel flow rates 160 g/hr and 180 g/hr and air flow rate 120 lpm. This condition represents leaner combustion representing equivalence ratio 0.2. For conventional stoves, the equivalence ratio might be higher than this. It is to be mentioned that at very lean condition in conventional stove, it is difficult to keep flame without being quenched. This would be possible only if there is recirculation of heat. Also it is to be noted that owing to the difference in supply of air, the efficiency of a conventional stove, in a true sense, cannot be compared with that a PB. The conventional stoves partially draws air through free convection, while, in the PB, air is drawn through forced convection. Although for purpose of comparison, the fuel flow rates in the two stoves were kept the same, in conventional stove, air flow rates were different. In the BIS

stove the air flow rate was not known, whereas, in the PB incorporated stove, to study the effect of equivalence ratio, air flow rate was regulated.

Table 4.2: Comparative study of thermal efficiencies and emissions of stove with and without PB

Casing type	Fuel flow rate (g/hr)	Air flow rate (lpm)	Thermal efficiencies (%)	CO (ppm)	NO_x (ppm)
70SCCWHS	160	120	51.0	50	1.5
70TCWHS	160	120	51.4	55	1.5
70CCWHS	160	120	**55.4**	58	1.6
BIS	*160*	--	*51.2*	*93*	*5*
70SCCWHS	180	120	47.7	45	1.5
70TCWHS	180	120	48.4	48	1.5
70CCWHS	180	120	**51.1**	50	1.7
BIS	*180*	--	*48.6*	*80*	*4*

It is observed from Table 4.2 that the thermal efficiencies of stove with and without PB are almost comparable. The PB with conical casing (70CCWHS) (Figure 3.5(d)) for both fuel flow rates 160 g/hr and 180 g/hr, gives higher thermal efficiencies 55.4% and 51.1% against 51.2% and 48.6%, respectively for the BIS stove. The increased thermal efficiency for 70CCWHS stove is owing to the higher radiative heat transfer to vessel/load. It is to be noted for 160 g/hr and 180 g/hr fuel flow rates, the stoichiometric air flow rates are 30 lpm and 45 lpm, respectively. Thus, the PB operating at 120 lpm air flow rate signifies a very lean air-fuel mixture. This result is very interesting, as it is normally thought, that a higher amount of excess air would result lower thermal efficiencies as it cools the burner. Further it is observed from Table 4.2 that emission-wise also the PB is better than the conventional BIS stove. Both CO and NO_x emissions

are lower. Better combustion quality i.e., better mixing of fuel and air resulted lower CO. Likewise lower combustion temperature attributed lower NO_x. Thus, both from emission and efficiency points of view, the stove with the PB is attractive.

Having discussed the results of performance of the new stove with SiC and Al_2O_3 burner at different air and fuel flow rates, next the results of some miscellaneous experiments relevant to the present study are presented. One of these experiments is the performance evaluation of the stove with different materials. The following section discusses the results.

4.5 MISCELLANEOUS EXPERIMENTS

4.5.1 Effect of material on thermal efficiencies and emissions

The material forming the porous bed has strong influence on the burner performance (Xiong et al., 1995). This is because, in PB there is a strong interaction between the combustion and the combined convective and radiative heat transfers. The solid materials having different thermal properties exhibit different levels of incandescence and hence different degree of thermal radiation. The higher emissive material yields higher thermal efficiencies owing to greater amount of radiative heat transfer to the load. Similarly, the high temperature burner results in improvement of convective heat transfer. Thus, it is necessary to find the effect of materials on thermal performance of the burner. Table 4.3 summarizes the results of the variation of thermal efficiencies and emissions with 5 sets of materials. For comparison CO_2 concentration calculated from stoichiometry is also presented. The experiments were conducted for the air and fuel flow rate of 120 lpm and 160 g/hr, respectively. The materials used are ZrO_2, Al_2O_3, SiC and metal ball (SS). These materials were enclosed in a conical casing (70CCWHS).

Table 4.3: Effect of materials on thermal efficiencies and emissions of 70CCWHS burner at air flow rate: 120 lpm and fuel flow rate: 160g/hr

Materials	Thermal efficiencies (%)	CO (ppm)	CO_2 (%)	CO/CO_2	NO_x (ppm)
SiC	48.5	44	2.10	0.002	1.8
SiC +Al_2O_3 balls	52	59	2.00	0.002	1.7
ZrO_2	46.8	48	1.82	0.002	1.6
ZrO_2+ Al_2O_3 balls	50.3	53	1.78	0.002	1.5
Metal (SS) balls	55.3	65	1.68	0.004	3

It is evident Table 4.3 that the material has a prominent effect on thermal efficiency. As expected, a single-layer burner made of SiC or ZrO_2 showed lower efficiencies. SiC and ZrO_2 are high emissive materials and in this case, radiative heat loss to the upstream was more. Emissivity and thermal conductivity of alumina (Al_2O_3) are low. In a bi-layer PB with Al_2O_3 in the upstream, the performance of the PB was better. Efficiencies of SiC +Al_2O_3 balls and ZrO_2+ Al_2O_3 balls were found to be 52% and 50.3%, respectively. Due to better radiative properties, the 7 mm diameter SS metal ball shows the highest efficiency. However, the emissions results revealed that with the metal balls CO and NO_x concentrations are higher. CO to CO_2 concentration ratio is also higher than the other configurations tested.

4.5.2 Thermal performance of PB with alumina paste

In order to investigate if efficiency can be increased by controlling upstream heat transfer, an experiment was conducted in 70SCC burner (Figure 3.5(a)). A little modification was made to the burner which included filling up the gap between vaporizer and the first layer of PM (Al_2O_3 ball) with a paste made of Al_2O_3 powder and sodium silicate. The idea of

putting Al_2O_3 paste was to restrict heat transfer to upstream so that the vaporizer could support combustion. The radiant heat flux from the PM was meant to be just sufficient for only vaporization not for combustion. Al_2O_3 being the low emissive material was expected to act as an insulating layer and vaporizer would not receive higher heat flux so that combustion could be self sustained. Since, the self ignition temperature of kerosene is low, higher heat flux results in ignition of the fuel below PM.

Figures 4.19 show (a) schematic and (b) picture of the burner, respectively. The thickness of Al_2O_3 insulation was 30 mm. 70SCC burner was chosen because of its constructional simplicity. This configuration resulted in the highest thermal efficiencies (60-62%). This increase is attributed to the reduced upstream heat loss. However, with this configuration, the ignition was difficult since the heat transfer from PM to vaporizer was shielded by Al_2O_3. It took more than 30 minutes to start the process and make the combustion reaction self sustained. A greater amount of heat had to be supplied through burning of kerosene in the oil plate. Thus, this configuration did not seem to be promising, although the thermal efficiency was higher than all other configurations, since for domestic use, short ignition time is one of the most desirable criteria.

Besides, emission readings were found very high (CO: 500 ppm, NO_x: 4 ppm). This was due to the blockage of air passages (Figure 4.2 (a)) which were present in 70SCC burner through sides of the casing. Inefficient air supply through central duct attached to vaporizer led poor mixing of fuel and air. Combustion was fuel rich giving rise to higher concentration of CO. Short residence time of reactants due to decreased volume for mixing also added to higher CO emissions. Local rise in equivalence ratio resulted in higher NO_x which is highly temperature dependent.

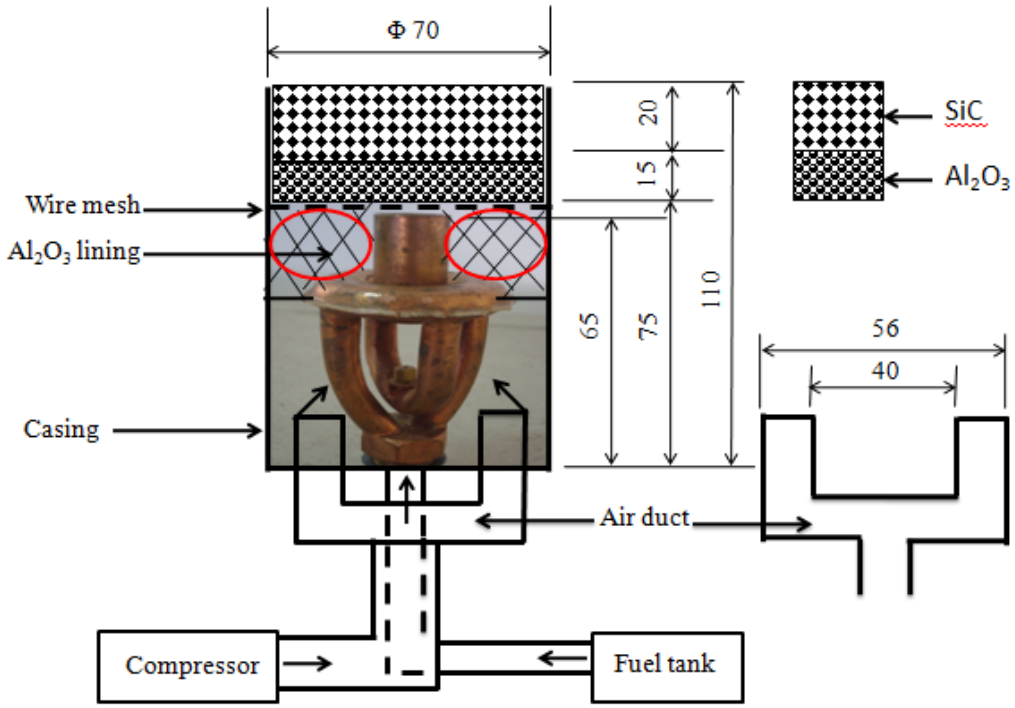

(a)

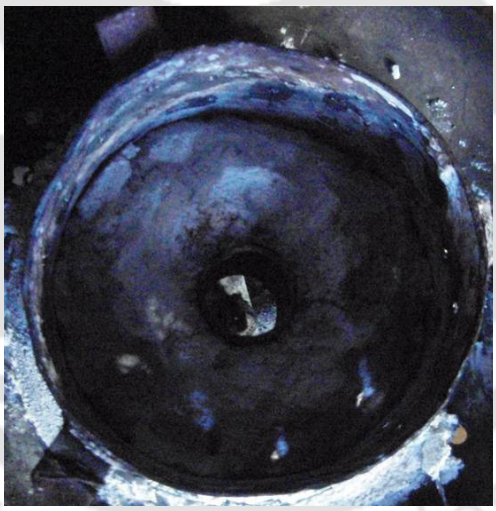

(b)

Fig. 4.19: (a) Schematic of Al_2O_3 pasted burner and (b) Picture of casing with Al_2O_3 paste.

4.5.3 Effects of distance between vaporiser and of air ducts on emissions

In the PB, air is supplied externally, and for this, the two air ducts are fed to the burner casing (Figure 3.2(a)). With reference to the vaporiser, the distance of the bottom layer of the bi-layer PB is kept fixed. For a better performance, a homogeneous air-fuel mixture is

desirable in the PM. For 70SCC, effect of the distance between outlet of the air ducts and the bottom of the PM on CO and NO_x emissions from PB are shown in Figures 4.20 and 4.21, respectively.

It is evident from the figures that with decrease in distance between air duct and vaporizer, both CO and NO_x emission increases. This is due to the inadequate residence time resulting in poor mixing of air and fuel. A minimum of 55 mm distance was found to suffice the requirement. When the distance was 45 mm, CO and NO_x emissions were very high. In this case, soot emitting orange flamelets signifying droplet combustion in diffusion mode was observed. When the distance was increased to 55 mm, a drastic reduction CO and NO_x emissions were observed. With further increase in distance, no marginal changes were observed.

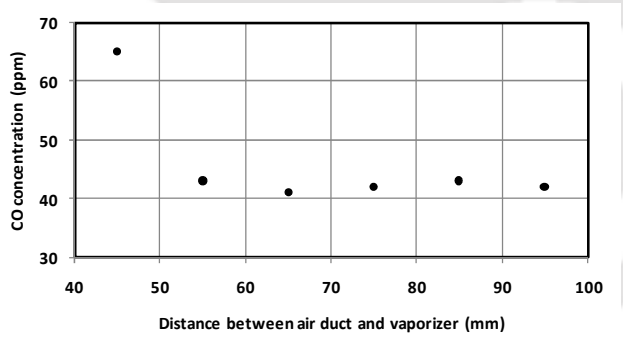

Fig. 4.20: CO concentration versus air duct location.

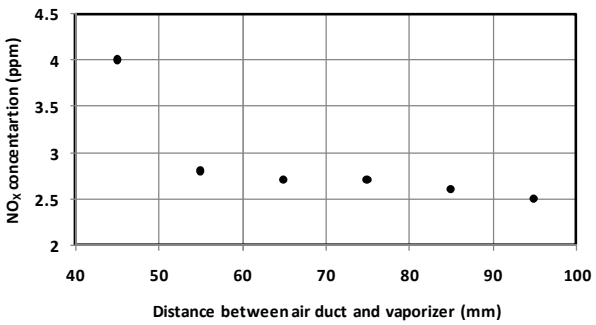

Fig. 4.21: NO_x concentration versus air duct location.

4.6 SUMMARY

With the objective of improving performance in terms of emissions and efficiency of the conventional kerosene pressure stoves, the concept of PMC was employed. A BIS kerosene pressure stove was modified to incorporate a combination of two different PM viz., Al_2O_3 and SiC in the combustion zone of the stove. SiC being highly conductive and radiative, promoted heat transfer to the downstream, and because of low thermal conductivity and emissivity, the Al_2O_3 could reduce the heat transfer to the upstream as well as in radial direction. This combination was found effective in recirculating heat from the reaction zone and maintaining the combustion temperature lower. Experiments were conducted for different air and fuel flow rates and its effects on temperature profiles, emissions and efficiencies were identified. Air flow rates were varied between stoichiometry to an extreme lean condition (equivalence ratio 0.18) and good combustion stability was found for the range 60-180 lpm. The temperatures measured at different radial locations were found nearly uniform. The axial temperature distribution showed an increasing trend with air and fuel flow rates. The lowest CO emission (30 ppm) was obtained for the fuel flow rate of 210 g/hr and air flow rate of 120 lpm. NO_x were found insensitive to heat input and air flow rates and remained low (1-2 ppm) for the whole operating range studied. This low value was attributed to better mixing of air and fuel assisted by the porous matrix. The observed value was much lower than the conventional stove. For a conventional stove, the CO level is found to be in the range 80-90 ppm.

The thermal efficiencies at different air and fuel flow rates showed a maximum improvement of 8% over the average thermal efficiencies of the conventional BIS stove (~48%) for a fuel flow rate of 160 g/hr and air flow rate of 120 lpm. The optimum vessel size for this efficiency was of 260 mm diameter and the distance between the vessel

bottom and the PM surface was 10 mm. The higher thermal efficiency was attributed to improvement in the convective heat transfer and also due to additional heat transfer through radiation to the vessel. Further, improvement in thermal performance of the stove was obtained by the use of a heat shield. Thus, the use of PM is beneficial not only in reducing emissions but also increasing thermal efficiencies.

Having studied the performance of the PB from the energy point of view (the first law of thermodynamics), and next the study of its performance is made on basis of the exergy analysis. Since, as mentioned in Chapter 2, literature review section (page 63), energy analysis can sometimes be misleading. To ascertain the performance of a thermal system, it is important to do the exergy analysis which measures closeness of the thermal performance with the ideal one. The next chapter deals with the exergy analysis.

CHAPTER 5

EXERGY ANALYSIS

5.1 INTRODUCTION

The common way of evaluating the performance of a combustion device is the energy analysis which is based on the first law of thermodynamic. Unfortunately, this energy analysis is not a realistic measure of performance, since it does not give information about quality or grades of energy (Kaushik and Gupta, 2008). In order to get a better insight about the performance of a thermal system, it is essential to do an analysis based on the second law of thermodynamics which introduces the concept of exergy. Exergy is defined as the maximum capacity of a body or an energy system to perform the useful work as it proceeds to a final equilibrium state with its surroundings (Utlu and Hepbasli, 2006). Unlike energy, exergy is not always conserved but it can be destroyed. Hence, to address this point, this chapter reports the exergy analysis of the kerosene pressure stove equipped with PM enclosed in 6 different types of casings, viz., (i) 60 mm straight cylindrical casing (60SCC) (ii) 70 mm straight cylindrical casing (70SCC) (iii) 80 mm straight cylindrical casing (80SCC) (iv) 70 mm straight cylindrical casing with heat shield (70SCCWHS) (v) 70 mm taper casing with heat shield (70TCWHS) and (vi) 70 mm conical casing with heat shield (70CCWHS). First, the exergy efficiencies of the burners at different air and fuel rates are calculated and presented in the form of Table. Following this, the variations of both the efficiencies with air and fuel flow rates are presented in the form of figures. From the figures, considering the trade off between the thermal efficiency and the exergy efficiency, the optimum operating conditions has been identified. Further, the efficiency of a BIS specified conventional kerosene pressure stove is evaluated and compared with the efficiency of the PM incorporated stove.

5.2 ENERGY AND EXERGY EFFICIENCY COMPARISON OF KEROSENE STOVE INCORPORATED WITH POROUS MEDIA

Energy is a thermodynamic property which can be transformed from one form to another. Figure 5.1(a) shows the energy flow diagram of a cooking stove which has 3 utilities viz., water, vessel and water vapour. These 3 components use a part of the heat released in combustion, and the rest of the heat is lost to the surroundings by different means. Figure 5.2 (b) shows the various possible losses while transferring heat to the utilities. As is evident, the losses can be from burner casing, through exhaust gases, and also, through walls of the vessel containing water. This heat transfer results in change in total energy of the system. The difference between the input and output energy indicates the change in total energy which is lost to the surroundings. The percentage of heat energy utilized is given by thermal efficiency or first law efficiency. It is basically the ratio of output energy to the input energy and depending upon the losses, it varies. One can improve the thermal efficiency of a system by minimizing the heat losses. However, there is a limit for obtaining the maximum efficiency, as in accordance with the second law of thermodynamics, even the best heat engine has to reject some of the heat supplied to it. This gives rise to the concept of exergy or available energy. The part of thermal energy that can be converted into useful work under ideal conditions (by reversible process) is called available energy and the rest of the energy which has to be rejected to the sink is known as unavailable energy. In thermal analysis, quantification of available energy or exergy is essential as having its idea, one can recover the destructed exergy and make the system to operate in its full potential. The calculation of non available energy gives the knowledge of the minimum energy that needs to be rejected by the system. In the present study, the second law efficiency is evaluated taking into account the loss of available energy during heat transfer with the finite temperature. The efficiency calculations are

done for the different burners enclosed under different casings. The difference is Table 5.1 presents the first and second law efficiency of 70SCC burner (Figure 3.5 (a)) at air flow rate 110-150 lpm and 4 different fuel flow rates viz., 160 g/hr, 180 g/hr, 210 g/hr and 220 g/hr. Sample calculation of the exergy efficiency is given in Annexure H. This is followed by Annexure I, in which calculation for specific heat of gas is shown.

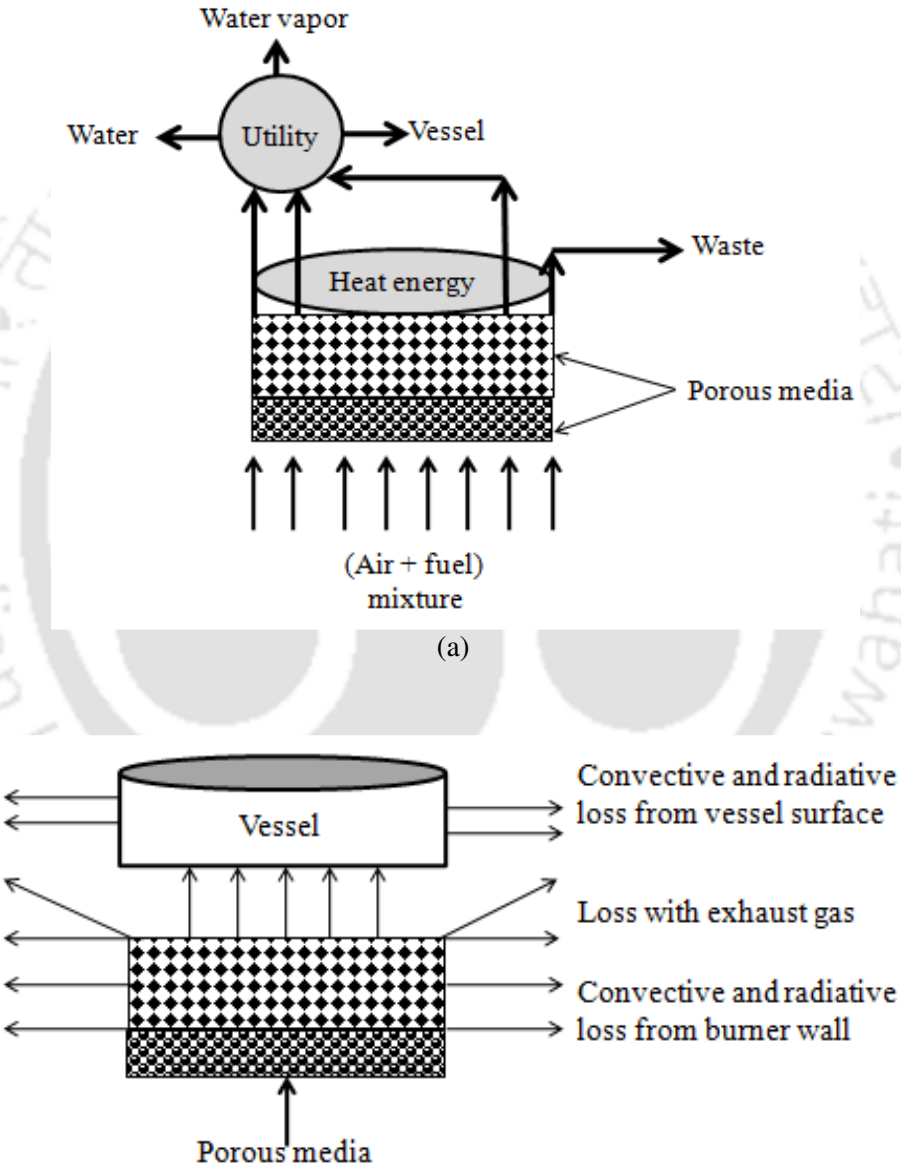

Fig. 5.1: (a) Energy flow diagram in cooking stove and (b) Losses in cooking stove.

Table 5.1: Energy and exergy efficiency of 70SCC burner

Fuel flow rate (g/hr)	Air flow rate (lpm)	Efficiency I (%)	Efficiency II (%)
160	110	47.2	9.2
160	120	48.3	8.4
160	130	48.8	7.9
160	140	49.4	7.3
160	150	50.2	6.9
180	110	44.0	9.5
180	120	45.4	8.9
180	130	46.0	8.5
180	140	46.5	7.9
180	150	47.0	7.6
210	110	40.1	10.0
210	120	41.3	9.7
210	130	42.1	9.4
210	140	42.6	8.8
210	150	43.1	8.5
220	110	36.9	10.1
220	120	38.5	9.9
220	130	38.9	9.7
220	140	39.6	9.0
220	150	40.0	8.3

It is evident from Table 5.1 that for a fixed fuel flow rate, with increase in air flow rate, the first law efficiency increases, while the second law efficiency decreases. This decrease in the second law efficiency with increase in air flow rate indicates more destruction of available energy. Thus, at higher air flow rate, although the first law efficiency increases, the burner actually does not operate to its full potential. The burner gives better performance when it is operated at lower air flow rate due to less destruction of exergy. With fuel flow rates, however, an exactly opposite trend is observed. For a fixed air flow rate, with increase in fuel flow rate, the first law efficiency decreases but the second law efficiency increases. Figures 5.2 (a)-(d) show the variations of first and second law efficiencies with air flow rates, for the 4 selected fuel flow rates viz., 160 g/hr, 180 g/hr, 210 g/hr and 220 g/hr.

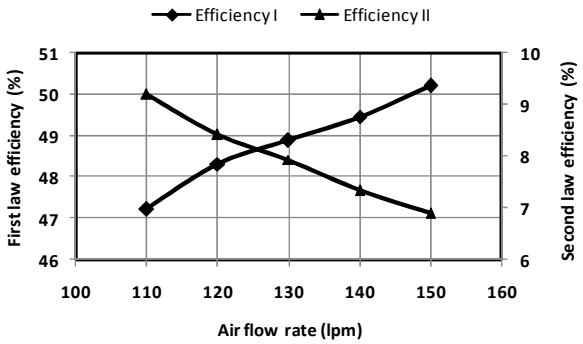

(a)

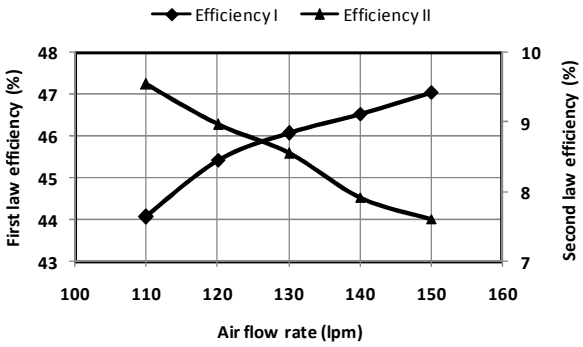

(b)

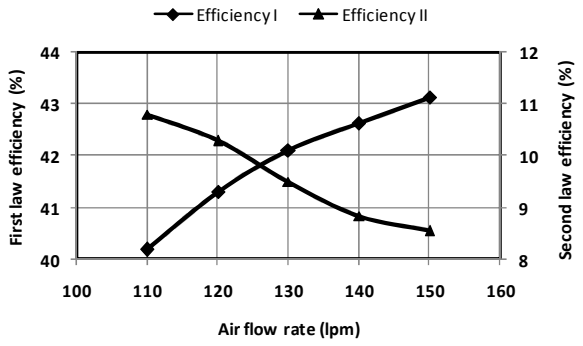

(c)

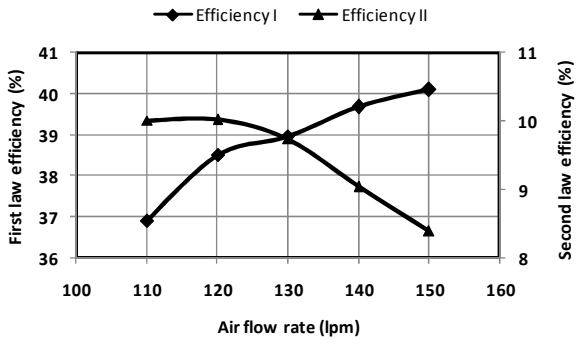

(d)

Fig. 5.2: Variations of first and second law efficiencies of 70SCC with air flow rate for the fuel flow rate of (a) 160 g/hr (b) 180 g/hr (c) 210 g/hr and (d) 220 g/hr.

It is evident from Figure 5.2(a) that at a fuel flow rate of 160 g/hr, when air flow rate increases from 110-150 lpm, the first law efficiency increases from 47.2% to 50.2%, while, the second law efficiency decreases from 9.2% to 6.9 %. The highest second law efficiency (10.1 %) is observed at an air flow rate of 110 lpm and a fuel flow rate of 220 g/hr. Conversely, the highest first law efficiency is observed at the air flow rate of 150 lpm and fuel flow rate of 160 g/hr. With increase in air flow rate from 110-150 lpm and at the fuel flow rate of 180 g/hr, the first law efficiency increases from 44% to 47%, and the second law efficiency decreases from 9.5% to 7.6%. Similarly, for the same range of air flow rate, at the fuel flow rate of 210 g/hr, the first law efficiency increases from 40.1% to 43.1%, and the second law efficiency decreases from 10.0% to 8.5%. Likewise, at the fuel flow rate of 220 g/hr, the first law efficiency increases from 36.9% to 40%, and the second law efficiency decreases from 10.1% to 8.3 %. It is to be noted that for the all the cases, for a particular fuel flow rate, the highest first law efficiency is observed at the air flow rate of 150 lpm and the highest second law efficiency is observed at 110 lpm, indicating minimum exergy destruction at this flow rate. Thus, the air flow rate supporting higher first law efficiency and second law efficiency is potentially different. The optimum air flow rates can be found out, considering the air flow rates corresponding to the average of four first law efficiencies for a particular fuel flow rates. For instance, at 160 g/hr, the average first law efficiency is 48.8%, and the average second law efficiency is 7.9%. These efficienies approximately corresponds to the air flow rate of 130 lpm. Similarly, for the other three fuel flow rates 180 g/hr, 210 g/hr and 220 g/hr respectively, the average first law efficiencies (45.8%, 41.8, 38.8%) and the average second law efficiencies (8.5%, 9.5, 9.6%) correspond to the air flow rates ranged between 120-130 lpm. Same behaviour is observed for the burner having heat shield, i.e., 70SCCWHS (Figure 3.6(b)). Table 5.2 presents the results.

Table 5.2: Energy and exergy efficiency of 70SCCWHS burner

Fuel flow rate (g/hr)	Air flow rate (lpm)	Efficiency I (%)	Efficiency II (%)
160	110	50.7	9.7
160	120	51.2	8.9
160	130	51.3	8.1
160	140	51.8	7.5
160	150	53.0	7.3
180	110	47.2	9.8
180	120	47.7	8.9
180	130	48.3	8.5
180	140	49.0	7.9
180	150	50.2	7.6
210	110	43.3	10.1
210	120	43.8	9.3
210	130	44.4	8.9
210	140	45.3	8.2
210	150	46.8	7.9
220	110	40.2	10.4
220	120	40.6	9.7
220	130	41.4	8.8
220	140	42.0	8.2
220	150	43.2	7.9

From Table 5.2 it is evident that like, the previous configuration, in this configuration also with increase in air flow rates the first law efficiency increases and the second law efficiency decreases. The highest first law efficiency is observed at the fuel flow rate of 160 g/hr and air flow rate 150 lpm. While, the highest second law efficiency is obtained at the fuel flow rate of 220 g/hr and the air flow rate of 110 lpm. Thus, the operating parameters for having higher first law efficiency and also, the higher second law efficiency are not same. Since the first law efficiency is higher at higher air flow rate and the second law efficiency is higher at lower air flow rate, it can be suggested that for better operation the burner has to operate in a flow rate between 110 lpm and 150 lpm. This can also be confirmed from Figures 5.3(a)-(d) which show the variations of efficiencies with air flow rates, for the 4 different fuel flow rates.

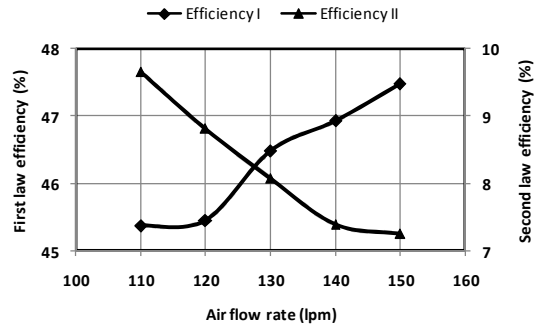

(a)

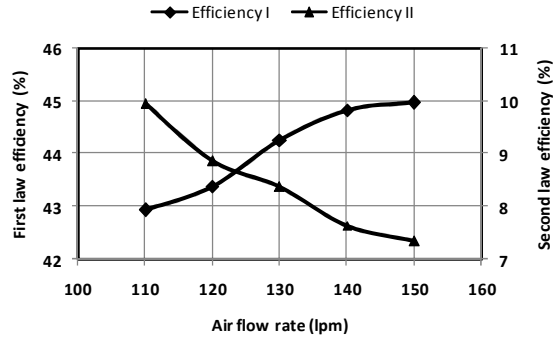

(b)

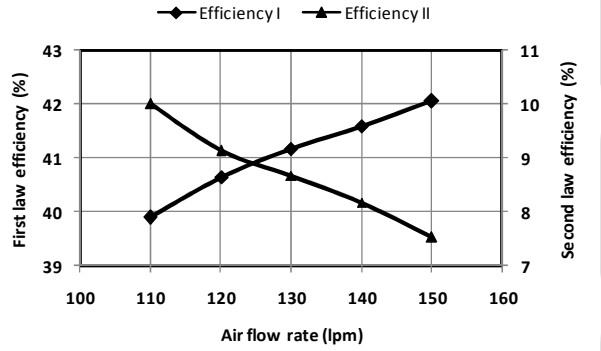

(c)

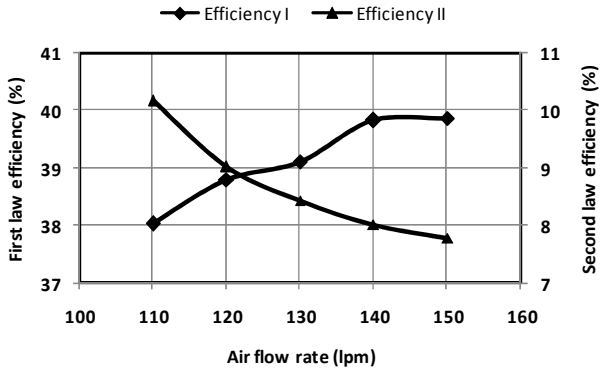

(d)

Fig. 5.3: Variations of first and second law efficiencies of 70SCCWHS with air flow rate for the fuel flow rate of (a) 160 g/hr (b) 180 g/hr (c) 210 g/hr and (d) 220 g/hr.

It is evident from Figure 5.3 (a)-(d) that the trends of variations of first and second law efficiencies are similar to 70SCC burner. Here also, for the four fuel flow rates 160 g/hr, 180 g/hr, 210 g/hr and 220 g/hr respectively, the average first law efficiencies (51.6%, 48.4, 44.4%, 41.4%) and the average second law efficiencies (8.3%, 8.5, 8.9, 8.6%) correspond to the air flow rates ranged between 120-130 lpm. Besides, it is observed that the first law efficiencies of this configuration, for all the air and fuel flow rates, are higher than the previous configuration i.e., 70SCC attributing to the addition of heat shield The second law efficiency is however, found similar, indicating the recovery potential to be the same. Next, the first and second law efficiencies of the 60SCC (Figure 3.5 (a)) burner are evaluated. Table 5.3 and Figures 5.4 (a)-(d) show the results. In Figures 5.4 (a)-(d) the variations of efficiencies are shown for different air and fuel flow rates.

Table 5.3: Energy and exergy efficiency of 60SCC burner

Fuel flow rate (g/hr)	Air flow rate (lpm)	Efficiency I (%)	Efficiency II (%)
160	110	45.3	9.6
160	120	45.4	8.8
160	130	46.4	8.0
160	140	46.9	7.3
160	150	47.4	7.2
180	110	42.9	9.9
180	120	43.3	8.8
180	130	44.2	8.3
180	140	44.8	7.6
180	150	44.9	7.3
210	110	39.8	10.0
210	120	40.6	9.1
210	130	41.1	8.6
210	140	41.5	8.1
210	150	42.0	7.5
220	110	38.0	10.1
220	120	38.8	9.0
220	130	39.1	8.4
220	140	39.8	8.0
220	150	39.8	7.7

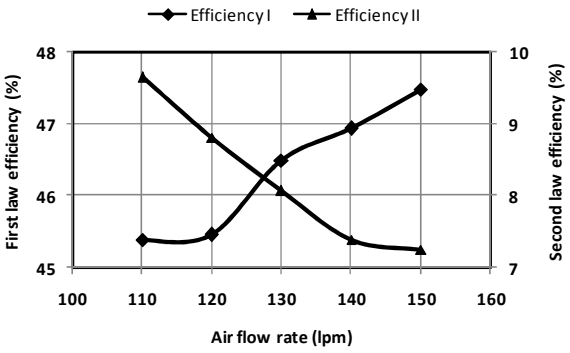

(a)

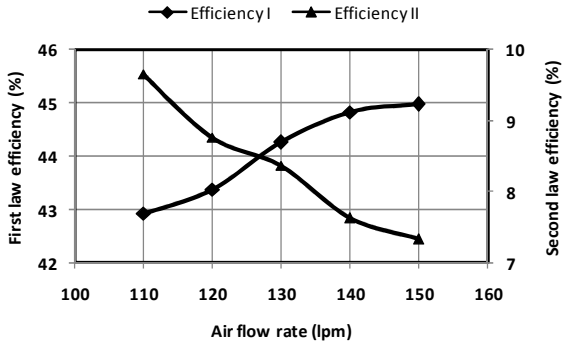

(b)

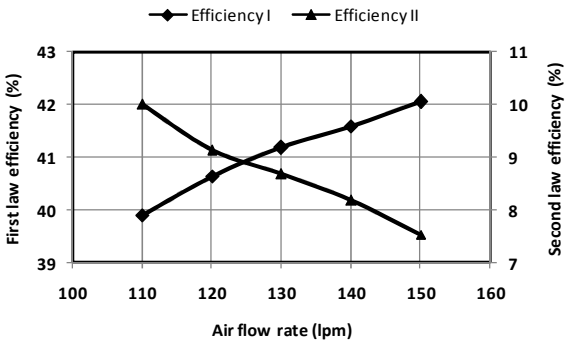

(c)

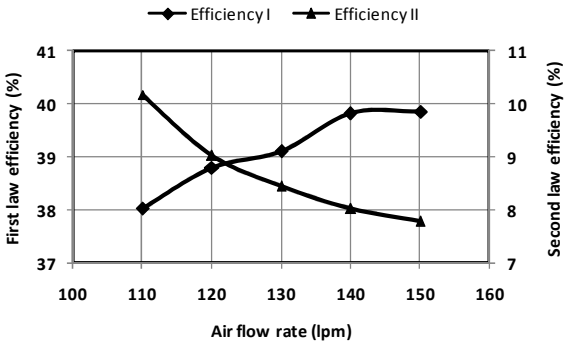

(d)

Fig. 5.4: Variations of first and second law efficiencies of 60SCC with air flow rate for the fuel flow rate of (a) 160 g/hr (b) 180 g/hr (c) 210 g/hr and (d) 220 g/hr.

It is seen from Table 5.3 and Figures 5.4(a)-(d) that in case of 60SCC burner also, with increase in air flow rate, the first law efficiency increases and the second law efficiency decreases. The optimum air flow rate ranges between 120-130 lpm. Same behaviour is observed for 80SCC (Figure 3.5 (a)) burner also. Table 5.4 includes the first and second law efficiency of 80SCC burner.

Table 5.4: Energy and exergy efficiency of 80SCC burner

Fuel flow rate (g/hr)	Air flow rate (lpm)	Efficiency I (%)	Efficiency II (%)
160	110	45.5	9.2
160	120	45.9	8.6
160	130	45.9	7.8
160	140	46.1	7.2
160	150	46.7	6.9
180	110	42.2	9.3
180	120	42.6	8.6
180	130	43.0	8.2
180	140	43.2	7.6
180	150	43.6	7.1
210	110	38.3	9.9
210	120	38.6	9.3
210	130	38.9	8.8
210	140	39.0	8.2
210	150	39.5	7.6
220	110	35.3	9.9
220	120	35.7	9.3
220	130	36.0	8.5
220	140	36.3	8.1
220	150	36.6	7.5

It is evident from Table 5.4 that the performance of 80SCC burner from first law point of view is not attractive. However, second law efficiency does not differ much with the previous configurations i.e., 70SCC, 70SCCWHS, 60SCC burners. This shows that the recovery potential of 80SCC burner and the other configurations are similar. Figures 5.5 (a)-(d) show the variations of efficiencies of 80SCC with air and fuel flow rates.

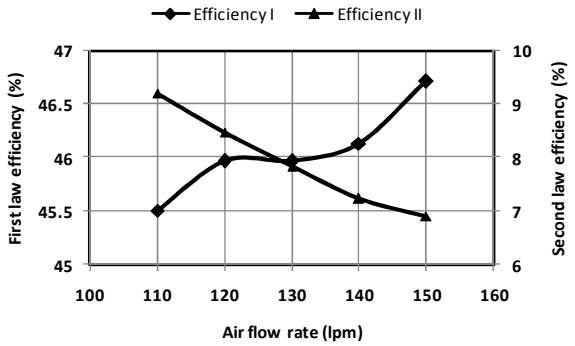

(a)

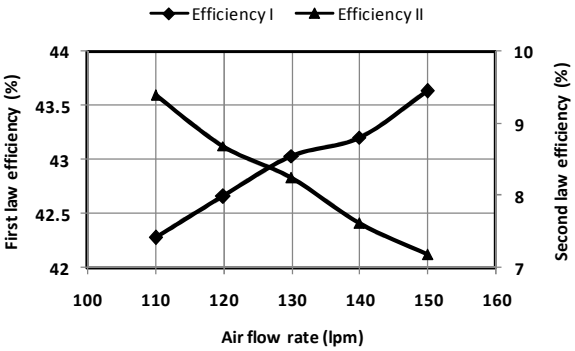

(b)

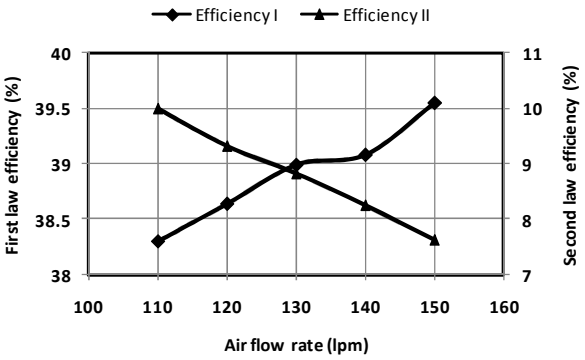

(c)

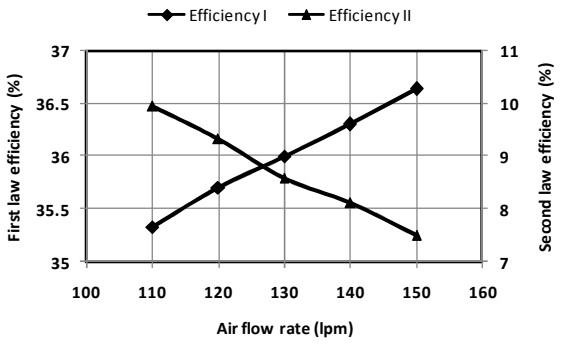

(d)

Fig. 5.5: Variations of first and second law efficiencies of 80SCC with air flow rate for the fuel flow rate of (a) 160 g/hr (b) 180 g/hr (c) 210 g/hr and (d) 220 g/hr.

It is evident from Figure 5.5(a)-(d) that for fuel flow rates of 160 g/hr, 180 g/hr, 210 g/hr and 220 g/hr respectively, the average first law efficiencies (53.5%, 50.4, 46.34%, 43.4%) and the average second law efficiencies (8.7%, 8.7, 9.2, 9.8%) correspond to the air flow rates ranged between 120-130 lpm. Hence, for this configuration also the air flow rate ranged between 120-130 lpm is considered optimum. Similar trend is observed for the burner in taper casing (70TCWHS). For 70TCWHS burner (Figure 3.5 (c)), the first and second law efficiencies are reported in Table 5.5 and their variations with air and fuel flow rates are presented in Figures 5.5(a)-(d). It is observed from Table 5.5 that the highest second law efficiency of this configuration is 10.9. While the same for 70SCC, 70SCCWHS, 60SCC and 80SCC burner as observed from Tables 5.1, 5.2, 5.3 and 5.4 are 10.1, 10.4, 9.9 and 10.1, respectively. Thus, 70TCWHS performs better.

Table 5.5: Energy and exergy efficiency of 70TCWHS burner

Fuel flow rate (g/hr)	**Air flow rate (lpm)**	**Efficiency I (%)**	**Efficiency II (%)**
160	110	52.6	9.9
160	120	53.3	9.4
160	130	53.4	8.7
160	140	54.1	8.0
160	150	54.2	7.5
180	110	49.5	10.0
180	120	50.0	9.4
180	130	50.1	8.7
180	140	50.7	8.0
180	150	51.4	7.4
210	110	45.6	10.7
210	120	46.0	9.8
210	130	46.6	9.1
210	140	46.6	8.4
210	150	47.3	7.8
220	110	42.6	10.9
220	120	43.0	9.9
220	130	43.0	8.8
220	140	43.6	8.6
220	150	44.6	7.9

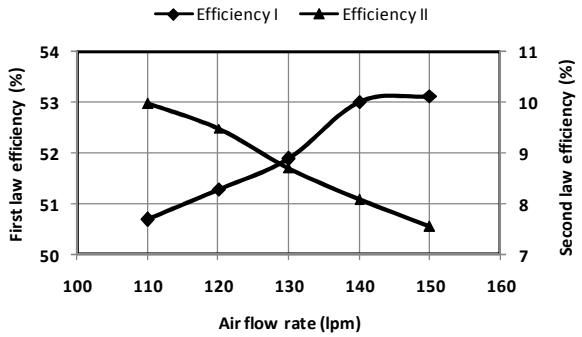

(a)

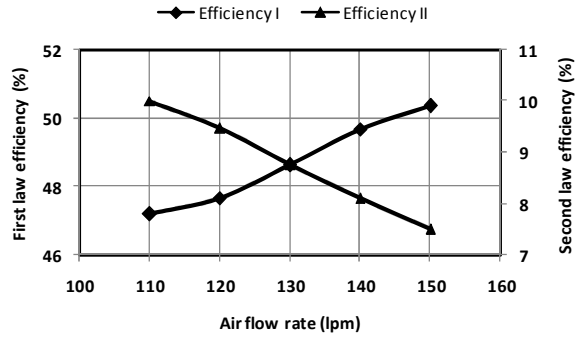

(b)

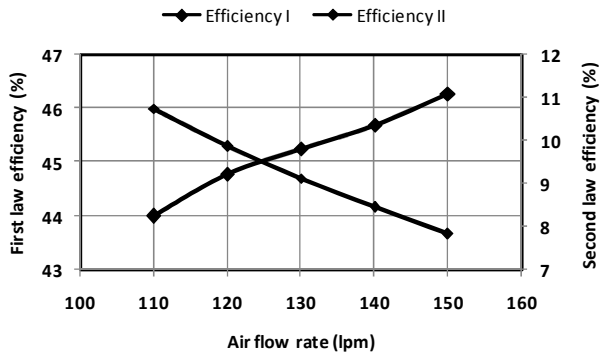

(c)

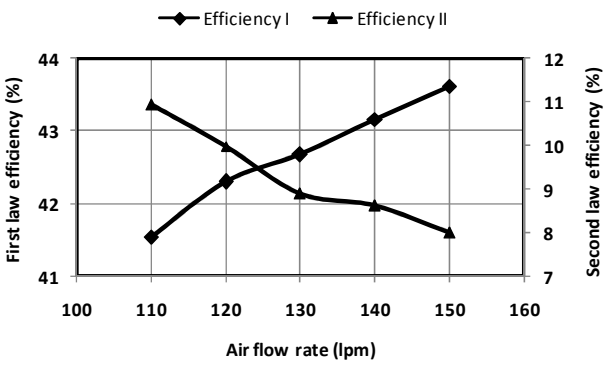

(d)

Fig. 5.6: Variations of first and second law efficiencies of 70TCWHS with air flow rate for the fuel flow rate of (a) 160 g/hr (b) 180 g/hr (c) 210 g/hr and (d) 220 g/hr.

Figure 5.6 (a)-(d) show similar trend of decreasing first law efficiencies and increasing second law efficiencies with increase in air flow rates. The range of optimum air flow rate found on the basis of average of four first law efficiencies and four second law efficiencies is 120-130 lpm. Table 5.6 shows the first law and second law efficiencies of 70CCWHS (Figure 3.5 (d)).

Table 5.6: Energy and exergy efficiency of 70CCWHS burner

Fuel flow rate (g/hr)	Air flow rate (lpm)	Efficiency I (%)	Efficiency II (%)
160	110	54.4	10.3
160	120	55.7	9.5
160	130	56.2	8.9
160	140	57.1	8.2
160	150	57.8	7.7
180	110	50.3	10.0
180	120	50.8	9.5
180	130	52.1	8.9
180	140	52.7	8.4
180	150	53.2	7.7
210	110	47.0	10.9
210	120	47.5	10.4
210	130	48.1	9.6
210	140	48.6	9.0
210	150	49.3	8.5
220	110	43.8	11.9
220	120	44.6	10.4
220	130	44.8	9.6
220	140	45.8	8.9
220	150	46.3	8.3

Among all the casings considered 70CCWHS burner showed the highest second law efficiency (11.9 %). Besides, it is also observed that with increase in air flow rate from 110-150 lpm, for a fixed fuel flow rate, first law efficiency increases by ~3%, and second law efficiency decreases by 1%. The variations of first law and second law efficiencies of this configuration at different air and fuel flow rates are shown in Figures 5.7(a)-(d).

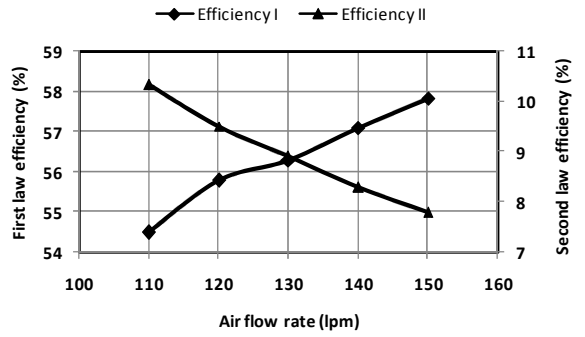

(a)

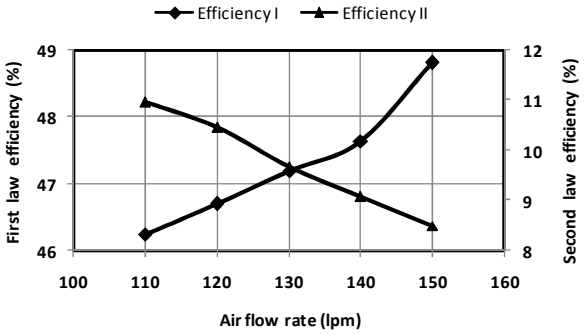

(b)

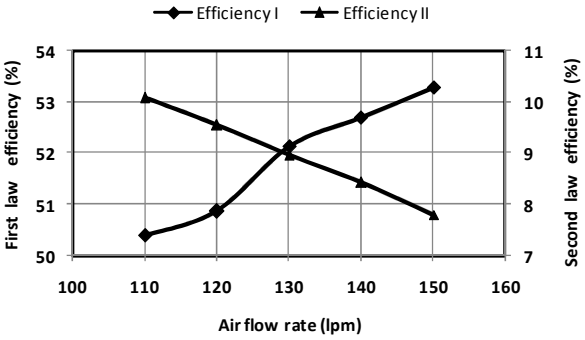

(c)

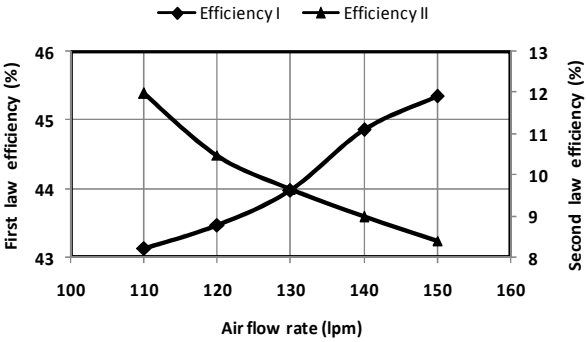

(d)

Fig. 5.7: Variations of first and second law efficiencies of 70CCWHS with air flow rate for the fuel flow rate of (a) 160 g/hr (b) 180 g/hr (c) 210 g/hr and (d) 220 g/hr.

Figures 5.7(a)-(d) clearly indicate that when the first law efficiency increases, the second law efficiency decreases. Thus, by considering Figures 5.7(a)-(d) together with the data presented in Table 5.7, the optimum air flow rate for better first and second law efficiencies is found to be ranged between 120-130 lpm. Further, in a broad sense, considering the variations of efficiencies of all the configurations with air flow rates it can be concluded that the optimum air flow rate ranges between 120-130 lpm.

Having optimized the air flow rate, next for a fixed air flow rate, variations of first and second law efficiencies with fuel flow rate was studied. With the air flow rate of 120 lpm, this study was made for 70CCWHS burner. Figure 5.8 shows the results.

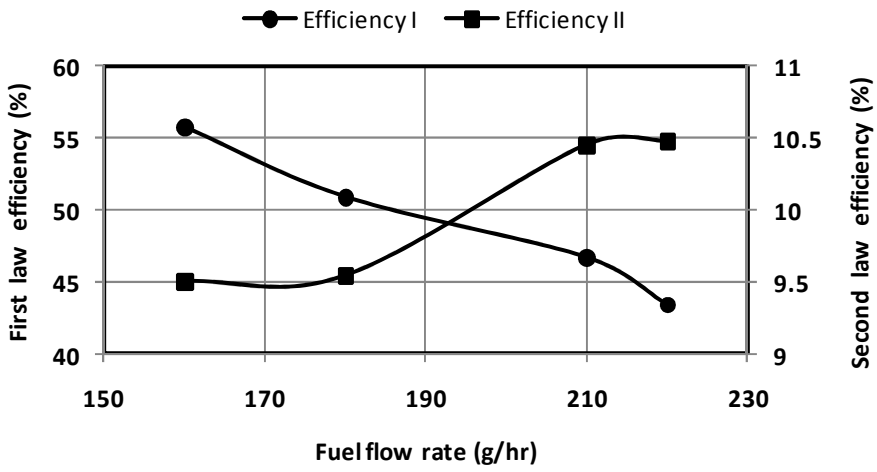

Fig. 5.8: Variations of first and second law efficiencies of 70CCWHS with fuel flow rate for the air flow rate of 120 g/hr.

As is evident from Figure 5.8 at an air flow rate of 120 lpm, when the fuel flow rate increases from 160-220 g/hr, the first law efficiency decreases from 55.8% to 43.4%, while, the second law efficiency increases from 9.5% to 10.4 %. Considering the averages of four first law efficiencies and the four second law efficiencies, for a fixed air flow rate, the optimum fuel flow rate is ~180 g/hr.

5.3 ENERGY AND EXERGY EFFICIENCIES OF BIS STOVE AND PB INCORPORATED STOVE WITH ALUMINA LINING

Having identified the optimum air and fuel flow rates for the stove with PM, next, second law efficiencies were found out for the stove with alumina lined burner (Figure 4.22 (a), (b) and also for the BIS stove (Figure 2.3). Table 5.7 shows the results.

Table 5.7: Energy and exergy efficiency of alumina lined burner and BIS burner.

Configuration	Fuel flow rate (g/hr)	Air flow rate (lpm)	Equivalence ratio	Efficiency I (%)	Efficiency II (%)
Alumina lined	180	120	0.31	62	12.6
BIS	160	-	-	51.2	11.7
	180	-	-	48.6	11.4

It is observed from Table 5.7 that the second law efficiencies of the BIS stove at two different fuel flow rates are 11.7 % and 11.4%. This indicates the improvement potential of the BIS stove and PM incorporated stoves, described in section 5.2, are similar. The Alumina lined 70SCC burner also shows similar second law efficiency with that of the BIS and configurations described before. The first law efficiency is however, higher.

From the discussions presented in section 5.2 and 5.3 it is evident that for a fixed fuel flow rate, the exergy efficiency of all the configurations at higher air flow rate is lower than that obtained at lower air flow rate. Similarly, for a fixed air flow rate, exergy efficiency is lower for lower fuel flow rate. These observations indicate that there is some improvement potential of the burners when operating at higher air or lower fuel flow rates. This point is not clear from the viewpoint of energy analysis. Thus, the energy analysis is sometimes misleading and in order to get the real picture of energy use, the

exergy analysis is essential. It is to be noted that in the present case, comparing both first and second law efficiencies as well as emissions, the burner conical casing 70CCWHS (Figure 3.5 (d)) shows the best thermal performance.

5.4 SUMMARY

Performances of a kerosene pressure stove equipped with PM enclosed in different shaped casings are reported in terms of first and second law efficiencies. The efficiencies are calculated at different air and fuel flow rates and with change in air and fuel flow rates, they are found to change. An increase in air flow rates resulted in increase in first law efficiency, and decrease in the second law efficiency. While, increase in fuel flow rate shows opposite trends. Higher the fuel flow rates, lower is the first law efficiency and higher the second law efficiency. The optimum air flow rate is found to lie between 120-130 lpm and the optimum fuel flow rate is found to be ~180 g/hr. The conical casing exhibits the highest first and second law efficiencies.

भारतीय प्रौद्योगिकी संस्थान गुवाहाटी
Indian Institute of Technology Guwahati

CHAPTER 6

SUMMARY AND CONCLUSIONS

6.1 SUMMARY AND CONCLUSIONS

With an objective of improving the performance of the conventional kerosene pressure stove, in terms of emissions and efficiency, the concept of PMC was employed. A BIS kerosene pressure stove was suitably modified. The geometrical parameters of the new stove were fixed on the basis of a series of parametric studies conducted to address some critical issues like air supply (natural or forced draft), vaporization, combustion stability, ignition, etc.

Experiments were conducted with different materials having different thicknesses and different porosities, and finally a combination of two different PM viz., alumina (Al_2O_3) and Silicon carbide (SiC) was chosen. SiC being highly conductive and radiative, promoted heat transfer to the downstream, and because of low thermal conductivity and emissivity, Al_2O_3 could reduce the heat transfer to the upstream as well as in radial direction. This combination was found effective in recirculating heat from the reaction zone, and maintaining the combustion temperature lower. A total of 35 mm thick porous bed with Al_2O_3 layer 15 mm and SiC 20 mm was found to retain the flame within PB with good combustion stability. Further increase in Al_2O_3 layer thickness resulted in higher pressure drop, restraining air-fuel mixture to move up and burn within SiC.

The combustion quality was found to be affected by pore density and porosity of the materials. For instance, 10 ppi SiC showed better performance than 20 ppi. Likewise, for the same bed thickness, 7 mm Al_2O_3 balls with 30% resulted in better mixing of air and

fuel than the 5 mm balls with 40% porosity. Owing to a large pressure drop, with 5 mm balls, there was soot deposition within the pores.

To see the effects of the flow fields on thermal efficiency and emissions, experiments were conducted with PM enclosed in 6 different types of casings, viz., (i) 60 mm straight cylindrical casing (60SCC) (ii) 70 mm straight cylindrical casing (70SCC) (iii) 80 mm straight cylindrical casing (80SCC) (iv) 70 mm straight cylindrical casing with heat shield (70SCCWHS) (v) 70 mm taper casing with heat shield (70TCWHS) and (vi) 70 mm conical casing with heat shield (70CCWHS). For each of the casings, experiments were conducted at different air and fuel flow rates. The fuel flow rates were maintained at 160 g/hr, 180 g/hr, 210 g/hr and 220 g/hr and the air flow rates varied between stoichiometry $(\phi = 1.0)$ to an extreme lean condition, viz., $(\phi = 0.18)$ with an air flow rate of 60 lpm and fuel flow rate of 160 g/hr. Good combustion stability was found for the air flow rate in the range: 60-180 lpm for all the fuel flow rate studied. Safe operation at such low air flow rate representing very low equivalence ratio was attributed to internal heat recirculation through PM to incoming mixture. At very high equivalence ratio viz., stoichiometric or near stoichiometric condition, however, the air-fuel mixture did not move up and started burning below the porous bed due to insufficient draft. To move the air-fuel into the PM by establishing a sufficient draft, a minimum of 60 lpm air at all selected fuel flow rates was found necessary.

The experiments with different air flow rate showed that with increase in air flow rate (from 60 to 180 lpm), the CO emissions first decreased and then increased. With respect to fuel flow rate, CO decreased with increase in fuel flow rate (from 160 g/hr to 220 g/hr). The lowest (30 ppm) CO emission was observed for the air and fuel flow rates of 120 lpm

and 220 g/hr, respectively. The emission of NO_x was found insensitive to heat input/fuel flow rate. It remained low (1-2 ppm) for the entire range of heat input studied. This low value was attributed to low combustion temperature owing to efficient heat removal.

With increase in air and fuel flow rates, the surface temperature was found to increase. When measured at different radial locations, nearly uniform temperature distribution was observed. However, with increase in air flow rate beyond 150 lpm, the distribution became non-uniform. Better uniformity was achieved at an air flow rate of 120 lpm. The measurement of axial temperature of the gas at two different locations viz., one at the interface and the other just below the bottom ceramic showed that with increase in air flow rates, the interface temperature increased, while the bottom temperature decreased.

The thermal efficiencies at different air and fuel flow rates showed that with increase in air flow rate (from 110 to 150 lpm) it increased by ~3%. Conversely, with increase in fuel rate (from 160 g/hr to 220 g/hr) the same was found to decrease. This trend was common for all the 6 configurations studied. There was ~3% improvement in efficiency of the burner enclosed in straight cylindrical casing with the use of a heat shield. The burner in conical casing (70CCWHS) showed the highest (~57%) thermal efficiency with air and fuel flow rates of 150 lpm and 160 g/hr respectively. This maximum efficiency is ~12% higher than the average thermal efficiencies of the conventional kerosene pressure stove reported in the literature review section. It is also higher (~8%) than the BIS stove tested under similar condition.

To investigate the dependence of thermal efficiencies on vessel size and explore the right vessel giving higher value, experiments were conducted with 3 different sizes of the

vessels. It was found that with increase in vessel size, the efficiency increases, it reaches the maximum and then it decreases. The best thermal efficiency was achieved for the vessel diamter of 260 mm. Besides the vessel size, the variation of thermal efficiency on the distance between the vessel bottom and the surface of the PM was also explored. A distance of 10 mm resulted in lower emissions.

Having analysed the performance of the burner from energy point of view, next at different air and fuel flow rates, the second law or the exergy efficiencies of the burner were evaluated. Unlike, thermal efficiency, the exergy efficiency was found to increase with decrease in air flow rate and increase in fuel flow rate. Considering the quantitative data of thermal efficiency and exergy efficiency at different air flow rates for a fixed fuel flow rate, a baseline to trade off was found between the air flow rates of 120-130 lpm. Similarly, for a fixed air flow rate, the optimum fuel flow rate was in the range of 190-200 g/hr.

The use of PM in kerosene pressure stove was found beneficial. It helped in reducing the emissions of CO and NO_x due to better mixing of air and fuel and low combustion temperature. The thermal efficiencies of the burners were also found improved. Among all the casings considered, the burner made of SiC and Al_2O_3 in conical casing exhibited the highest efficiency. Hence, this combination is preferable. It was found that the conditions for higher efficiency and lower emissions are contradictory. Likewise, the conditions for higher thermal efficiency and higher exergy efficiency are also not same. Hence, depending upon the actual requirement, user can choose any flow rate within the stated operating range, exhibiting good combustion stability. In the present study,

considering the trade off between the thermal efficiency and the exergy efficiency, the optimum operating conditions has been identified.

6.2 SCOPE FOR FUTURE WORK

In this work, for improvement of thermal performance of the kerosene pressure stove, the concepts of PMC was introduced and as expected promising results were obtained. However, there is scope for further improvement. To start with, one can try to redesign the vaporizing system so that the vaporizer would receive the heat flux just sufficient for vaporization without supporting combustion. This would prevent ignition of the mixture, and allow complete combustion within the PM. The first layer of the PM would then act as the preheating layer. One can also try to design a stove without a vaporizing system, allowing kerosene to vaporize within the PM. However, this would require a better distribution system, a new spray nozzle with wide spray angle, and also for initial heating of the PM, a preheater. Without preheater, it would be difficult to retain the flame without being quenched. One can use either LPG or electricity for preheating, and can check their usability with a detailed cost analysis in terms of energy. In addition to preheater, one can also focus on workability of the stove on natural draft. An alternate design without the use of compressor might be explored. Way for controlling upstream heat transfer can also be investigated. For better understanding of the complex phenomena of heat and mass transfer, phase change and chemical kinetics that takes place simultaneously inside the porous system, a theoretical investigation would be appropriate. Detailed experiments can be performed with materials other than SiC and Al_2O_3 with different porosities.

भारतीय प्रौद्योगिकी संस्थान गुवाहाटी
Indian Institute of Technology Guwahati

REFERENCES

1. Alam M, Sathaye J and Barnes D., 1998. Urban household energy use in India: efficiency and policy implications. Energy Policy 26: 885-891.
2. Artur G, Jozef J, Shenqyang S et al., 2009. Different methods of flame quenching in Jarosinski J and Veyssiere B (eds), Combustion phenomena: selected mechanisms of flame formation, propagation and extinction, chapter 6, CRC press, London.
3. Avdic F., 2004. Application of the porous medium gas combustion technique to household heating systems with additional energy sources, PhD thesis, University of Erlangen Nuremberg, Nuremberg.
4. Avdic F, Adzic M and Durst F., 2010. Small scale porous medium combustion system for heat production in households. Appl. Energy 87: 2148-2155.
5. Babkin VS, Korzhavin AA and Bunev VA., 1991. Propagation of premixed gaseous explosion flames in porous media. Combust. Flame 87:182-190.
6. Barra AJ and Ellzey JL., 2004. Heat recirculation and heat transfer in porous burners. Combust. Flame 137:230-241.
7. Bejan A., 2006. Advanced engineering thermodynamics, 2nd edn, Wiley Interscience publishers, New York.
8. Bhattacharya SC, Albina DO and Khaing AM., 2002. Effects of selected parameters on performance and emission of biomass fired cook stoves. Biomass Bioenergy 23: 387-395.
9. Bozzelli ZW and Dean AM., 1995. O+NNH a possible new route for NO_x formation in flames. Int. J. Chem. Kinet. 27:1097-1109.

10. Brenner G, Pickenäcker K and Pickenäcker O et al., 2000. Numerical and experimental investigation of matrix-stabilized methane/air combustion in porous inert media. Combust. Flame 123:201-213.
11. Buckmaster J and Takeno T., 1981. Blow off and flashback of an excess enthalpy flame. Combust. Sci. Technol. 25:153-158.
12. Delalic N, Mulahasanovic Dz., and Ganic EN., 2004. Porous media compact heat exchanger unit-experimental analysis. Exp. Therm. Fluid Sci. 28; 185-192.
13. Dendukuri G and Mittal JP., 1993. Some field experiences with improved chulhas (cookstoves) introduced in rural households of Andhra Pradesh, India. Energy Convers. Mange.34:457-464.
14. Dillon J., 1999. Combustion in porous media. Ae104 final report, viewed 10 December 2100, <www.osti.gov/bridge/servlets/purl/765956-VvNtsP/webviewable/>.
15. Dixit CSB, Paul PJ and Mukunda HS 2006. Experimental studies on a pulverized fuel pulverized fuel stove, Biomass Bioenergy 30: 673-683.
16. Dunkerley J, Macauley M and Naimuddin M et al., 1990. Consumption of fuelwood and other household cooking fuels in Indian cities. Energy policy 18: 92-99.
17. Dincer I, Hussain MM and Al-Zaharnah I., 2004. Energy and exergy utilization in transportation sector of Saudi Arabia. Appl. Therm. Eng. 24:525-538.
18. Fuse T, Araki Y and Kobayashi N., 2003.Combustion characteristics in oil-vaporizing sustained by radiant heat reflux enhanced with higher porous ceramics. Fuel 82:1411-1417.

19. Fuse T, Kobayashi N and Hasatani M., 2005. Combustion characteristics of ethanol in a porous ceramic burner and ignition improved by enhancement of liquid-fuel intrusion in the pore with ultrasonic irradiation. Exp. Therm. Fluid Sci. 29:467-476
20. Gangopadhyay S, Ramaswami B and Wadha W., 2005. Reducing subsidies on household fuels in India: how will it affect the poor?. Energy Policy 33:2326-2336.
21. Glassman I., 1996. Combustion, 3rd edn, Academic Press, California.
22. Goeckner BA, Helmich DR and McCarthy TA et al., 1992. Radiative heat transfer augmentation of natural gas flames in radiant tube burners with porous ceramic inserts. Exp. Therm. Fluid Sci. 5:848-860.
23. Gupta G and Köhlin G., 2006. Preference for domestic fuel: Analysis with socio-economic factors and rankings in Kolkata, India. Ecological Economics 57:107-121.
24. Hardesty DR, Weinberg FJ., 1974. Burners producing large excess enthalpies. Combust. Sci. Technol.8:201-214.
25. Howell JR, Hall MJ and Ellzey JL., 1996. Combustion of hydrocarbon fuels within porous inert media. Prog. Energy Combust. Sci. 22:121-145.
26. Hsu PF, Evans WD and Howell JR., 1993. Experimental and numerical study of premixed combustion within nonhomogeneous porous ceramics. Combust. Sci. Technol. 90:149-172.
27. Huang Y, Chao CYH and Cheng P., 2002. Effects of preheating and operation conditions on combustion in a porous medium. Int. J. Heat Mass Transfer 45:4315-4324.
28. Indian Standard, Burners for oil pressure stoves and oil pressure heaters, specification, (Second Revision): IS 10109, 2002, Bureau of Indian Standard.

29. Jugjai S and Phothiya C., 2007. Liquid fuels-fired porous combustor-heater. Fuel 86: 1062-1068.

30. Jugjai S and Polmart N., 2003. Enhancement of evaporation and combustion of liquid fuels through porous media. Exp. Therm. Fluid Sci. 27:901-909.

31. Jugjai S and Pongsai C., 2007. Liquid fuels-fired porous burner. Combust. Sci. Technol. 179:1823-1840.

32. Jugjai S and Rungsimuntuchart N., 2002. High Efficiency heat-recirculating domestic gas burners. Exp. Therm. Fluid Sci. 26: 581-592.

33. Jugjai S, Wongpanit N and Laoketkan T et al., 2002. The combustion of liquid fuels using a porous medium. Exp. Therm. Fluid Sci.26: 15-23.

34. Jungbluth N, Kollar M and Koβ V., 1997. Life cycle inventory for cooking-some results for the use of liquefied petroleum gas and kerosene as cooking fuels in India. Energy Policy 25: 471-480.

35. Kakati S, Mahanta P and Kokoty SK., 2007. Performance analysis of pressurized kerosene stove with porous medium inserts. J. Sci.Ind. Res. 66:565-569.

36. Kandpal JB, Maheshwari RC and Kandpal TC., 1995. Indoor air pollution from domestic cookstoves using coal, kerosene and LPG. Energy Convers. Manage. 36:1067-1072.

37. Kamal MM and Mohamad AA., 2006. Combustion in porous media, a review. Proc. Inst. Mechanical Engineers - Part A: J. Power Energy 220:487-508.

38. Kamal MM and Mohamad AA., 2007. Investigation of liquid fuel combustion in a cross flow burner. Proc. Inst. Mechanical Engineers - Part A: J. Power Energy 221:371-385.

39. Kaplan M and Hall MJ., 1995. The combustion of liquid fuels within a porous media radiant burner. Exp. Therm. Fluid Sci. 11:113-120.

40. Kaushik SC and Gupta MK., 2008. Energy and exergy efficiency comparison of community - size and domestic - size paraboloidal solar cooker performance. Energy Sustainable Dev. 12: 60-64.
41. Kaushik SC, Mishra RD and Singh N., 2000. Second law analysis of a thermal power system. Int. J. Solar Energy 20:239-253.
42. Kayal TK and Chakravarty M., 2005. Combustion of liquid fuel inside inert porous media: an analytical approach. Int. J. Heat Mass Transfer 48:331-339.
43. Kayal TK and Chakravarty M., 2006. Modeling of trickle flow liquid fuel combustion in inert porous medium. Int. J. Heat Mass Transfer 49:975–983.
44. Kayal TK and Chakravarty M., 2007. Modeling of a conceptual self-sustained liquid fuel vaporization–combustion system with radiative output using inert porous media. Int. J. Heat Mass Transfer 50:1715-1722.
45. Kee RJ, Gracer JF and Smooke MD et al., 1985. A fortran program for modeling steady laminar one dimensional premixed flames, Sandia Technical Report SAND85-8240.
46. Khalil MAK and Rasmussen RA., 1985. Causes on increasing atmospheric methane: dependence of hydroxyl radicals and the rise of emissions. Atmos. Environ. 19:397-407.
47. Khanna R, Goel R and Ellzey JL.,1994. Measurements of emissions and radiations for methane combustion within a porous medium burner. Combust. Sci. Technol. 99:133-142.
48. Kline SJ and Mc Clintock FA., 1953. Describing uncertainties in single-sample experiments. Mech. Eng. 75:3-8.
49. Ko YC and Ta HL., 2003. Emissions and efficiency of a domestic gas stove burning natural gases with various compositions. Energy Convers. Manage. 44: 3001-3014.

50. Kumar TS, Vasudevan P and Patwardhan SV., 1985. Pattern of non-commercial energy consumption and availability in the Indian domestic sector-A case study. Agric. Wastes. 12:55-60.

51. Leonardi SA, Viskanta R and Gore JP., 2002. Radiation and thermal performance measurements of a metal fiber burner. J. Quant. Spectrosc. Radiat. Transfer. 73: 491-501.

52. Liu JF and Hsieh WH., 2004. Experimental investigation of combustion in porous heating burners. Combust. Flame 138: 295-303.

53. Lucky AR and Hossain I., 2001. Efficiency study of Bangladeshi cookstoves with an emphasis on gas cookstoves. Energy 26: 221-237.

54. Malico I and Pereira JCF., 1999. Numerical predictions of porous burners with integrated heat exchanger for house hold applications. J. Porous Media 2:153-162.

55. Martynenko VV, Echigo R and Yoshida H., 1998. Mathematical model of self-sustaining combustion in inert porous medium with phase change under complex heat transfer. Int. J. Heat Mass Transfer 41:117-126.

56. Mathis Jr WM andEllzey JL., 2003. Flame stabilization, operating range, and emissions for a methane/air porous burner. Combust. Sci. Technol. 175:825-839.

57. Meng WH, McCordic C and Gore JP et al., 1991. A study of effects of porous ceramic inserts on heat transfer and combustion in a fired heat exchanger. In: Proceedings of the 1991 ASME/JSME Thermal Engineering Joint Conference. Maui, Hawai, 181-188.

58. Min DK and Shin HD. 1991.Laminar premixed flame stabilized inside a honeycomb ceramic. Int. J. Heat Mass Transfer 34:341-356.

59. Mishra TK, Datta A and Mukhopadhyay A., 2006. Comparisons of the structures of methane-air and propane-air partially premixed flame. Fuel 85:1254-1263.

60. Meng WH, McCordic C and Gore JP et al., 1991. A study of effects of porous ceramic inserts on heat transfer and combustion in a fired heat exchanger. In: Proceedings of the 1991 ASME/JSME Thermal Engineering Joint Conference. Maui, Hawai, 181-188.
61. Mital R, Gore JP and Viskanta R., 1997. A study of the structure of submerged reaction in porous ceramic radiant burners. Combust. Flame 11:175-184.
62. Mößbauer S, Pickenäcker O and Pickenäcker K et al., 1999. Application of the porous burner technology in energy and heat engineering. In: Proceeding of the Fifth International Conference on Technologies and Combustion for a Clean Environment. Lisbon, Portugal 519-523.
63. Mößbauer S, Grüber W and Trimis D., 2001. Exhaust gas recirculation in porous burners for the target application zero emission steam engines. In: Proceeding of the Sixth International Conference on Technologies and Combustion for a Clean Environment. Porto, Portugal, 9-12.
64. Mujeebu A, Abdullah MZ and Bakar MZA et al., (2009a). Applications of porous media combustion technology-a review. Appl. Energy 86:1365-1375.
65. Mujeebu A, Abdullah MZ and Bakar MZA et al.,(2009b). Combustion in porous media and its applications - a comprehensive survey J. Environ. Mange. 90:2287-2312.
66. Mujeebu A, Abdullah MZ and Bakar MZA et al.,(2009c). A review of investigations on liquid fuel combustion in porous inert media. Prog. Energy Combust. Sci. 35:1-15.
67. Mujeebu A, Abdullah MZ and Bakar MZA et al.,(2010d). Trends in modeling of porous media combustion. Prog. Energy Combust. Sci. 6:627-650.
68. Mukunda HS, Dasappa S and Paul PJ et al., 2010. Gasifier stoves - science, technology and field outreach. Curr. Sci. 98: 627-638.

69. Mukunda HS, Shrinivasa U and Dasappa S., 1988. Portable single pan wood stove for high efficiency. Sadhana 13: 237-270.

70. Natarajan J, Kochar Y and Lieuwen T et al., 2009. Pressure and preheat dependence of laminar flame speeds of H2/CO/CO2/He mixtures. Proc. Combust. Inst. 32:1261-1268.

71. Natarajan R, Karthikeyan NS and Agarwaal A et al., 2008. Use of vegetable oil as fuel to improve efficiency of cooking stove. Renewable Energy 33:2423-2427.

72. Ozturk HH., 2004. Experimental determination of energy and exergy efficiency of the solar parabolic cooker. Solar Energy 77: 67-71.

73. Pandit GG, Srivastava PK and Rao AMM., 2001. Monitoring of indoor volatile organic compounds and polycyclic aromatic hydrocarbons arising from kerosene coking fuel. The Sci. Total Environ.279:159-165.

74. Pantangi VK,. 2010. Development and performance analysis of porous radiant burners for cooking applications, PhD Thesis, Indian Institute of Technology Guwahati, Guwahati.

75. Panwar NL, Kothari S and Kaushik SC., 2010. Experimental investigation of energy and exergy efficiency of masonry-type solar cooker for animal feed. Int. J Sustainable Energy 29: 178-184

76. Periasamy C, Sankara SK, Gollahalli SR., 2007. An experimental evaluation of evaporation enhancement with porous media in liquid-fuelled burners. J. Porous Media 10:137-150.

77. Petela R., 2005. Exergy analysis of the solar cylindrical – parabolic cooker. Solar Energy. 79:221-233.

78. Pickenäcker O, Pickenäcker K, and Wawrzinek K et.al., 1999. Innovative ceramic materials for porous-medium burners. Interceram, Germany. 48:424-433.

79. Pohekar SD, Kumar D and Ramachandran M., 2005. Dissemination of cooking energy alternatives in India- a review. Renewable Sustainable Energy Rev. 9:379-393.

80. Pope K. Dincer I and Naterer GF., 2010. Energy and exergy efficiency comparison of horizontal and vertical axis wind turbines. Renewable Energy 35: 2102-2113.

81. Primus stove, Wikipedia 2010, viewed 10 December 2010, <http://en.wikipedia.org/wiki/Primus_stove>.

82. Purohit P, Kumar A and Rana S et al., 2002. Using renewable energy technology for domestic cooking in India: a methodology for potential estimation. Renewable Energy 26:235-246.

83. Qiu K and Hayden ACS., 2006. Premixed gas combustion stabilized in fiber felt and its application to a novel radiant burner. Fuel 85:1094-2000.

84. Ravindranath NH, Somasekar HI and Nagaraja MS et al., 2005. Assessment of sustainable non-plantation biomass resources potential for energy in India. Biomass Bioenergy 29:178-190.

85. Reddy BS., 2003., Overcoming the energy efficiency gap in India's household sector. Energy Policy 31:1117-1127.

86. Rumminger MD, Dibble RW and Heberle NH et al., 1996. Gas temperature above a porous radiant burner: comparison of measurements and model predictions. Proc. Combust. Inst. 26:1755-1762.

87. Sahoo BB, Saha UK and Sahoo N et al., 2009. Analysis of throttle opening variation impact on a diesel engine performance using second law of thermodynamics. In: Proceedings of the ASME Internal Combustion Engine Division Spring Technical Conference, Milwaukee, Wisconsin, USA.

88. Saidur R, Sattar MA and Masjuki HH et al., 2007. An estimation of the energy and exergy efficiencies for the energy resources consumption in the transportation sector in Malaysia. Energy Policy 35:4018-4026.

89. Sathe SB, Peck RE and Tong TW., 1990. A numerical analysis of heat transfer and combustion in porous radiant burners. Int. J. Heat Mass Transfer 33: 1331-1338.

90. Sharma M, Mukunda HS and Sridhar G., 2009. Solid fuel block as an alternate fuel for cooking and barbecuing: preliminary results. Energy Convers. Manage.50: 955-961.

91. Sharma M, Nishioka M and Mishra SC et al., 2010a. A modeling study of premixed CH4/air mixtures: dependence of laminar flame speed on pressure and preheating temperature. In: Proceedings of the ISHMT-ASME Heat and Mass Transfer Conference. Mumbai, India.

92. Sharma M, Nishioka M and Mishra SC et al., 2010b. A numerical study on laminar preheated premixed propane/air flame. In: Proceedings of the International Conference on Flow Dynamics, Sendai, Japan.

93. Sharafat S, Ghoniem N and Williams B et al. 2005. Cellular foams: a potential innovative solid breeder material for fusion applications. Fusion Sci. Technol. 47: 886-890.

94. Smith K, Uma Rand Kishore VVN et al., 2000. Greenhouse gases from small-scale combustion devices in developing countries, Phase IIa, Household stoves in India, USEPA, EPA-600-00-052.

95. Suzukawa Y, Sugiyama S and Hino Y et al., 1997. Heat transfer improvement and NOx reduction by highly preheated air combustion. Energy Convers. Manage. 38:1061-1071.

96. Takami H, Suzuki T and Itaya Y et al., 1998. Performance of flammability of kerosene and NO_x emission in the porous burner. Fuel 77:165-171.

97. Takeno T and Sato K., 1979. An excess enthalpy flame theory. Combust Sci. Technol. 20:7-84.

98. Thukral K and Bhandari PM., 1994. The rationale for reducing subsidy on LPG in India. Energy Policy 22:81-87.

99. Tong TW, Sathe SB and Peck RE., 1990. Improving the performance of porous radiant burners through use of sub-micron size fibres. Int. J. Heat Transfer 33:1339-1346.

100. Trimis D and Durst F. 1996. Combustion in a porous medium-advances and applications. Combust. Sci. Technol.121:153-168.

101. Trimis D, Wawrzinek K and Hetzfeld O et al., 2001. High modulation burner for liquid fuels based on porous media combustion and cool flame vaporization. In: Proceedings of the sixth international conference on technologies and combustion for clean environment, Porto, Portugal 1-8.

102. Tseng CJ and Howell JR., 1996. Combustion of liquid fuels in a porous radiant burner. Combust. Sci. Technol. 112:141-161.

103. Utlu Z and Hepbasli A., 2006. Estimating the energy and exergy utilization efficiencies for the residential-commercial sector: an application. Energy policy 34:1097-1105.

104. Vijaykant S and Agrawal AK., 2007. Liquid fuel combustion within silicon-carbide coated carbon foam. Exp. Therm. Fluid Sci. 32:117-125.

105. Viswanathan B and Kumar KSK., 2005. Cooking fuel use patterns in India: 1983-2000. Energy policy 33:1021-1036.

106. Warnatz J, Mass U and Dibble RW. 2001. Combustion: Physical and chemical fundamentals, modeling and simulation, experiments and pollutants formation, Springer-Verlag Berlin, Heidelberg.

107. Weclas M., 2006. Porous media in internal combustion engines in M. Scheffler, (ed). Cellular Ceramics, Chapter 5.10, 580-595.

108. Wei M, Wang Y and Reh L., 2002. Experimental investigation of the pre vaporized premixed (vpl) combustion process for liquid fuel lean combustion. Chem. Eng. Process 41:157-164.

109. Weinberg FJ., 1971. Combustion temperatures: the future? Nature. 233:239-241.

110. Wood S and Harris AT., 2008. Porous burners for lean-burn applications. Prog. Energy Combust. Sci.34:667-684.

111. Xiong T-Y, Khinkis MJ and Fish FF., 1995. Experimental study of a high-efficiency, low emission porous matrix combustor-heater. Fuel 74:1641-1647.

112. Zhang J, Smith KR and Uma R et al., 1999. Carbon monoxide from cookstoves in developing countries: 2. Exposure potentials. Chemos. Global Change Sci. 1: 367-375.

Annexure A

CALCULATIONS OF FLAME SPEEDS IN FREE SPACE FOR METHANE-AIR AND PROPANE-AIR MIXTURE AND COMPARISONS OF THE RESULTS OF EFFECTIVE FLAME SPEEDS OF THE SAME MIXTURES IN PM

PBs are characterized by higher flame speeds. In comparison combustion in free space, the combustion within PM results in higher reaction rates and higher effective flame speeds, mostly in excess of the laminar flame speed. This increase in flame speed in PM is caused due to preheating of the reactants due to radiation and conduction heat transfers from the reaction zone. Preheating may be external or internal. Considering external preheating, Figure A.1 shows the variations of laminar flame speed of a preheated premixed methane-air mixture with equivalence ratios, computed using PREMIX code with GRI Mech 3.0 kinetic mechanism by Sharma et al. (2010a). The unburnt temperature was varied from 300-800K.

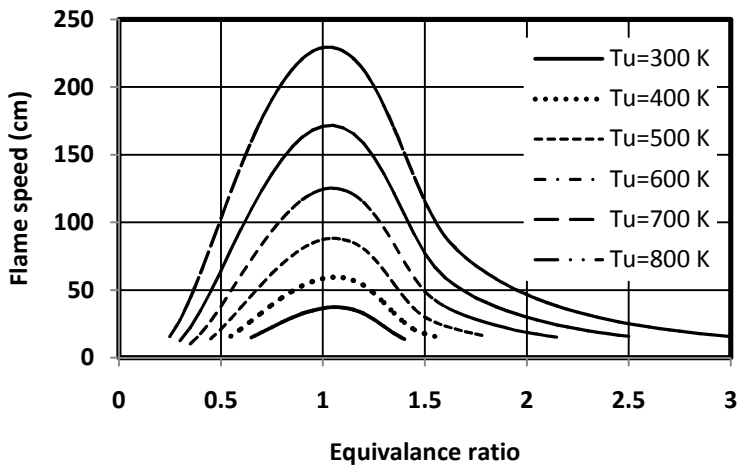

Fig.A.1: Variations of laminar flame speed of preheated premixed methane-air mixture with equivalence ratios.

It is observed in Figure A.1 that with preheating the laminar flame speed increases. Similar inference can be drawn in PMC, where there is internal heat recirculation. Barra and Ellzey (2004) computed the flame speed of methane-air mixture in a PM and also in free space. They quantified the ratio of effective flame speed to laminar flame speed as flame speed ratio. The results are presented in Table A.1. For comparison the results of Sharma et al. (2010a) are also included.

Table A.1: Equivalence ratios and corresponding laminar flame speed, effective flame speed.

Equivalence ratio (Φ)	Laminar flame speed (cm/s)		Flame speed ratio (max.)	Effective flame speed (cm/s)
	Barra and Ellzey (2004)	Sharma et al., (2009)		
0.55	7.2	-	5.1	**36.7**
0.60	11.2	-	4.9	54.8
0.65	15.5	14.9	4.8	74.4
0.70	19.9	18.7	4.9	97.5
0.75	24.3	22.5	5.0	121.5
0.80	28.5	26.2	5.1	145.3
0.85	-	29.6	-	-
0.90	35.5	32.5	5.3	188.1

As observed from Table A.1, the results of Sharma et al. (2010a) and Barra and Ellzey (2004) are nearly same. Besides, it is observed that in PB, the effective flame speed is higher than laminar flame speed. For the same equivalence ratio, similar ranged effective flame speed is obtained for the mixture having higher unburnt temperature. Table A.2 shows the detail results of Sharma et al. (2010a) on the computations of laminar flame speed of methane-air flame at various unburned temperatures ranging from 300-800K.

Table A.2: Laminar flame speed of methane-air flame at various unburned temperatures

Equivalence ratio	Laminar flame speed at various unburned temperature (Tu)					
	Tu= 300K	Tu= 400K	Tu=500K	Tu= 600K	Tu= 700K	Tu= 800K
0.25	-	-	-	-	-	15.56687
0.3	-	-	-	-	12.46486	27.98265
0.35	-	-	-	10.1684	22.27329	44.10809
0.4	-	-	-	17.75043	34.68562	62.61857
0.45	-	-	14.00715	27.2392	48.93169	82.59088
0.5	-	-	21.06384	**37.98691**	64.17441	102.82161
0.55	-	15.79493	28.99736	49.41586	79.79128	122.7222
0.6	-	21.42699	37.36564	**61.17283**	95.06512	141.91885
0.65	14.91188	27.30455	45.89337	**72.70988**	109.68605	159.91005
0.7	18.75824	33.21101	54.30166	83.58451	123.39252	176.25217
0.75	22.5713	38.99093	62.1758	93.6182	135.82571	190.67633
0.8	26.2338	44.40521	69.29672	102.65733	**146.71174**	203.03731
0.85	29.62729	49.21193	75.52405	110.45115	155.83729	213.18381
0.9	32.56631	53.25278	80.70649	116.77951	163.03619	220.99247
0.95	34.91073	56.4069	84.67577	121.46021	168.1854	226.3558
1	36.52739	58.52698	87.24133	124.33291	171.13656	229.16246

It is evident from Table A.1 that at equivalence ratio 0.55, the effective flame speed is 36.7 cm/s. This value is matched with the results in Table A.2, when the unburnt temperature is 600K. Similarly, at equivalence ratio 0.8, a matching flame speed is observed at an unburnt temperature of 700K. This confirmed the fact of increasing laminar flame speed with preheating. Similar conclusions can be made from Figure B.2 in which the variations of flame speed of a preheated premixed propane-air mixture with equivalence ratios are shown. The flame speeds were computed using PREMIX code with Dagaut kinetic mechanism by Sharma et al. (2010b). Table A.3 shows the laminar flame speeds of propane-air flame at various unburned temperatures.

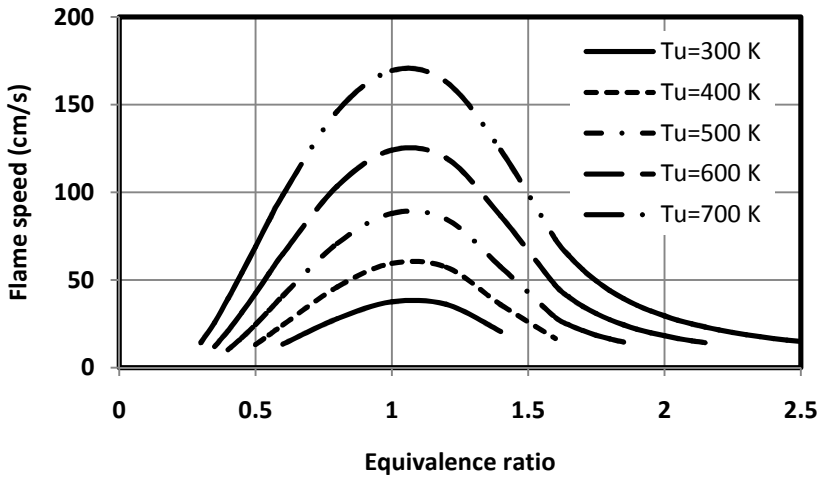

Fig.A.2: Variations of laminar flame speed of preheated premixed propane-air mixture with equivalence ratios.

Table A.3: Laminar flame speed of propane-air flame at various unburned temperatures

Equivalence ratio	Laminar flame speed at various unburned temperature (Tu)				
	Tu=300K	Tu=400K	Tu=500K	Tu=600K	Tu=700K
0.3	-	-	-	-	14.1
0.35	-	-	-	12.0	25.7
0.4	-	-	10.1	21.0	39.3
0.45	-	-	16.9	31.3	54.0
0.5	-	13.1	24.5	42.3	68.9
0.55	-	18.5	32.6	53.6	83.9
0.6	13.2	24.2	40.7	64.7	98.3
0.8	27.8	45.9	70.7	**103.5**	146.1
1	37.5	59.5	87.9	124.0	169.4

As evident from Table A.3, at equivalence ratio of 0.8, and 300K unburnt temperature of the mixture, the flame speed is 27.8. While, for the same mixture (at equivalence ratio 0.8), the effective flame speed in PM was found to be 110 cm/s by Babkin et al. (1991).

Annexure B

MANUFACTURE OF CERAMIC FOAM (Sharafat et al., 2006)

Reticulated foam is an assembly of irregularly shaped prismatic or polyhedral cells connected to each other with solid edges/ faces. It can be of 2 types, viz., (i) open cell and (ii) closed cell. In open cell, the cells are connected with edges of the solids, and in closed cell, the connections are with the faces. These cells are manufactured from polymers, metals, glasses, and ceramics. Ceramic foams are porous brittle materials with closed, fully open or partially interconnected pores. The ceramic foam manufacturing techniques can be classified into 3 general categories: sponge-replication, foaming agent based, or space holder method. In sponge-replication method, a natural sponge or polyurethane foam is used and infiltrate with ceramic slurry. The ceramic slurry is then dried, fired and sintered to form ceramic foam. In foaming agents method, some gas evolving constituents are added to preceramic melt and during the treatment, bubbles are generated causing the material to form foam. In the third method, i.e., the space holder method, first, a space holder is formed by sintering a salt and then the space holder is infiltrated with polymer. After dissolving the salt, the polymer foam remains which is then pyrolysed. Figure B.1 shows a picture of square and circular ceramic foams.

.

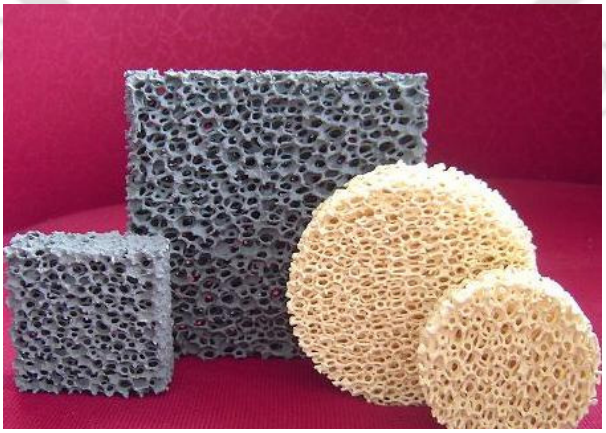

Fig. B.1: Picture of ceramic foam.

Annexure C

TECHNICAL SPECIFICATIONS OF THE INSTRUMENTS USED IN THE SET UP

1. Pressure regulator

Make	:	Norgren
Model	:	R73G-2GK-RMN
Maximum pressure	:	10 bar
Operating Temperature	:	-20 °C to +50 °C

2. Pressure gauge

Make	:	Waree instruments
Dial size	:	100 mm
Range	:	0-2 bar
Readability	:	0.05 bar
Housing Materials	:	300 Series SS
Accuracy	:	±0.05% full scale
Temperature Limits	:	0 °C to 120 °C

3. Compressor

Type	:	Reciprocating
Maximum Pressure	:	12 kg/cm^2
Free air delivery	:	400-450 lpm
Type	:	Two stage
Tank capacity	:	250 litres

4.Weighing balance

Make	:	SARTORIUS
Model:	:	CLWP1 – 30ED-I
Capacity	:	30 kg
Platform size	:	400 mm × 300 mm
Least count	:	1 g

5. Thermocouple

Type	:	K
Range	:	20 ^oC to 1350 ^oC
Accuracy	:	±1.5 ^oC

6. Rotameter I

Make	:	Flow tech engineers
Operating fluid	:	LPG
Pressure	:	Atmospheric
Measuring range:	:	0-2.5 lpm
Least count	:	0.1 lpm
Accuracy	:	±2% FS
Housing		Glass fibred

Rotameter II

Make	:	Flow tech engineers
Operating fluid	:	Air
Pressure	:	up to 15 bar
Measuring range	:	0-400 lpm
Least count	:	10 lpm
Accuracy	:	±3% FS

Rotameter III

Make	:	Flow tech engineers
Operating fluid	:	Kerosene
Pressure	:	Atmospheric
Measuring range	:	0-10 mlpm
Least count	:	0.2 mlpm
Accuracy	:	±3% FS

7. Bomb calorimeter

Make	:	IKA
Model	:	C4000 A
Measurement range	:	375 to 12000 Kcal/Kg
Measurement accuracy	:	± 0,1%

8. Flue Gas Analyzer

Model	:	TESTO 350XL
O_2	:	0-25%, accuracy: ±0.8% of f.v.
CO	:	0-10000 ppm, accuracy: ±5% of mv
NO	:	0-3000 ppm, accuracy: ±5% of mv
NO_2	:	0-500 ppm, accuracy: ±5% of mv
CO_2	:	Calculated (%)
Default O_2 reference:	:	3%
Resolution	:	0.1 ppm
Storage temperature	:	-4 to +122 °F
Operating temperature	:	+20 to +113 °F

Annexure D

SAMPLE CALCULATION FOR CALORIFIC VALUE IN BOMB CALORIMETER

Bomb calorimeter is used to determine the enthalpy of combustion, for hydrocarbons. Basically, it consists of a small cup to contain the sample, oxygen, a stainless steel bomb, water, a stirrer, a thermometer, and an ignition circuit connected to the bomb. Electrical energy is used to ignite the fuel and this leads to rise in temperature of water. The change in temperature is noted with a thermometer.

Before the use of bomb for determination of heat of combustion of any compound, it is generally calibrated with a known compound. In the current study, the calorimeter was standardized by burning pure and dry benzoic acid and calculating the heat capacity of the calorimeter. Once the standardization was over, experiments were done to determine the calorific value of the IOCL (Indian Oil Corporation Limited) certified kerosene. Measurements were done in triplicate and the average was taken. ASTM standard 240D was followed. The calculation procedure is described below.

Initially, the heat capacity of the calorimeter was evaluated using Benzoic acid with known heat of combustion.

Heat capacity (C) of the calorimeter is given by

$$C = \frac{(H_{OB} \times m_{OB}) + Q_F}{\Delta T} \qquad \text{D.1}$$

Heat of combustion of Benzoic acid, H_{OB}=26456 J/g

Mass of combustion of Benzoic acid, m_{OB}=0.520 g

Change in water temperature, ΔT=1.5817 K

Q_F =Calorific value of thread + ignition wire + ignition energy

$Q_F = (2\times 50)+30+0.91=130.91\text{J}$

$$\therefore C=\frac{(26456\times 0.520)+130.91}{1.5817}=8780.45\text{J/K}$$

Having found the heat capacity of the calorimeter with Benzoic acid, next, the calorific value of the fuel was evaluated. For calculation the following formula was used.

$$LCV=\frac{(C\times\Delta T)-Q_F}{m_f} \qquad \text{D.2}$$

$C = 8780.45\,\text{J/K},\ \Delta T$=2.1810 K, $Q_F=(2\times 50)+30+1.51=131.51\text{J},\ m_F$=0.4360 g, ΔT=2.1810 K

$$\therefore LCV=\frac{(8780.45\times 2.1810)-131.51}{0.4332}$$

=439020.70 kJ/kg

Annexure E

SAMPLE CALCULATION FOR UNCERTAINTY OF THERMAL EFFICIENCY

Uncertainty is a measure of the 'goodness' of a result. In physical experiments uncertainty analysis deals with assessing the uncertainty in measurement. Without such analysis, it is impossible to judge the fitness of the value as a basis for making decisions relating to physical experiments. Kline and McClintok (1953) proposed a precise method for estimating the uncertainty in the experimental results. The method is based on a careful specification of the uncertainties in the various primary experimental measurements. These are systematic errors which are dependent on the resolution of the measuring device. The theory involved in the method can be described as follows.

Consider an experimental result where R is a function of several independent variables viz., $x_1, x_2, x_3.....x_n$.

Thus, $R = R(x_1, x_2, x_3.....x_n)$ E.1

Now, each of these independent variables has its own uncertainty viz. $(\Delta R_1, \Delta R_2, \Delta R_3.....\Delta R_n)$ and this will propagate. For calculation of the uncertainty in the value of the result ΔR, the propagated uncertainties of the independent variables should be considered. The uncertainty in the result ΔR can be calculated by the following formula.

$$\Delta R = \left[\left(\frac{\partial R}{\partial x_1} \Delta R_1 \right)^2 + \left(\frac{\partial R}{\partial x_2} \Delta R_2 \right)^2 + \left(\frac{\partial R}{\partial x_3} \Delta R_3 \right)^2 ..... + \left(\frac{\partial R}{\partial x_n} \Delta R_n \right)^2 \right]^{1/2} \quad \text{E.2}$$

In this work, the uncertainty associated with the estimation of thermal efficiency is calculated. The results are presented below.

Thermal efficiency is given by

$$\eta_I = \left(\frac{Q_1 + Q_2 + Q_3}{Q_i + W_c}\right)\left(\frac{1}{t}\right) \qquad \text{E.3}$$

$$where\ Q_1 = m_w \times c_{pw} \times \left(T_f - T_i\right),\ (kJ)$$

$$Q_2 = m_{wvp} \times L,\ (kJ)$$

$$Q_3 = m_v \times c_{pv} \times \left(T_f - T_i\right),\ (kJ)$$

$$Q_i = \dot{m} \times LCV,\ (\text{kW})$$

$$W_c = \frac{1}{0.80 \times 0.90}\left[\dot{m}_a \times R \times T_1\left[\left(\frac{n}{n-1}\right)\left(\frac{P_2}{P_1}\right)^{\frac{n-1}{n}} - 1\right]\right] = 0.035\,\text{kW}$$

Considering the compressor work to be constant and expressing the heat input $\left(Q_i\right)$ and heat output $\left(Q_1 + Q_2 + Q_3\right)$ in kJ, the expression for efficiency will be as follows.

$$\eta_I = \left(\frac{Q_1 + Q_2 + Q_3}{Q_i}\right)$$

$$\eta_I = \left(\frac{\left(m_w \times c_{pw} \times \left(T_f - T_i\right)\right) + \left(m_{wvp} \times L\right) + \left(m_v \times c_{pv} \times \left(T_f - T_i\right)\right)}{\left(m \times LCV\right)}\right) \qquad \text{E.4}$$

where m is the total mass of fuel consumed during the WBT, when water was heated from room temperature to 90 ^{o}C.

Uncertainty in the result

$$\Delta\eta = \left[\left(\frac{\partial \eta}{\partial m_w} \Delta m_w \right)^2 + \left(\frac{\partial \eta}{\partial m_v} \Delta m_v \right)^2 + \left(\frac{\partial \eta}{\partial m_{wvp}} \Delta m_{wvp} \right)^2 + \left(\frac{\partial \eta}{\partial (\Delta T_w)} \Delta (\Delta T_w) \right)^2 + \left(\frac{\partial \eta}{\partial (\Delta T_v)} \Delta (\Delta T_v) \right)^2 + \left(\frac{\partial \eta}{\partial m_f} \Delta m_f \right)^2 \right]^{1/2} \quad \text{E.5}$$

where,

$\Delta m_v = \pm 1\,\text{g}$, $\Delta m_w = \pm 1\,\text{g}$, $\Delta m_{wvp} = \pm 5\,\text{g}$, $\Delta m_f = \pm 2\,\text{g}$,

$\Delta(\Delta T_w) = \pm 1\,^{\circ}\text{C}$ $\Delta(\Delta T_v) = \pm 10\,^{\circ}\text{C}$

At a condition of

$m_w = 6\,\text{kg}$, $m_v = 0.894\,\text{kg}$, $m_{wvp} = 0.020\,\text{kg}$, $\Delta m_f = 0.094\text{kg}$,

$\Delta T_w = 65\,^{\circ}\text{C}$, $\Delta T_v = 415\,^{\circ}\text{C}$

$\Delta\eta = 2.1\%$

Annexure F

SAMPLE CALCULATION FOR COMPRESSOR POWER

The compressor work $W_c\,(kW)$ is calculated from the following equation.

$$W_c = \frac{1}{0.80 \times 0.90}\left[\dot{m}_a \times R \times T_1\left[\left(\frac{n}{n-1}\right)\left(\frac{P_2}{P_1}\right)^{\frac{n-1}{n}} - 1\right]\right] \qquad \text{F.1}$$

The compressor work $W_c\,(kW)$ is varied with the air flow rates. One sample calculation is shown below.

$\dot{m}_a = 120\,\text{lpm or } 0.144\,\text{kg/min}$

$R = 0.287\,\text{kJ/kgK}$

$T_1 = 298\,\text{K}$

$n = 1.2$

$P_2 = 1.2\,\text{bar}$

$P_1 = 1.013\,\text{bar}$

$W_c = 0.035\,\text{kW}$

For calculation of compressor work $W_c\,(kW)$ other than the stated air flow rate, R, T_1, P_2 and P_1 are assumed to be same as the above.

Annexure G

SAMPLE CALCULATION OF STOICHIOMETRIC AIR-FUEL RATIO AND EQUIVALENCE RATIO

Equivalence ratio (φ): It is defined as the ratio of stoichiometric air-fuel ratio to the actual air-fuel ratio.

$$\varphi = \frac{(\text{A/F})_{stoich}}{(\text{A/F})_{actaul}} \qquad \text{G.1}$$

where

$\varphi \succ 1$, rich mixture

$\varphi = 1$, stoichiometric mixture

$\varphi \prec 1$, lean mixture

The stoichiometric quantity of oxidizer is just that amount needed to burn a fuel completely. The stoichiometric air fuel ratio is determined by writing simple atomic balances, assuming that the fuel reacts to form an ideal set of products. Kerosene is a mixture of several hydrocarbons. Assuming the representative formula of kerosene as $C_{13}H_{26}$ the stoichiometric equation is:

$$C_{13}H_{26} + 19.5(O_2 + 3.76N_2) = 13CO_2 + 13H_2O + (3.76 \times 19.5)N_2 \qquad \text{G.2}$$

$\therefore$ Stoichiometric air-fuel ratio of kerosene is

$$(A/F)_{stoich} = \frac{4.76 \times 19.5 \times 29}{182} = 14.8:1$$

For air flow rate: 120 lpm and kerosene flow rate: 160 g/hr 0.00325 lpm

$$\text{Equivalence ratio } (\phi) = \frac{(A/F)_{stoich}}{(A/F)_{actual}} = \frac{14.8 \times 0.00325 \times 820}{120 \times 1.2} = 0.27$$

Annexure H

SAMPLE CALCULATION FOR FIRST LAW AND SECOND LAW EFFICIENCY

First law efficiency or thermal efficiency is given by

$$\eta_I = \left(\frac{Q_1 + Q_2 + Q_3}{Q_i + W_c}\right)\left(\frac{1}{t}\right)$$

$$where\ Q_1 = m_w \times c_{pw} \times \left(T_f - T_i\right),\ (kJ)$$

$$Q_2 = m_{wvp} \times L,\ (kJ)$$

$$Q_3 = m_v \times c_{pv} \times \left(T_f - T_i\right),\ (kJ) \qquad \text{H.1}$$

$$Q_i = \dot{m} \times LCV,\ (\text{kW})$$

$$W_c = \frac{1}{0.80 \times 0.90}\left[\dot{m}_a \times R \times T_1\left[\left(\frac{n}{n-1}\right)\left(\frac{P_2}{P_1}\right)^{\frac{n-1}{n}} - 1\right]\right] = 0.035\,\text{kW}$$

For air flow rate of 120 lpm and fuel flow rate of 160g/hr,

$$Q_1 = m_w \times c_{pw} \times \left(T_f - T_i\right) = 6 \times 4.2 \times (90 - 25) = 1638\,\text{kJ}$$

$$Q_2 = m_{wvp} \times L = 0.020 \times 2257 = 45.14\,\text{kJ}$$

$$Q_3 = m_v \times c_{pv} \times \left(T_f - T_i\right) = 0.894 \times 0.881 \times (417 - 25) = 308.74\ \text{kJ}$$

$$Q_i = \dot{m} \times LCV = \frac{160 \times 43.90}{3600} = 1.95\,\text{kW}$$

$$W_c = \frac{1}{0.80 \times 0.90}\left[\dot{m}_a \times R \times T_1\left[\left(\frac{n}{n-1}\right)\left(\frac{P_2}{P_1}\right)^{\frac{n-1}{n}} - 1\right]\right] = 0.035\,\text{kW}$$

$$\eta_I = \left(\frac{Q_1 + Q_2 + Q_3}{Q_i + W_c}\right)\left(\frac{1}{t}\right) = \left(\frac{1638 + 45.14 + 308.74}{1.95 + 0.035}\right)\left(\frac{1}{31 \times 60}\right) = 53.90\%$$

Second law efficiency or exergy efficiency is given by

$$\eta_{II} = \frac{A_1 + A_2 + A_3}{A_g}$$

$$where\ A_1 = \left(\left(m_w \times c_{pw} \times \left(T_f - T_i\right) - \left(T_o \Delta S_w\right)\right) / t\right),\ (kW)$$

$$A_2 = \left(\left(\left(m_{wvp} L\right) - T_o \Delta S_{wvp}\right) / t\right),\ (kW)$$

$$A_3 = \left(\left(m_v \times c_{pv} \times \left(T_f - T_i\right) - T_o \Delta S_v\right) / t\right),\ (kW)$$

$$A_g = \dot{m}_g \times c_{pg} \times \left(T_g - T_o\right)\left(1 - \frac{T_o}{T_g}\right),\ (kW)$$

H.2

For air flow rate of 120 lpm and fuel flow rate of 160 g/hr,

$$A_1 = \left(\left(\left(m_w \times c_{pw} \times \left(T_f - T_i\right)\right) - \left(T_o \Delta S_w\right)\right) / t\right),\ (kW)$$

$$= \left(\left(\left(m_w \times c_{pw} \times \left(T_f - T_i\right)\right) - \left(T_o \left(m_w C_{pw} \ln \frac{T_f}{T_i}\right)\right)\right) / t\right)$$

$$= \left(\left(\left(6 \times 4.2 \times \left(\left(90 - 25\right)\right)\right) - \left(25 \times \left(6 \times 4.2 \times \ln\left(\frac{363}{298}\right)\right)\right)\right) / t\right)$$

$$= 0.083\,\text{kW}$$

$$A_2 = \left(\left(\left(m_{wvp} L\right) - T_o \Delta S_{wvp}\right) / t\right)$$

$$= \left(\left(\left(m_{wvp} L\right) - T_o \left(\frac{m_{wvp} L}{T_f}\right)\right) / t\right)$$

$$= \left(\left(\left(0.020 \times 2257\right) - 298\left(\frac{0.020 \times 2257}{363}\right)\right) / t\right)$$

$$= 0.004\,\text{kW}$$

$$A_3 = \left(\left(m_v \times c_{pv} \times \left(T_f - T_i \right) - T_o \Delta S_v \right) / t \right), \ (kW)$$

$$A_3 = \left(\left(0.894 \times 0.881 \times \left(417 - 25 \right) - \left(0.894 \times 0.881 \ln \left(\frac{417}{25} \right) \right) \right) / t \right), \ (kW)$$

$$= 0.06 \, \text{kW}$$

$$A_g = \dot{m}_g \times c_{pg} \times \left(T_g - T_o \right) \left(1 - \frac{T_o}{T_g} \right)$$

$$= \left(\frac{2.7 + 132}{60 \times 1000} \right) \times 1.29 \times \left(1011 - 298 \right) \left(1 - \frac{1011}{298} \right)$$

$$= 1.43 \, \text{kW}$$

$$\eta_{II} = \left(\frac{A_1 + A_2 + A_3}{A_g} \right) = \left(\frac{0.083 + 0.004 + 0.06}{1.43} \right) = 10.2\%$$

Annexure I

SAMPLE CALCULATION FOR SPECIFIC HEAT OF GAS

Assuming the representative formula of kerosene as $C_{13}H_{26}$

The stoichiometric equation can be written as

$$C_{13}H_{26} + 19.5\left(O_2 + 3.76N_2\right) = 13CO_2 + 13H_2O + \left(3.76 \times 19.5\right)N_2$$

For air flow rate of 120 lpm and fuel flow rate of 160 g/hr, (equivalence ratio 0.28 and 260.36% excess air), the equation will be

$$C_{13}H_{26} + 19.5\left(O_2 + 3.76N_2\right) + 70.27\left(O_2 + 3.76N_2\right) = 13CO_2 + 13H_2O + 264.21N_2 + 50.77O_2$$

At the stated condition (equivalence ratio 0.28), the temperature of burned gas is 1025 K. At this temperature, $\left(c_{pg}\right)$ values for the 4 stated constituents are

Table I1: Specific heat $\left(c_{pg}\right)$ of gas

Constituent	Mole fraction	$\left(c_{pg}\right)$ (kJ/kgK)	$\left(c_{pg}\right)$ of the mixture (kJ/kgK)
CO_2	0.041	1.247	
H_2O	0.041	4.2	$\left(0.041 \times 1.247\right) + \left(0.041 \times 4.2\right) +$
N_2	0.773	1.177	$\left(0.773 \times 1.177\right) + \left(0.143 \times 1.1097\right) = 1.28$
O_2	0.143	1.1097	

List of publications

International journals

1. **M. Sharma** and S.C Mishra and P Acharjee. Thermal efficiency study of conventional kerosene pressure stoves with porous radiant inserts. International Energy Journal 2009, 10:247-254.

2. **M. Sharma**, S.C Mishra and P. Mahanta. An experimental investigation on efficiency improvement of a conventional kerosene pressure stove. Journal of Enhanced Heat transfer (Under review).

3. **M. Sharma**, S.C Mishra and P. Mahanta. Use of porous media for improvement in thermal performance of kerosene pressure stoves. Energy Conversion and Management (Under review).

4. **M. Sharma**, P. Mahanta and S.C Mishra. Parametric studies on performance of kerosene pressure stove with porous media. International Energy Journal (Under review).

5. **M. Sharma**, P. Mahanta and S.C Mishra. Energy and exergy analyses of a kerosene pressure stove equipped with porous media enclosed in different casings. Thermal Engineering (Under review).

International Conferences

1. **M. Sharma** and S.C Mishra and P Acharjee. Use of ceramic heat shield ring with embedded porous zirconia: an approach to enhance thermal efficiency of conventional pressure stove. ICAER, December 2009, Mumbai, India.

National Conferences

1. **M.Sharma** and S.C Mishra. A review of combustion of hydrocarbon fuel within porous media. CHEMCON, December 2006. Gujrat.

2. **M.Sharma** and S.C Mishra. Emission analysis of pressurized kerosene stove equipped with porous burners. CHEMCON, December 2007, Kolkata.